Thesis

Adjuvanted trimethyl chitosan based nanoparticle formulations to improve immunogenicity of DNA vaccines

POECHEIM, Johanna

Abstract

The aim of this thesis was to formulate nanoparticles with DNA plasmid (pDNA), encoding the Mycobacterium tuberculosis (Mtb) antigen 85A. The design of cationic N-trimethylated chitosan (TMC) nanoparticles, adjuvanted with the pattern recognition ligands TLR-9 and NLR-2, is a novel approach for improving DNA vaccines. To provide a potential context for future design of DNA vaccines, important parameters of TMC nanoparticle formulations with pDNA were evaluated and characterized. Successful binding of pDNA to the nanoparticles was confirmed as well as integrity of the secondary structure of pDNA after being released. It was shown that two pattern-recognition ligands co-delivered by nanoparticles synergistically activate innate immune responses in vitro and enhance cell-mediated immune responses in vivo. TMC nanoparticles, formulated with Mtb antigen 85A expressing pDNA, successfully induced robust Th1 immune responses in mice and may render pDNA/TMC nanoparticles a potential vaccine candidate for further investigations of protective efficacy against Mtb infections.

Reference

POECHEIM, Johanna. *Adjuvanted trimethyl chitosan based nanoparticle formulations to improve immunogenicity of DNA vaccines*. Thèse de doctorat : Univ. Genève, 2015, no. Sc. 4909

URN : urn:nbn:ch:unige-867173
DOI : 10.13097/archive-ouverte/unige:86717

UNIVERSITÉ DE GENÈVE
Section des Sciences Pharmaceutiques
Biopharmacie

FACULTÉ DES SCIENCES
Professeur Gerrit Borchard

Adjuvanted Trimethyl Chitosan based Nanoparticle Formulations to Improve Immunogenicity of DNA Vaccines

THÈSE

présentée à la Faculté des Sciences de l´Université de Genève, pour obtenir le grade de Docteur ès Sciences, mention Sciences Pharmaceutiques

par

Johanna POECHEIM

de
Satteins (Autriche)

Thèse N° 4909

Genève

Atelier d´impression Uni-Mail

2016

UNIVERSITÉ
DE GENÈVE

FACULTÉ DES SCIENCES

Doctorat ès sciences
Mention sciences pharmaceutiques

Thèse de *Madame Johanna POECHEIM*

Intitulée :

"Adjuvanted Trimethyl Chitosan Based Nanoparticle Formulations to Improve Immunogenicity of DNA Vaccines"

La Faculté des sciences, sur le préavis de Monsieur G. BORCHARD, professeur ordinaire et directeur de thèse (Section des sciences pharmaceutiques), Madame M. CUENDET, professeure associée (Section des sciences pharmaceutiques), Madame E. ROBLEGG, professeure associée (Institut für Pharmarzeutische Wissenschaften, Karl Franzens University, Graz, Austria) et Monsieur B. A. GANDER, professeur (Institut für Pharmarzeutische Wissenschaften, Eidgenössische Technische Hochschule Zürich, Zürich), autorise l'impression de la présente thèse, sans exprimer d'opinion sur les propositions qui y sont énoncées.

Genève, le 26 septembre 2015

Thèse - 4909 -

Le Doyen

N.B. - La thèse doit porter la déclaration précédente et remplir les conditions énumérées dans les "Informations relatives aux thèses de doctorat à l'Université de Genève".

Table of Contents

Preface

The introduction of vaccines against infectious diseases at the beginning of the twentieth century has had an extraordinary impact on human health worldwide. There is remarkable success of current vaccines against pathogens with a predominantly extracellular lifestyle, and protection can be induced by immunizing with components of these infectious agents (Titball, 2008). Despite the success of such traditional vaccines there is still a clear need for vaccine development against intracellular microbes such as human immunodeficiency virus (HIV), hepatitis C virus (HCV), *Plasmodium falciparum* and *Mycobacterium tuberculosis*, for which vaccines are not yet available or shown to be inadequate (WHO, 2013). Cell-mediated immune response is critical for controlling such intracellular pathogens, involving recognition of cell-associated foreign antigens by lymphocytes, followed by destruction of the infected host cells. In contrast to antibody mediated humoral immune responses, this arm of the immune response is stimulated by T-helper type I (Th1) lymphocytes and pro-inflammatory cytokines.

Strategies for developing T-cell-inducing vaccines against intracellular pathogens aim to deliver the antigen to antigen presenting cells (APCs) in order to induce antigen presentation by major histocompatibility complex (MHC) molecules on the cell surface. So-called new generation vaccines make use of vectors such as plasmid DNA, recombinant proteins, or live recombinant vaccines using bacterial or viral vectors. However, displaying highly purified components, representing only subunits without other, less defined structures of the pathogen, vaccines currently in development are often poorly immunogenic (Cui and Mumper, 2003, O'Hagan, 2007). Efficient vaccines will require the combination of diverse strategies, such as different delivery systems and

adjuvants, to present the antigen in a manner that can elicit an adequate and efficient immune response against these antigens (Nascimento and Leite, 2012).

In DNA vaccines an antigen coding sequence is inserted into a bacterial plasmid vector. The plasmid contains a eukaryotic gene promoter to express the antigenic proteins in mammalian cells *in vivo* (Robinson and Torres, 1997). The protein encoded by the plasmid DNA (pDNA) normally does not occur in vertebrates except in pathological conditions, such as for example proteins associated with *Mycobacterium tuberculosis (Mtb)* (Romano and Huygen, 2009). Upon pDNA administration, these exogenous proteins are expressed by the host's own cells and processed by MHC system in the same way as when an actual infection occurs. Hence, DNA vaccines are capable to induce humoral as well as cell-mediated immune responses, including cytotoxic T-lymphocyte responses, which are important for acquisition of protection against intracellular pathogens like *Mtb* (Kutzler and Weiner, 2008). Moreover, the presence of unmethylated cytosine-phosphate-guanosine (CpG) motifs characteristically present in bacterial DNA can act as an effective adjuvant by targeting the endosomal innate immune receptor Toll-like receptor 9 (TLR-9). Because only one or several selected antigens of a pathogen, rather than the whole pathogen are administered, there is no risk of infection by the vaccine. However, displaying only highly purified components, without other less defined structures of the target pathogen, DNA vaccines applied in the naked form are poorly immunogenic (Cui and Mumper, 2003). Furthermore, being poorly taken up by immune cells and quickly cleared from the circulation after injection, less pDNA is available for antigen processing and higher doses of naked pDNA would have to be applied (Liu *et al.*, 2007).

Nanotechnology in DNA vaccines is of great scientific interest as nanoparticles may serve as gene delivery systems and adjuvants to improve immunogenicity. Non-viral vectors based on chitosan hold great promise for the delivery of DNA in terms of biodegradability, biocompatibility and safety (Borchard, 2001). Nanocarrier adjuvanted

DNA vaccines are more efficiently localized to the targeted tissues, improving bioavailability, and are more efficiently taken up by antigen presenting cells (APC) because of their dimensions, which are comparable to pathogens. Moreover, according to their size or composition the desired type of immune response may be directed (Zaman *et al.*, 2013). Hence, DNA delivered with nanoparticles would lead to improved success of DNA vaccines and account for the interest of nanotechnology in vaccination.

The realization of this thesis has been divided into four chapters:

Current influences of nanotechnology on the development of new vaccines, with focus on particle characteristics interacting with the immune system, immune receptor targeting and antigen delivery, are reviewed in Chapter 1.

The synthesis and characterization of N-trimethylated chitosan (TMC), pDNA integrity upon interaction with TMC nanoparticles and nanoparticle stability are described in Chapter 2.

In Chapter 3, N-trimethyl chitosan (TMC) nanoparticles, a cationic squalene-in-water emulsion, and the cationic oil-in-water emulsion Cationorm® are compared *in vitro* and *in vivo* as delivery systems for pDNA. Moreover, involvement of TLR and NLR in immunity to CpG containing pDNA and muramyl dipeptide (MDP), respectively, and interaction of TLR and NLR pathways by simultaneous activation with both receptor ligands, are investigated.

Finally, in Chapter 4, influences of variations in pDNA doses on the outcome of immune responses, pharmaceutical and immunological properties of pDNA-TMC nanoparticles and co-delivery of pDNA with TMC nanoparticles and MDP to induce cellular immune responses *in vivo*, are described.

Aims of this thesis

- Formulation and characterization of trimethyl chitosan nanoparticles with pDNA.

- *In vitro* investigations of adjuvant effects of pDNA with regards to TLR and NLR stimulation.

- Investigations of dose effects of pDNA / TMC nanoparticles, with regards to their pharmaceutical characteristics.

- *In vivo* evaluation of potentiating effects of adjuvants on immunogenicity of pDNA.

References

Borchard, G. (2001). Chitosans for gene delivery*, Advanced Drug Delivery Reviews,* 52, pp. 145-150.

Cui, Z. and Mumper, R.J. (2003). Microparticles and nanoparticles as delivery systems for DNA vaccines*, Critical Reviews™ in Therapeutic Drug Carrier Systems,* 20, 103-137.

Kutzler, M.A. and Weiner, D.B. (2008). DNA vaccines: ready for prime time?*, Nature Reviews Genetics,* 9, pp. 776-788.

Liu, F., Shollenberger, L.M., Conwell, C.C., Yuan, X., and Huang, L. (2007). Mechanism of naked DNA clearance after intravenous injection*, The Journal of Gene Medicine,* 9, pp. 613-619.

Nascimento, I.P. and Leite, L.C.C. (2012). Recombinant vaccines and the development of new vaccine strategies*, Brazilian Journal of Medical and Biological Research,* 45, pp. 1102-1111.

O'Hagan, D.T. (2007). New generation vaccine adjuvants*, eLS.* DOI: 10.1002/ 9780470015902.a0020177.

Robinson, H.L. and Torres, C.A.T. (1997). DNA vaccines*, Seminars in Immunology,* 9, pp. 271-283.

Romano, M. and Huygen, K. (2009). DNA vaccines against mycobacterial diseases*, Expert Review of Vaccines*, 9, pp. 1237-1250.

Titball, R.W. (2008). Vaccines against intracellular bacterial pathogens*, Drug Discovery Today,* 13, pp. 596-600.

WHO (2013). The Global vaccine action plan 2011-2020*, from* http://www.who.int/immunization/global_vaccine_action_plan/GVAP_doc_2011_2020/en/index.html

Zaman, M., Good, M.F., and Toth, I. (2013). Nanovaccines and their mode of action*, Methods,* 60, pp. 226-231.

Chapter I:

Immunotherapy and Vaccines

Johanna Poecheim and Gerrit Borchard

School of Pharmaceutical Sciences, University of Geneva, University of Lausanne, Quai Ernest Ansermet 30, 1211 Geneva, Switzerland

Published in: Poecheim, J., Borchard, G. (2015), *Controlled Release Systems: Advances in Nanobottles and Active Nanoparticles*, Editor(s): J. Forcada, A. v. Herk, G. Pastorin, “Immunotherapie and Vaccines”, Pan Stanford Publishing, ISBN 978-981-4613-21-7 (Hardcover), 978-981-4613-22-4 (eBook).

1. Introduction

The human immune system has evolved to recognize antigenic properties of pathogens and initiate an immune response resulting in the restriction of the pathogen from entering the body, or in the clearance of the pathogen after infection. Among the signals leading to an activation of the immune system are the pathogen's surface properties, its size and its shape. It is therefore not surprising that the general paradigm of vaccine development demands the preparation of vaccines combining both antigen and adjuvant in the same - particulate - formulation. Vaccine development today, though, is fraught with the failure to achieve the required sufficient level of protection, possibly due to the lack of appropriate adjuvants - especially for mucosal vaccines - and delivery systems (Doroud and Rafati, 2011). However, and unfortunately, there is a bias between current knowledge on specific immune activation and its translation into real products. Whereas groundbreaking discoveries in the field of pathogenic pattern recognition by dedicated receptor families have been made over the last decades, only few ligands specifically interacting with these receptors have been introduced into clinical studies. One reason for this pause in vaccine development may have been the reluctance of manufacturers to introduce these novel adjuvants into the pipeline; another lies in the fact that they need to be presented to the cells of the immune system in an appropriate way to exploit their full potential. It may even be necessary to include combinations of novel adjuvants in one vaccine formulation to achieve synergistic effects.

Nanotechnology may offer the possibility to design of novel, more effective vaccines. These nanoparticulate carrier systems should be of appropriate size, have favorable surface parameters for immune recognition, are targeted to antigen-presenting cells (APCs) and suitable for the inclusion of the respective antigen. In addition, such novel vaccines may prove to have enhanced shelf-life stability, rendering refrigeration unnecessary, and to be applicable by mucosal pathways, allowing for the avoidance of needles for injection and the health risks related.

This chapter discusses the current influence of nanotechnology on the development of vaccines.

2. The Immune System

Vaccines are meant to elicit an immune response and to create long-lasting immune memory against a pathogen-specific antigen by staging an "artificial" infection. In order to rationally design novel vaccines it is essential to understand the function of the immune system itself. The vertebrate immune system consists of the innate and adaptive branches that cooperate to protect against infection and subsistence of pathogenic agents in the host. How both arms of the immune response are orchestrated is described in the following sections and illustrated in Figure 1.

2.1 The innate immune system

When pathogens overcome the barriers formed by the skin and the mucosae and gain access to the body's soft tissues, the innate immune system detects the invading agent and is activated as a fast and early- stage immune response. Innate immunity provides immune surveillance and immediate defenses that are always available and do not improve with repeated exposure to the same antigen. The immune system has to identify danger signals related to the pathogen, by detecting antigenic properties or patterns of a pathogen in the absence of prior immune recognition (first infection). Such danger signals are for example the recognition of pathogen associated molecular patterns (PAMPs) by pattern-recognition receptors (PRR), missing components or "missing self" signals distinguishing between bacterial cells and healthy human cells, tissue damage caused by pathogens, and alarm signals such as the release of certain cytokines. Upon recognition, complement activation is triggered, consisting in a system of plasma proteins and cell-surface molecules that mark pathogens for destruction. These interactions assist resident macrophages to phagocytose the microbiological invaders, as well as to induce macrophages to secrete inflammatory cytokines that in turn attract

neutrophils and natural killer (NK) cells to the site of infection (Parham, 2000) (Figure 1).

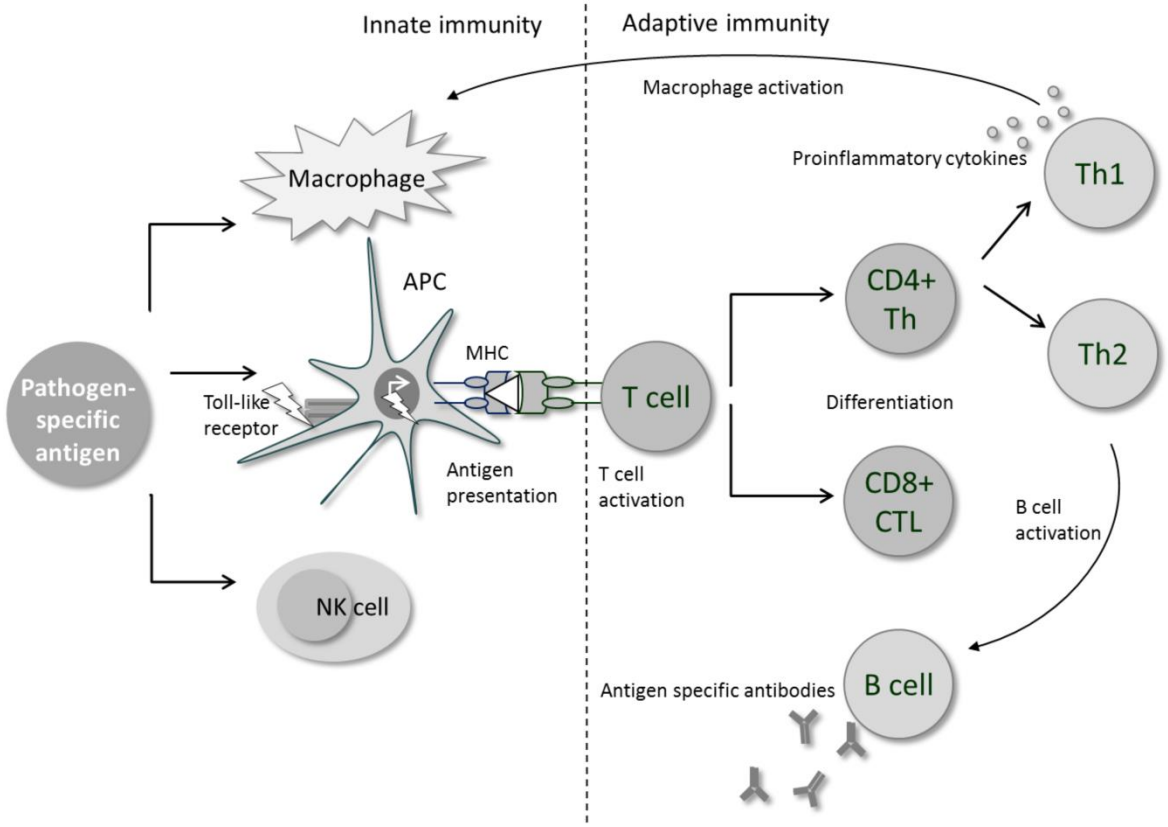

Figure 1. The role of innate and adaptive immune responses following vaccination with pathogen-specific antigen. Antigen presenting cells (APCs), which activate naïve T-cells through antigen presentation activate the adaptive immune system and induce T-cell differentiation. Activated CD4+ T-helper cells of type 1 activate macrophages and cytotoxic T-cells (CTL) through proinflammatory cytokine release. Type 2 helper T-cells activate B-cells to release specific antibodies against the antigen. Additionally to those antigen specific B- and T-cells spread as effector cells, long-lived clones of memory cells are produced that form the immunological memory.

2.2 The adaptive immune system

Under normal conditions, the adaptive immune system is silent and is only called into action directly when pathogens evade or overcome the innate immune defense. Thus, the adaptive immune response is initiated only if the innate immune system is activated and signals the presence of a pathogen. It “adapts” to the presence of a

pathogen by activating, proliferating, and creating potent mechanisms to neutralize and/or eliminate pathogens.

Two types of adaptive immune responses are to be distinguished. Humoral immunity is mediated by antibodies, also known as immunoglobulines (Ig), which are produced by B lymphocytes. The most abundant isotypes are IgG, found in blood serum and lymph, and IgA as the main effector of the mucosal immune system. Ratios of IgG2a/IgG1 subclasses >1 are associated with Th1 responses, whereas any ratio <1 corresponds to Th2-biased immune responses. Simultaneously cell-mediated immunity is induced, mediated by T lymphocytes. The main difference between these lymphocyte subtypes is that immunoglobulin receptors of B cells bind whole molecules and intact pathogens, whereas T-cells recognize only short peptide antigens (Kumar *et al.*, 2012), the so-called T-cell epitopes. At the site of infection (APC internalize, process and present T-cell epitopes by the major histocompatibility complex (MHC or CD1) molecules expressed at the cell surface. These cells subsequently migrate to the draining lymph nodes (LN), a collection point where APC interact with naïve T-cells. The T-cell receptor (TCR) recognizes peptide antigens presented at the surface of these immune cells and, thus, activates the T-cell (Von Andrian and Mackay, 2000). Antigen structures from intracellular infections are presented by MHC class I molecules and antigens from extracellular pathogens by MHC class II molecules. Depending on these two classes, T-cells differentiate into one of two types of effector T-cells: T helper cells ($CD4^+$ cells) to fight off extracellular pathogens, or cytotoxic T-cells ($CD8^+$ cells) to eliminate infected cells. The CD4+ T-helper (Th) lymphocytes are commonly divided into Th1 and Th2 subtypes. Th1 cells release pro-inflammatory cytokines to activate macrophages and cytotoxic T-cells (CTL) that are a part of the cellular immune system. Th2 cells help B-cells to maturate to antibody producing plasma cells, thereby supporting humoral immunity (Figure1).

2.3 Immunological memory

In the course of the adaptive immune response to infection, clones of pathogen-specific B- and T-cells spread as effector cells. Additionally, long-lived clones of memory T-cells that form the immunological memory are produced. Subsequent immune responses to the same pathogen will be faster and stronger, since memory cells are more quickly activated than naïve cells. Unlike naïve T-cells, memory T-cells can patrol non-lymphoid tissues, such as mucosae, and detect infection at an earlier stage. The greater power of a secondary immune response supports the generation of vaccine-mediated protection. By applying antigenic structures of the pathogen to the body without inducing the disease, immunological memory is elicited. Additionally, Th1 and Th2 polarizing adjuvants may be introduced to direct the desired immune response (Parham, 2000, Plotkin *et al.*, 2013).

3. Nanotechnology in vaccines

3.1 Particle characteristics interacting with the immune system

In the following section some of the key parameters of nanoparticles suitable for targeting to specific cells of the immune system will be discussed. Nanoparticles are of great scientific interest as they are effectively a bridge between bulk materials and atomic or molecular structures (Pignataro, 2010). To design an optimal vaccine carrier, physicochemical properties of nanoparticles such as size, surface charge, functional material(s) and their composition, hydrophilicity/hydrophobicity and biodegradability have to be taken into consideration. Nanoparticles activate APC, which phagocytose them and travel from the application site, i.e. lung, skin, nose to the lymph nodes where immune reactions are initiated.

3.1.1 Particle size

3.1.1.1 Size-dependent uptake

Particle size is a critical parameter that influences uptake by phagocytic immune cells via either direct penetration through the cell membrane (i.e. energy-

independent mechanism) or by endocytosis (i.e. energy-dependent mechanism). Various types of endocytosis have been identified: virus sized particles (20 – 200 nm) are taken up by clathrin-dependent endocytosis (particles < 150 nm), through caveolae-mediated endocytosis (particles within 50 – 80 nm), or clathrin- and caveolae-independent pathways. Endocytosis of bacteria and larger sized particles (> 0.5 µm) occurs mainly *via* macropinocytosis and phagocytosis, effected only by macrophages and immature dendritic cells (Xiang *et al.*, 2006). It was verified *in vitro* that APC are able to ingest particles up to 5 µm (Tabata and Ikada, 1988). Although nanoparticles' size seems to deeply influence the uptake mechanisms inside the cells, many reported data are still controversial. Some studies have shown that the most efficient uptake is achieved for particles in the nanosize range (Joshi *et al.*, 2012, Yue *et al.*, 2010), other studies have demonstrated a similar or even preferred internalization of microparticles of a size of up to 5 µm (Chua *et al.*, 2011, Kobiasi *et al.*, 2012).

It has been suggested that the immune system has evolved to react to particles on the scale of viruses (< 0.5 µm) and bacteria (> 0.5 µm) (Fifis *et al.*, 2004). Uptake and immunostimulating mechanisms of nanoparticles and microparticles may be related to their similarity in size to these pathogens, and the immune system reacts to particles that fall within this size range (Chua *et al.*, 2011). *In vivo*, the particles are either phagocytosed by macrophages at the site of application and transported to the lymph nodes, or they diffuse to the lymph nodes by interstitial flow where they become phagocytosed by LN resident APC. Studies have shown that only nanoparticles below 100 nm were taken up into the lymphatic system directly and activated lymph node resident APC more efficiently than nanoparticles of larger sizes (Reddy *et al.*, 2006, Reddy *et al.*, 2007, Xie *et al.*, 2009). This size-dependency of absorption into the lymph nodes is likely to be related to the process of particle transport through the interstitium. Large particles (> 100 nm) will penetrate the interstitium less easily and will remain at the site of injection, targeting peripheral rather than LN resident APC (Oussoren and Storm, 2001). Manolova *et al.* reported on the impact of particle size on the specific targeting of distinct

dendritic cell (DC) populations. Whereas small nanoparticles (20 nm) were found in lymph node-resident APC, larger particles (500 – 2000 nm) were mainly associated with DC at the injection site. This size dependent manner of transport to the lymph nodes implicates a delayed appearance of nanoparticles > 500 nm in the lymph nodes after subcutaneous injection and is consistent with the active transport of these particles by skin resident dendritic cells. Small particles of 20 nm were detected in the lymph nodes within two hours after injection and taken up by lymph node resident APC, suggesting free drainage (Manolova *et al.*, 2008). This explains the findings in other studies, where a more rapid appearance of chitosan nanoparticles in the lymph nodes compared to chitosan microparticles after subcutaneous injection was observed (Chua *et al.*, 2011, Kobiasi *et al.*, 2012). From these findings it can be concluded that both nano- and microparticles are internalized by cells at comparable efficiency, but nanoparticles are transported to LN much faster.

These results, however, do not necessarily implicate an increased immunogenicity for nanoparticles. Besides investigation of particle uptake into the LN, their ability to elicit immune responses was examined. Both nano- and microparticles showed the ability to induce antigen-specific antibody responses. 40 nm polystyrene particles were found in more LN cells and induced higher levels of interferon gamma (IFN-γ) and antibody titers in mice than other smaller or larger sized beads (Fifis *et al.*, 2004). 1 µm particles elicited higher serum immunoglobulin G (IgG) levels than smaller particles (Gutierro *et al.*, 2002). Some studies revealed no significant differences in IgG production between different sized particles after parenteral administration (Chua *et al.*, 2011, Gutierro *et al.*, 2002, Nagamoto *et al.*, 2004). However, it has to be mentioned that nanoparticles up to 1 µm applied intranasally elicited a significantly higher production of mucosal IgA when compared to microparticles (Nagamoto *et al.*, 2004). Intranasal immunization with 200 nm nanoparticles enhanced CD4+ T-cell responses in the lungs compared to 30 nm nanoparticles (Stano *et al.*, 2012). Regarding the route of administration, following intranasal application, higher serum IgG2a/IgG1 ratios were found for 500 nm PLGA

nanoparticles than for 200 nm particles indicating a Th1 polarized response (Gutierro *et al.*, 2002).

In general, these findings suggest that local immunization may be preferably induced by nanoparticles at a size range between 200 and 1000 nm. However, there is not always a clear size-dependency with regard to particle uptake and immunogenicity. Extent and type of immune responses are presumably also associated with other physicochemical properties of the particles, the various materials used, the antigen type transferred, the route of administration as well as the vaccination regimen (Chua *et al.*, 2011, Kobiasi *et al.*, 2012).

3.1.1.2 Nanoparticle size and Th response

The concept of immune activation can be further extended by investigating the type of immune response induced. Particle size may influence Th cell differentiation, whereas Th1 cells are mainly developed following infections by intracellular bacteria and some viruses. Th1 cells produce cytokines that activate macrophages, are responsible for cell-mediated immunity and phagocyte-dependent protective responses. Th2 cells are predominant in responding to large extracellular pathogens and are responsible for antibody production and activation of eosinophils (Romagnani, 1999).

Seen the conflicting data available in literature, it is difficult to accurately predict particle size ranges that will induce a Th1 or a mixed Th1/Th2 immune response outcome (Oyewumi *et al.*, 2010). Some data are suggesting that nanoparticles promote cellular immune responses. For instance, co-delivery of the hepatitis B viral protein HBcAg and monophosphoryl lipid A (MPLA) in the copolymer poly(lactic-co-glycolic) acid (PLGA) nanoparticles of around 300 nm promoted antigen specific Th1 immune responses including IFN-γ production (Chong *et al.*, 2005). In a different study, mice vaccinated with 300 nm sized PLGA particles loaded with a model antigen (ovalbumin, OVA) generated the highest fraction of OVA specific cytotoxic T lymphocytes (CTL). They also induced more than a 50-fold increase in

the IgG2a/IgG1 ratio compared to microparticles, suggesting polarization towards a Th1-type immune response (Joshi *et al.*, 2012).

Unlike these observations, Henriksen-Lacey *et al.* described how DDA:TDB liposomes, regardless of their size, stimulated a characteristic Th1 immune response with production of IgG2 antibodies and IFN-γ (Henriksen-Lacey *et al.*, 2011). Other reports showed that 200 – 600 nm particles favored induction of Th1 responses associated with higher levels of IFN-γ production, whereas microparticles of 2 – 8 µm in size promoted interleukin-4 (IL-4, a cytokine that induces differentiation of naïve helper T-cells (Th0 cells) to Th2 cells) secretion inducing humoral immunity (Kanchan and Panda, 2007).

It has also been reported that as the particle size increases from the nanometer to the micrometer range, antibody titers increase, as well. Gutierro *et al.* showed that 1 µm particles elicited higher total serum IgG levels than nanoparticles. IgG2a/IgG1 ratios typical for a Th1 response, on the other hand, were similar for all particle sizes (Gutierro *et al.*, 2002). In addition, according to Katare *et al.*, microparticles in the size range of 2 – 8 µm elicited highest antibody titers whereas decreasing the particles size resulted in lower peak antibody titers (Katare *et al.*, 2005).

By contrast, subcutaneous application of several particle types present in the environment led to different results. Diesel exhaust particles below a size of 500 nm increased the production of IgE and IgG1 antibodies as indicators for Th2-like responses, while IgG2a titers remained low. Carbon black particles, on the other hand, induced a mixed Th1/Th2 response, and the larger silica particles (1 – 5 µm) induced a Th1 bias (van Zijverden and Granum, 2000). In addition, data from Samuelsen *et al.* applying polystyrene particles of different diameters intratracheally, as well as from Mann *et al.* using orally applied bile salt stabilised vesicles (named bilosomes), showed that larger particles (≥ 1 µm) generated stronger Th1 responses than nanoparticles (Mann *et al.*, 2009, Samuelsen *et al.*, 2009).

Not only nanoparticle size as a parameter has been determined to initiate immunostimulatory reactions through mediating release of pro-inflammatory

cytokines, also the surface charge and the material used for nanoparticles production itself, may modulate immune responses.

The studies described here are listed in Table 1 summarizing the effects of particle size on the resultant immune responses. Abbreviations used in this table are CBP: carbon black particle; DEP: diesel exhaust particle; i.d.: intradermal; i.m.: intramuscular; i.n.: intranasal; i.p.: intraperitoneal; i.t.: intratracheal; p.o.: per os; s.c.: subcutaneous; MP: microparticles; NP: nanoparticles; PLGA: Poly (lactic-co-glycolic) acid; PPS: Polypropylene sulfide; PS: Polystyrene; SIP: silica particles.

3.1.2 Charge

Charged nanoparticles have been shown to be more likely taken up by phagocytes than neutral particles of the same size. Polyethylene glycol (PEG) modified neutral nanoparticles had the lowest percentage of uptake when compared to particles with cationic or anionic surface charges (Dobrovolskaia *et al.*, 2008, Zahr *et al.*, 2006). Nanoparticles rendered negatively charged, e.g., by adsorption of mucus components after mucosal administration, again may interact to a much lesser extent with the negatively charged cell membrane surface. Consequently, it is more likely that positively charged particles are internalized by immune cells and induce mucosal immune responses, which was confirmed in a study showing a positive correlation between particle uptake and increasing zeta potential (Kwon *et al.*, 2005). Usually particles displaying a cationic surface charge are thought to be more toxic, since they can penetrate into cells more easily.

However, some studies revealed a higher uptake of negatively charged particles compared to cationic ones, which was explained by nonspecific binding and clustering of the particles at cationic cell membrane domains and subsequent endocytosis (Verma and Stellacci, 2010). Another possibility in this case would be that these positively charged particles become neutralized by adsorption of negatively charged components of the mucus to their surface and thus reduced in their targeting ability (Rajapaksa and Lo, 2010).

Table 1. List of representative studies demonstrating the effects of particle size on immune responses.

Materials	Particle size (nm)	Route	Parameters measured	Comments
PS (Manolova *et al*., 2008), Chitosan (Chua *et al*., 2011, Kobiasi *et al*., 2012)	20/500/1000 150/1300, 163/2100	s.c.	Particle trafficking	Faster appearance of NP in lymph nodes than MP.
PS (Fifis *et al*., 2004)	20/40/100/500/ 1000/2000	i.d.	IFN-γ, IgG	40 nm beads induced the highest levels of IFN-γ and IgG.
PLGA (Gutierro *et al*., 2002)	200/500/1000	s.c., p.o., i.n.	IgG	1 μm particles elicited higher total serum IgG levels than smaller particles for all tested routes.
Chitosan (Chua *et al*., 2011, Nagamoto *et al*., 2004)	163/2100 700/1300/3000	s.c., ip., i.n.	IgG, IgA	Similar ability in inducing IgG after parenteral, IgA levels higher for smaller particles after i.n. administration.
PPS sulfide (Stano *et al*., 2012), PLGA (Gutierro *et al*., 2002)	30/200, 200/500/1000	i.n.	IFN-γ, TNF-α, IL-2, IgG1, IgG2a	Higher Th1 responses were obtained with NP of 200 – 500 nm after i.n. administration.
PLGA (Chong *et al*., 2005)	633	s.c.	IFN- γ, IL-4, IgG	Only NP induced Th1 responses with IFN- γ production.
Liposomes (Henriksen-Lacey *et al*., 2011)	<200/700/1500/ 2000-3000	i.m.	IL-1β, IL-2, IL-6, IFN-γ, IgG1, IgG2a, IL-10, IL-5	High levels of IFN- γ and IgG2a and low levels of IL-5 and IL-10 were noted regardless of the size. Particles of ~700 - 1000 nm produced the highest levels of IFN-γ and IL-1β.
PLA (Kanchan and Panda, 2007)	200-600/2000-8000	i.p.	IFN-γ, IL-4	NP favored IFN- γ secretion, microparticles IL-4 secretion and higher IgG1/IgG2a ratios.
PLA (Katare *et al*., 2005)	<2000/ 2-8 μm/> 8 μm	i.m.	IgG	MP of 2 – 8 μm elicited highest antibody titers.
DEP, CBP, SIP (van Zijverden and Granum, 2000)	<500/1000-5000	s.c.	IgE, IgG1, IgG2a	NP induced a strong Th2 response, MP induced Th1.
PS (Samuelsen *et al*., 2009)	64/ 202/ 1053/ 4646	i.t.	TNF-α, IL-1β	MP induced higher cellular responses than NP.
Bilosomes (Mann *et al*., 2009)	250/980	p.o.	IFN-γ, IgG1, IgG2a	Large vesicles are better inducers of Th1 responses, assessed by IFN- γ and IgG2a production.

Not only surface charge, but also surface charge density is crucial for interactions between nanoparticle surface and proteins, i.e. opsonins. Nanoparticles have been shown to be covered with serum proteins in the blood stream shortly after injection. This process is called opsonization and enables macrophages to recognize and subsequently phagocytose foreign particles. How different coating patterns of particles may change the pathway of opsonization (classic, alternative, lectin-mediated) has recently been described by Moghimi *et al.* (Moghimi *et al*., 2011, Moghimi *et al*., 2012). Particles of neutral surface potential may have slower opsonization kinetics, a much lower opsonization rate and very possibly show a different opsonization pattern than charged particles (Nie, 2010). Such particles avoiding opsonization are used when a "stealth effect" for prolonged circulation in the blood stream and reduced immunogenicity is desired. Serum proteins bound to charged particles on the other hand have been shown to activate immune cell receptors upon unfolding of the protein (Deng *et al.*).

Last not least, surface charge may also have an effect on the intracellular transport and processing following phagocytosis. As shown for instance by Harush-Frenkel *et al*., anionic nanoparticles are targeted to the degradative lysosomal route, whereas cationic particles, bound to the transcytotic pathway, are not found in lysosomes suggesting a longer intracellular residence time (Harush-Frenkel *et al.*, 2008).

3.1.3 Immunogenicity of nanoparticle materials

Nanoparticles are classified as transport vehicles and their adjuvant activity is mainly related to enhanced delivery of antigens to APC or to the lymph nodes. However, mere transport function and interaction with target cells determining overall effect cannot be separated for these complex systems. Different types of bulk materials used for nanoparticle preparation may induce cytokine release, as has been shown in several studies (Plotkin *et al*., 2013). Materials used for nanoparticle preparation include (bio)polymers (e.g., PLGA and chitosan), lipids and metals, of which certain substances have been shown to be immunogenic and/or have adjuvant properties themselves.

3.1.3.1 Polymers

Response to polymeric particles is characterized by mild inflammation, differentiation of immune cells, and degradation of the particles. (Chakravarthi *et al.*, 2007). Biomaterials used in nanoparticulate vaccines have the potential to control the host response in order to reduce or enhance immune responses. Babensee *et al.* investigated the effect of biomaterial-induced DC phenotype changes and observed differential levels of DC maturation depending on the biomaterial used. PLGA or chitosan films induced maturation of DCs, as seen in augmentation of pro-inflammatory cytokine production and expression of co-stimulatory molecules, such as CD86, providing increased interaction with T-cells. By contrast, this effect was not observed when DCs were treated with alginate or agarose films, and was even inhibited by hyaluronic acid (Babensee, 2008, Rogers and Babensee, 2011, Yoshida *et al.*, 2007).

In addition, a different effect on TNF-α secretion by the shape of biomaterials was observed, showing stronger effects for particles than for films of the same material (Yoshida *et al.*, 2007). PLGA is considered to be safe and biocompatible at low immunogenicity, and is therefore approved by the U.S. Food and Drug Administration (FDA). However, several studies exhibited the induction of weak inflammatory responses to PLGA, which in vaccine carriers could lead to an adjuvant effect enhancing the overall immunogenicity of the vaccine. After tracheal application of PLGA, an acute inflammatory response was demonstrated by the increase of neutrophils when compared with animals treated with saline solution. By contrast, the inflammatory response seen in animals instilled with saline and polystyrene was similar. This suggests that polystyrene under these conditions behaves as an inert material and does not induce a sustained inflammatory response in the airways (Avital *et al.*, 2002, Springer *et al.*, 2005).

Fiore *et al.* suggested that the degradation of PLGA into acidic by-products could be responsible for its potential to induce inflammatory responses. Having assessed macrophage and lymphocyte numbers, PLGA treated lungs of mice displayed a slight

increase in inflammation. By contrast, upon intratracheal administration of polyketal particles, which degrade into neutral compounds, no significant inflammatory reactions were detected (Fiore *et al.*, 2010).

The adjuvant properties of chitosan, a biodegradable biopolymer, have also been subjected to investigations. Chitosan potently activated the NLRP3 (NOD-like receptor family, pyrin domain containing 3) inflammasome (a multiprotein oligomer that is a component of the innate immune system) in a phagocytosis-dependent manner. Chitosan is the deacetylated derivative of chitin, which was shown to be relatively inert, suggesting the influence of charge on the immunostimulatory properties of chitosan because of the presence of a secondary amino group (Bueter *et al.*, 2011). Also Tokura *et al.*, who studied the immunological aspects of chitin and chitin derivatives administered to animals, pointed out that chitosan itself, as an adjuvant, can induce polarized Th2 responses (Borchard *et al.*, 2012, Tokura *et al.*, 1999). Whether this activation is based on the interaction of chitosan with PRR in a lectin-like fashion is still under discussion.

3.1.3.2 Lipids

Lipid-based delivery systems have been subjected to investigation as vaccine adjuvants, as well. It is generally assumed that hydrophobic surfaces of particles enhance their phagocytosis (Thiele *et al.*, 2003). Among lipid-based vaccine deliver systems, such as solid lipid nanoparticles (SLN), liposomes, polymerized and non-polymerized liposomes, and new classes of lipid drug carriers such as ISCOMs (immune stimulating complexes) and multilamellar vesicles (Alonso-Romanowski *et al.*, 2003, Cai *et al.*, 2011, Moon *et al.*, 2011, Wilson *et al.*, 2012), oil-in-water emulsions are the most extensively studied particulate vaccine carriers. In Europe, nanoscale emulsion-based adjuvants are licensed for influenza vaccines, containing MF59 (Novartis; 1997) or AS03 (GlaxoSmithKline; 2009). AF03 (Sanofi Pasteur) is another emulsion containing squalene, a naturally occurring intermediate metabolite of cholesterol. AF03 has been tested in humans, but is not yet licensed for use in humans

(Montomoli *et al.*, 2011, Salvador *et al.*, 2011). The potential to improve vaccine performance has been shown, yet the mechanism of adjuvanticity of these oil-in-water emulsions remains unknown or undisclosed. However, as described above, several studies suggest that these nanoemulsions do not act only as antigen delivery systems, but also as immune modulators.

In a study on the influence of squalene-based nanoemulsions on the activation of the innate immune system, it was hypothesized that changes in lipid metabolism and innate immunity are closely linked. Uptake of squalene-based nanoemulsions induced accumulation of neutral lipids that have been shown to have pro-inflammatory properties (Kalvodova, 2010, Lorentzen, 1999, Prieur *et al.*, 2010). Other findings show that the non-ionic surfactant polysorbate 80, used in the above mentioned emulsions, may have an immunomodulatory effect, inducing Th2 responses (Kozutsumi *et al.*, 2006). The systemic expression of IL-5 is in agreement with the Th2 immune response elicited by the polysorbate 80 containing nanoemulsion MF59 (Mosca *et al.*, 2008). The contribution of vitamin E to the overall adjuvanticity in AS03 was investigated by Morel *et al.*, where higher antibody responses with the inclusion of α-tocopherol than with the plain squalene-in-water emulsion were observed (Morel *et al.*, 2011).

3.1.3.3 Inorganic materials

As an alternative to organic compounds, inorganic materials such as metals and metal oxides are also known to form nanoparticles. Due to their rigid non-deformable shape and much smaller size, they exhibit many distinct biological properties compared to polymeric or lipid nanoparticles (Huang *et al.*, 2010). Being non-biodegradable, these nanoparticles remain at the site of injection for extended periods of time, resulting in long-lasting presentation and thus enhanced immunogenicity (Maquieira *et al.*, 2012). Among the most widely used metal nanoparticles, gold, silver, or copper, and as magnetic metals iron or cobalt are taken into consideration for drug delivery, however, few attempts have been made to develop solid inorganic nanoparticles as vaccine platforms (Bhattacharyya *et al.*, 2011, Pusic *et al.*, 2012).

The main advantage of this type of nanoparticles is that they can be manufactured in fine-tunable sizes between 5 and 100 nm. In addition, they show a high affinity for sulfhydryl groups, which facilitates the binding of various biomolecules through chemisorption of thiol residues onto the metal nanoparticles (Algar *et al.*, 2011, Cruz *et al.*, 2012). Gold, silver and copper are known for being antimicrobial materials, probably due to their ability to react with the –SH groups of enzymes and hence inactivating these proteins (Bhattacharya and Mukherjee, 2008, Yoon *et al.*, 2007). As an example, inhibitory effects on HIV-1 infection in CD4+MT-2 cells (human T-cell leukemia HTLV-1 virus carrier cell line) and cMAGI HIV-1 reporter cells (HeLa cell clone expressing human CD4 and HIV-*long terminal repeat*-coupled genes) due to the interaction of silver nanoparticles with the virus was reported by Elechiguerra *et al*. (Elechiguerra *et al.*, 2005).

Furthermore, the inflammatory potential of metals could be of interest in vaccine development. Goebel *et al.* showed that the T cell response in mice treated with gold(I) compounds for 12 weeks is directed against the oxidized gold(III), which is a metabolite generated *in vivo* by macrophages (Goebel *et al.*, 1995). In another study the inflammatory potential of colloidal silver on macrophages was evaluated through assessing the release of IL-8, cell viability, and induction of oxidative stress. While reactive oxygen species (ROS) are generated as part of the normal oxidative metabolism, their overproduction can lead to cell death. Early stage oxidative stress, on the contrary, can stimulate inflammatory responses, and the generated ROS were found to trigger the release of IL-8 in macrophages (Park *et al.*, 2011). While different types of metallic nanoparticles without any specific antigen loading reportedly exert antimicrobial activity, other studies revealed a compromise of innate immune response and clearance of bacterial pathogens after exposure. Shedova *et al*. suggested that elimination of microbes depends to a larger extent on nitric oxide production than ROS from the oxidative burst (Nathan and Hibbs Jr, 1991, Shvedova *et al.*, 2008). This could explain the controversial findings of decreased pulmonary bacterial clearance in mice

after exposure to copper nanoparticles, despite induction of robust inflammatory responses (Kim *et al*., 2011).

Also metal oxide nanoparticles and their soluble ions were investigated with regard to their immunostimulatory/inflammatory effects. *In vitro*, nanoparticles made of nickel, copper, and zinc oxide, respectively, all showed toxic effects, but only zinc and copper oxide nanoparticles induced IL-8 production and activation of transcription factors. Aqueous extracts of zinc and copper oxide nanoparticles showed similar profiles of cytotoxicity and inflammatory effects, whereas nickel ions did not induce any cytotoxicity or immune responses. The inflammatory response assessed in rats given by nanoparticles was also different to the aqueous extracts, with zinc and copper oxide nanoparticles leading to the recruitment of eosinophils, but not their soluble ions (Cho *et al.*, 2012).

3.2 Immune receptor targeting and antigen delivery

Currently, intense research efforts are aimed at the development of novel formulations and delivery systems for vaccines. By the use of nanoparticles, antigens are expected to be adequately presented to the immune system to elicit immune responses appropriate for sufficient protection against infectious diseases. Ideally, the nanoparticulate vaccine carrier system should have sufficient antigen- and adjuvant-loading capacity, through either incorporation or surface adsorption.

Formulation strategies can facilitate the capture by and the entry of the antigen into APC. T cell antigens, in the form of peptides, proteins, plasmid DNA or RNA formulated into nanoparticles appear to increase CTL responses *in vivo*. Such particulate formulations significantly increase efficiency as compared to the soluble antigen alone, as they are in general readily recognized as antigenic and ingested by immune cells, which subsequently leads to antigen processing and presentation to other cells of the immune system. (Moingeon *et al*., 2002). Ligands of APC-specific pattern recognition receptors, such as Toll-like receptors (TLR), can be grafted onto the surface of particle-

based vaccines to increase specific delivery to immune cells (Heuking and Borchard, 2012).

Application of vaccines in particulate form not only allows moving the antigen within the tissue to individual cells, it also facilitates its penetration through the cell membrane. This transfection process is a major requirement for making use of intracellular mechanisms, such as signaling pathways and antigen processing, to activate the immune system. Many biomolecules, used as antigens for vaccines, are not able to diffuse within tissues and through the plasma membrane, due to their size and other physicochemical properties. Particle-based strategies to overcome this problem have been developed for genetic vaccination relying on chemical materials used as carriers and physical treatment. In the “gene gun technique” DNA is coated on gold particles, energy is transferred to the DNA carriers to accelerate and propel the particles into the cells (Villemejane and Mir, 2009). This method is limited to low-depth penetration of particles in tissues, but is sufficient for skin DNA vaccination (Luz Garcia-Hernandez *et al.*, 2008). Magnetic nanoparticles have attracted attention because of their potential use for direct targeting to diseased tissues and organs by applying an external magnetic field. “Magnetofection” describes a technique of gene transfection involving naked plasmid DNA or DNA vectors associated to the surface of magnetic nanoparticles. Superparamagnetic iron oxide nanoparticles (SPIONs) are applied for magnetofection by delivering genes to the target cells, hence increasing their local concentration (Al-Deen *et al.*, 2011, Vasir and Labhasetwar, 2007). Application of an external alternating magnetic field leads to the production of energy, in the form of heat. Hyperthermia has been demonstrated to stimulate the innate immune response through the release of heat shock proteins that activate neighboring immune cells (Baronzio *et al.*, 2006, Colombo *et al.*, 2012). As such, SPIONs may have adjuvant properties activating the immune system in a non-specific manner. These two methods are still under investigation. Although a few clinical trials have already been performed or are in progress, long-term safety and potential risks have not been sufficiently

evaluated (Villemejane and Mir, 2009). Another approach is impalefection, by functionalizing nanoscale carbon fibers with DNA to impale cells. It is a useful tool for exploring gene delivery in vitro, but has yet to be used in the therapeutic field (Pearce *et al.*, 2013).

The types of effective immune responses against infectious diseases depend on the localization of the pathogens after infection. Generally, extracellular pathogens are combated by antibodies mediated by humoral immune responses, whereas protection against intracellular pathogens depends on cell-mediated immunity via CD4+ type 1 helper (Th1) cells. In addition, CD8+ CTL play an important role in the protection against these pathogens by directly killing infected cells (Nagata and Koide, 2010). Antigen recognition by T lymphocytes depends on the ability of APC to process protein antigen into peptides and to present them via major histocompatibility complex (MHC) molecules at the cell surface. The MHC I presentation pathway allows CD8+ T cells to identify and eliminate cells infected by intracellular pathogens. By contrast, MHC II and CD1 molecules present peptides derived from captured exogenous antigens to CD4+ T cells and natural killer (NK) cells (Makidon *et al.*, 2008) (Figure 1).

3.3 Current nanoparticle vaccines on the market and in clinical studies

Nanotechnology is enabling novel vaccines to enter clinical trials, which often show superiority of the particulate systems over traditional vaccine types. We will discuss here several examples of nanoparticle-based vaccines.

On the basis of antigen presentation by dendritic cells and innate immune system stimulation via Toll-like receptors, a vaccine against melanoma was designed. Melanoma-specific peptide Melan-A/Mart-1 was linked to virus-like nanoparticles (VLPs) loaded with CpG oligonucleotides as activators of Toll-like receptor 9 located in the endosomal compartment of target cells (Speiser *et al.*, 2005). Already vaccination of HLA-A2 transgenic mice in pre-clinical studies showed strong Melan-A-specific CD8 T cell responses. A phase I/II study in stage II-IV melanoma patients confirmed good

tolerability of the vaccine and *ex vivo* T cell responses. Increased activated Melan-A-specific CD8 T cell populations were detected directly *ex vivo* as well as cytokine production of INF-γ, TNF-α, and IL-2 and LAMP-1 expression by vaccine induced T cells. Furthermore, a central memory phenotype of those specific T cells was frequently observed and an enhancement of T cell responses was achieved by subsequent vaccination with the peptide emulsified in incomplete Freund's adjuvant (Speiser *et al.*, 2010). Other vaccines using nanotechnology based on VLPs have already been licensed for the prevention of cervical and anogenital infections, i.e. by GlaxoSmithKline (Engerix® and Cervarix®), and Merck and Co. (Recombivax HB and Gardasil®) (Buonaguro and Buonaguro, 2013). These products are non-infectious viral subunit vaccines with proteins of the respective pathogens assembled in nanosized VLPs, structures resembling the virus itself and thus recognized as antigens, but lacking the genetic repertoire necessary for replication.

A novel liposomal influenza subunit vaccine is currently under clinical investigation. It consists of liposomes containing the viral surface proteins hemagglutinin (HA) and neuraminidase (NA) derived from various influenza strains (Babai *et al.*, 2001). An IL-2 supplemented liposomal formulation injected intramuscularly has proven to be both safe and effective in inducing strong anti-HA and anti-NA antibody responses in mice and humans (Ben-Yehuda *et al.*, 2003).

DNA vaccines with one specific or even several pathogenic antigenic epitopes encoded by the plasmid are known to drive cellular and humoral immune responses at least in the animal model. To increase transfection efficiency, and to enhance and direct immune responses to DNA vaccines, particle based delivery systems have been explored (Bivas-Benita *et al.*, 2009, Bivas-Benita *et al.*, 2004). FDA-controlled Phase I studies to assess safety and immunogenicity of particle-mediated DNA vaccines against influenza and hepatitis B viruses have been completed only for microparticles. These studies were a part of the clinical development of a particle mediated epidermal delivery (PMED) DNA vaccine or "gene gun" based on a dry powder formulation with

DNA plasmid adsorbed onto microscopic gold particles (PowderMed, 2007, PowderMed, 2008). Particle-mediated DNA administration permits the use of small quantities of DNA and application *via* the skin as an immunological active tissue increases the efficacy of the vaccine. Hepatitis B virus (HBV) specific protective antibody responses of at least 10 mIU/ml and antigen specific CD8+ cells were detected. Hepatitis B surface antigen specific IFN-γ secreting Th cells were measured in the majority of individuals treated, indicating Th1-biased responses. Current data demonstrate that particle-mediated DNA administration with this needle-free method of administration was safe and well-tolerated. Since Th1 and CD8+ T cell responses are associated with resolution of HBV and other chronic viral infections, the results reported suggest a potential for particle-mediated DNA vaccine delivery (Roy *et al.*, 2000).

Another topical vaccine, DermaVir Patch for skin delivery of DNA vaccine has already entered clinical trials for the treatment of HIV infections (Genetic Immunity, 2013). Treatment of HIV-1/AIDS requires a vaccine to induce robust and long-lasting HIV-1 specific T cells to control viral replication. A plasmid DNA encoding the majority of HIV-1 genes has been chemically formulated into polyethylenimine mannose (PEIm), a cationic polymer that forms nanoparticles with the negatively charged plasmid through condensation. The mannose moiety targets the vaccine to receptors on the surface of APC (Lisziewicz *et al.*, 2007). Based on the potent induction of Gag, Tat and Rev antigen-specific memory T cells, it is assumed that DermaVir boosts T cell responses specific to all the 15 HIV antigenic epitopes expressed by a single plasmid applied. Furthermore, a dose-dependent expansion of HIV-specific memory T cells with high proliferation capacity was detected (Lisziewicz *et al.*, 2012).

Just recently a phase II clinical trial evaluated the safety and immunogenicity of a respiratory syncytial virus fusion (RSV F) protein vaccine, formulated as nanoparticles. The protein was extracted and purified from insect cell membranes and assembled into 40 nm nanoparticles composed of multiple RSV F oligomers arranged in the form of rosettes (Smith *et al.*, 2012). The primary immune response measured confirmed the

vaccine to be a potent antigen eliciting immune responses at levels that would be predicted to protect infants through maternal immunization (Novavax, 2013). A study using a polypeptide vaccine against malaria that self-assembles into spherical nanoparticles, displaying repetitive epitopes of the *Plasmodium falciparum* circumsporozoite protein, showed promising results in pre-clinical testing. The outcome was high-titer, long-lasting protective antibody and long-lived central memory CD8+ T-cells and could provide sterile protection against a lethal challenge of the transgenic parasites in mice (Kaba *et al*., 2012).

From a soluble type of chitosan, Viscosan, a hydrogel was formed, which was further mechanically processed into gel particles. This so- called ViscoGel was mixed with a commercial vaccine against *Haemophilus influenza* type b (Act-HIB). ViscoGel-Act-HIB with a tenth of the vaccine dose is as efficient in eliciting a humoral response in mice as the high dose vaccine alone (Neimert-Andersson *et al.*, 2011).

Mixing saponin, cholesterol and phospholipid under controlled conditions, 40 nm spherical negatively charged immune stimulating complexes (ISCOMs) of ISCOMATRIX® adjuvant are formed. A range of ISCOMATRIX® vaccines have been tested in clinical trials, generating both antibody and T-cell responses. The adjuvant has been combined with influenza viral proteins or recombinant antigens for two cancer/neoplasia vaccines and one Hepatitis C (HCV) vaccine to be tested in humans. Higher and faster antibody responses compared to conventional influenza vaccines and virus-specific CTL responses were observed. Furthermore, strong virus-specific humoral and cellular immune responses were detected in vaccinated subjects of the two types of human papillomavirus (HPV)- and of the HCV core ISCOMATRIX® vaccines (Pearse and Drane, 2005).

4. Conclusion

Prevention is better than treatment. Preventing a pathogen from gaining access to the body is better than to fight it off after infection. Antibiotics are failing, occurrence of multidrug resistance is on the rise, and new pathogens are emerging: we are in dire need of novel vaccines that elicit long-lasting and protective immune responses. By our growing understanding of how adjuvants may work, the "dirty little secrets" of vaccinologists may be no more, and through nanotechnology we may have the opportunity to design vaccine delivery systems as Nature intended them to be. In practical terms, which antigens would be good candidates to be used in a novel (nanoparticulate) formulation, possibly using novel adjuvants? Using known antigens, for which successful vaccines already exist, might not be a good choice: the danger of non-acceptance by regulatory authorities and/or the public may be to high. Therefore, one would choose novel antigens that are being identified through sequencing of pathogen genomes, or a combination thereof. The concept of "new formulations for new vaccines" might rightfully apply, as tolerance towards undesired side effects is certainly higher for first-in-man vaccines than for new formulations of vaccines that have been tried and tested. The use of adjuvants, on the other hand, is fraught with their sometimes difficult handling, the skepticism of regulatory authorities towards new, not well-defined excipients/active principles, and the ongoing discussion in a public that remains often closed to scientific argumentation. The way out of this dilemma would in our opinion be to enhance the immunogenicity of protein- and peptide-vaccines themselves, to use particulate systems to better target and present the antigen to the immune system, and to finally use well-characterized small molecular weight entities of a defined mechanism of action and known toxicity. These avenues are followed in modern vaccine development, and will result in highly effective vaccines against old and new threats to our health. Nanotechnology is playing a prominent part in this endeavor.

References

Al-Deen, F.N., Ho, J., Selomulya, C., Ma, C., and Coppel, R. (2011). Superparamagnetic Nanoparticles for Effective Delivery of Malaria DNA Vaccine*, Langmuir,* 27, pp. 3703-3712.

Algar, W.R., Prasuhn, D.E., Stewart, M.H., Jennings, T.L., Blanco-Canosa, J.B., Dawson, P.E., and Medintz, I.L. (2011). The Controlled Display of Biomolecules on Nanoparticles: A Challenge Suited to Bioorthogonal Chemistry*, Bioconjugate Chemistry,* 22, pp. 825-858.

Alonso-Romanowski, S., Chiaramoni, N.S., Lioy, V.S., Gargini, R.A., Viera, L.I., and Taira, M.C. (2003). Characterization of diacetylenic liposomes as carriers for oral vaccines*, Chemistry and Physics of Lipids,* 122, pp. 191-203.

Avital, A., Shapiro, E., Doviner, V., Sherman, Y., Margel, S., Tsuberi, M., and Springer, C. (2002). Polystyrene Microspheres as a Specific Marker for the Diagnosis of Aspiration in Hamsters*, American Journal of Respiratory Cell and Molecular Biology,* 27, pp. 511-514.

Babai, I., Barenholz, Y., Zakay-Rones, Z., Greenbaum, E., Samira, S., Hayon, I., Rochman, M., and Kedar, E. (2001). A novel liposomal influenza vaccine (INFLUSOME-VAC) containing hemagglutinin–neuraminidase and IL-2 or GM-CSF induces protective anti-neuraminidase antibodies cross-reacting with a wide spectrum of influenza A viral strains*, Vaccine,* 20, pp. 505-515.

Babensee, J.E. (2008). Interaction of dendritic cells with biomaterials*, Seminars in Immunology,* 20, pp. 101-108.

Baronzio, G., Gramaglia, A., and Fiorentini, G. (2006). Hyperthermia and Immunity. A Brief Overview*, In Vivo,* 20, pp. 689-695.

Ben-Yehuda, A., Joseph, A., Zeira, E., Even-Chen, S., Louria-Hayon, I., Babai, I., Zakay-Rones, Z., Greenbaum, E., Barenholz, Y., and Kedar, E. (2003). Immunogenicity and safety of a novel liposomal influenza subunit vaccine (INFLUSOME-VAC) in young adults*, Journal of Medical Virology,* 69, pp. 560-567.

Bhattacharya, R. and Mukherjee, P. (2008). Biological properties of “naked” metal nanoparticles*, Advanced Drug Delivery Reviews,* 60, pp. 1289-1306.

Bhattacharyya, S., Kudgus, R., Bhattacharya, R., and Mukherjee, P. (2011). Inorganic Nanoparticles in Cancer Therapy*, Pharmaceutical Research,* 28, pp. 237-259.

Bivas-Benita, M., Lin, M.Y., Bal, S.M., van Meijgaarden, K.E., Franken, K.L.M.C., Friggen, A.H., Junginger, H.E., Borchard, G., Klein, M.R., and Ottenhoff, T.H.M. (2009). Pulmonary delivery of DNA encoding Mycobacterium tuberculosis latency antigen Rv1733c associated to PLGA–PEI nanoparticles enhances T cell responses in a DNA prime/protein boost vaccination regimen in mice*, Vaccine,* 27, pp. 4010-4017.

Bivas-Benita, M., van Meijgaarden, K.E., Franken, K.L.M.C., Junginger, H.E., Borchard, G., Ottenhoff, T.H.M., and Geluk, A. (2004). Pulmonary delivery of chitosan-DNA nanoparticles enhances the immunogenicity of a DNA vaccine encoding HLA-A*0201-restricted T-cell epitopes of Mycobacterium tuberculosis*, Vaccine,* 22, pp. 1609-1615.

Borchard, G., Esmaeili, F., and Heuking, S. (2012) *Chitosan-Based Systems for Biopharmaceuticals* eds. B. Sarmento and Neves, J.D., Chapter 12 "Chitosan-Based Delivery Systems for Mucosal Vaccination", (Wiley, UK) pp. 211-224.

Bueter, C.L., Lee, C.K., Rathinam, V.A.K., Healy, G.J., Taron, C.H., Specht, C.A., and Levitz, S.M. (2011). Chitosan but Not Chitin Activates the Inflammasome by a Mechanism Dependent upon Phagocytosis*, Journal of Biological Chemistry,* 286, pp. 35447-35455.

Buonaguro, F. and Buonaguro, L. (2013). The application of virus-like particles to human diseases*, Expert Review of Vaccines,* 12, pp. 99-99.

Cai, S., Yang, Q., Bagby, T.R., and Forrest, M.L. (2011). Lymphatic drug delivery using engineered liposomes and solid lipid nanoparticles*, Advanced Drug Delivery Reviews,* 63, pp. 901-908.

Chakravarthi, S.S., Robinson, D.H., and De, S. (2007) *Nanoparticulate Drug Delivery Systems* 166, eds. D. Thassu, Deleers, M., and Pathak, Y., Chapter 3 "Nanoparticles Prepared Using Natural and Synthetic Polymers", (CRC Press, USA) pp. 51-60.

Cho, W.-S., Duffin, R., Poland, C.A., Duschl, A., Oostingh, G.J., MacNee, W., Bradley, M., Megson, I.L., and Donaldson, K. (2012). Differential pro-inflammatory effects of metal oxide nanoparticles and their soluble ions in vitro and in vivo; zinc and copper nanoparticles, but not their ions, recruit eosinophils to the lungs*, Nanotoxicology,* 6, pp. 22-35.

Chong, C.S.W., Cao, M., Wong, W.W., Fischer, K.P., Addison, W.R., Kwon, G.S., Tyrrell, D.L., and Samuel, J. (2005). Enhancement of T helper type 1 immune responses against hepatitis B virus core antigen by PLGA nanoparticle vaccine delivery*, Journal of Controlled Release,* 102, pp. 85-99.

Chua, B.Y., Al Kobaisi, M., Zeng, W., Mainwaring, D., and Jackson, D.C. (2011). Chitosan Microparticles and Nanoparticles as Biocompatible Delivery Vehicles for Peptide and Protein-Based Immunocontraceptive Vaccines*, Molecular Pharmaceutics,* 9, pp. 81-90.

Colombo, M., Carregal-Romero, S., Casula, M.F., Gutierrez, L., Morales, M.P., Bohm, I.B., Heverhagen, J.T., Prosperi, D., and Parak, W.J. (2012). Biological applications of magnetic nanoparticles*, Chemical Society Reviews,* 41, pp. 4306-4334.

Cruz, L.J., Tacken, P.J., Rueda, F., Domingo, J.C., Albericio, F., and Figdor, C.G. (2012). Targeting Nanoparticles to Dendritic Cells for Immunotherapy*, Methods in Enzymology,* 509, pp. 143-163.

Deng, Z.J., Liang, M., Toth, I., Monteiro, M., and Minchin, R.F. (2012). Plasma protein binding of positively and negatively charged polymer-coated gold nanoparticles elicits different biological responses*, Nanotoxicology,* 7, pp. 314-322.

Dobrovolskaia, M.A., Aggarwal, P., Hall, J.B., and McNeil, S.E. (2008). Preclinical Studies To Understand Nanoparticle Interaction with the Immune System and Its Potential Effects on Nanoparticle Biodistribution*, Molecular Pharmaceutics,* 5, pp. 487-495.

Doroud, D. and Rafati, S. (2011). Leishmaniasis: focus on the design of nanoparticulate vaccine delivery systems*, Expert Review of Vaccines,* 11, pp. 69-86.

Elechiguerra, J., Burt, J., Morones, J., Camacho-Bragado, A., Gao, X., Lara, H., and Yacaman, M. (2005). Interaction of silver nanoparticles with HIV-1*, Journal of Nanobiotechnology,* 3, pp. 6.

Fifis, T., Gamvrellis, A., Crimeen-Irwin, B., Pietersz, G.A., Li, J., Mottram, P.L., McKenzie, I.F.C., and Plebanski, M. (2004). Size-Dependent Immunogenicity: Therapeutic and Protective Properties of Nano-Vaccines against Tumors*, The Journal of Immunology,* 173, pp. 3148-3154.

Fiore, V.F., Lofton, M.C., Roser-Page, S., Yang, S.C., Roman, J., Murthy, N., and Barker, T.H. (2010). Polyketal microparticles for therapeutic delivery to the lung*, Biomaterials,* 31, pp. 810-817.

Genetic Immunity (2013), Single DermaVir Immunization in HIV-1 Infected Patients on HAART (GIHU004), (NCT00712530), 2013 May 6, from http://clinicaltrials.gov.

Goebel, C., Kubickamuranyi, M., Tonn, T., Gonzalez, J., and Gleichmann, E. (1995). Phagocytes render chemicals immunogenic: oxidation of gold(I) to the T cell-sensitizing gold(III) metabolite generated by mononuclear phagocytes.*, Archives of Toxicology,* 69, pp. 450-459.

Gutierro, I., Hernández, R.M., Igartua, M., Gascón, A.R., and Pedraz, J.L. (2002). Size dependent immune response after subcutaneous, oral and intranasal administration of BSA loaded nanospheres*, Vaccine,* 21, pp. 67-77.

Harush-Frenkel, O., Rozentur, E., Benita, S., and Altschuler, Y. (2008). Surface Charge of Nanoparticles Determines Their Endocytic and Transcytotic Pathway in Polarized MDCK Cells*, Biomacromolecules,* 9, pp. 435-443.

Henriksen-Lacey, M., Devitt, A., and Perrie, Y. (2011). The vesicle size of DDA:TDB liposomal adjuvants plays a role in the cell-mediated immune response but has no significant effect on antibody production*, Journal of Controlled Release,* 154, pp. 131-137.

Heuking, S. and Borchard, G. (2012). Toll-like receptor-7 agonist decoration enhances the adjuvanticity of chitosan–DNA nanoparticles*, Journal of Pharmaceutical Sciences,* 101, pp. 1166-1177.

Huang, Y., Yu, F., Park, Y.-S., Wang, J., Shin, M.-C., Chung, H.S., and Yang, V.C. (2010). Co-administration of protein drugs with gold nanoparticles to enable percutaneous delivery*, Biomaterials,* 31, pp. 9086-9091.

Joshi, V., Geary, S., and Salem, A. (2013). Biodegradable Particles as Vaccine Delivery Systems: Size Matters*, The AAPS Journal,* 15, pp. 85-94.

Kaba, S.A., McCoy, M.E., Doll, T.A.P.F., Brando, C., Guo, Q., Dasgupta, D., Yang, Y., Mittelholzer, C., Spaccapelo, R., Crisanti, A., Burkhard, P., and Lanar, D.E. (2012). Protective antibody and CD8+ T-cell responses to the Plasmodium falciparum circumsporozoite protein induced by a nanoparticle vaccine*, PLoS ONE,* 7, pp. 1-11.

Kalvodova, L. (2010). Squalene-based oil-in-water emulsion adjuvants perturb metabolism of neutral lipids and enhance lipid droplet formation*, Biochemical and Biophysical Research Communications,* 393, pp. 350-355.

Kanchan, V. and Panda, A.K. (2007). Interactions of antigen-loaded polylactide particles with macrophages and their correlation with the immune response*, Biomaterials,* 28, pp. 5344-5357.

Katare, Y.K., Muthukumaran, T., and Panda, A.K. (2005). Influence of particle size, antigen load, dose and additional adjuvant on the immune response from antigen loaded PLA microparticles*, International Journal of Pharmaceutics,* 301, pp. 149-160.

Kim, J.S., Adamcakova-Dodd, A., O'Shaughnessy, P., Grassian, V., and Thorne, P. (2011). Effects of copper nanoparticle exposure on host defense in a murine pulmonary infection model*, Particle and Fibre Toxicology,* 8, pp. 29.

Kobiasi, M.A., Chua, B.Y., Tonkin, D., Jackson, D.C., and Mainwaring, D.E. (2012). Control of size dispersity of chitosan biopolymer microparticles and nanoparticles to influence vaccine trafficking and cell uptake*, Journal of Biomedical Materials Research Part A,* 100A, pp. 1859-1867.

Kozutsumi, D., Tsunematsu, M., Yamaji, T., Murakami, R., Yokoyama, M., and Kino, K. (2006). PS80 interferes with the antiallergic effect of Cry-consensus peptide, a novel recombinant peptide for immunotherapy of Japanese cedar pollinosis, at very low concentration through modulation of Th1/Th2 balance*, Immunology,* 118, pp. 392-401.

Kumar, V., Abbas, A.K., Fausto, N., and Mitchell, R. (2012) *Robbins Basic Pathology,* 9th Ed. (Elsevier Saunders, USA).

Kwon, Y.J., Standley, S.M., Goh, S.L., and Fréchet, J.M.J. (2005). Enhanced antigen presentation and immunostimulation of dendritic cells using acid-degradable cationic nanoparticles*, Journal of Controlled Release,* 105, pp. 199-212.

Lisziewicz, J., Bakare, N., Calarota, S.A., Bánhegyi, D., Szlávik, J., Újhelyi, E., Tőke, E.R., Molnár, L., Lisziewicz, Z., Autran, B., and Lori, F. (2012). Single DermaVir Immunization: Dose-Dependent Expansion of Precursor/Memory T Cells against All HIV Antigens in HIV-1 Infected Individuals*, PLoS ONE,* 7, e35416. DOI: 10.1371/journal.pone.0035416.

Lisziewicz, J., Calarota, S.A., and Lori, F. (2007). The potential of topical DNA vaccines adjuvanted by cytokines*, Expert Opinion on Biological Therapy,* 7, pp. 1563-1574.

Lorentzen (1999). Identification of Arthritogenic Adjuvants of Self and Foreign Origin*, Scandinavian Journal of Immunology,* 49, pp. 45-50.

Luz Garcia-Hernandez, M., Gray, A., Hubby, B., Klinger, O.J., and Kast, W.M. (2008). Prostate stem cell antigen vaccination induces a long-term protective immune response against prostate cancer in the absence of autoimmunity*, Cancer Research,* 68, pp. 861-869.

Mann, J.F.S., Shakir, E., Carter, K.C., Mullen, A.B., Alexander, J., and Ferro, V.A. (2009). Lipid vesicle size of an oral influenza vaccine delivery vehicle influences the Th1/Th2 bias in the immune response and protection against infection*, Vaccine,* 27, pp. 3643-3649.

Manolova, V., Flace, A., Bauer, M., Schwarz, K., Saudan, P., and Bachmann, M.F. (2008). Nanoparticles target distinct dendritic cell populations according to their size*, European Journal of Immunology,* 38, pp. 1404-1413.

Maquieira, Á., Brun, E.M., Garcés-García, M., and Puchades, R. (2012). Aluminum Oxide Nanoparticles as Carriers and Adjuvants for Eliciting Antibodies from Non-immunogenic Haptens*, Analytical Chemistry,* 84, pp. 9340-9348.

Moghimi, S.M., Andersen, A.J., Ahmadvand, D., Wibroe, P.P., Andresen, T.L., and Hunter, A.C. (2011). Material properties in complement activation*, Advanced Drug Delivery Reviews,* 63, pp. 1000-1007.

Moghimi, S.M., Hunter, A.C., and Andresen, T.L. (2012). Factors Controlling Nanoparticle Pharmacokinetics: An Integrated Analysis and Perspective*, Annual Review of Pharmacology and Toxicology,* 52, pp. 481-503.

Moingeon, P., de Taisne, C., and Almond, J. (2002). Delivery technologies for human vaccines*, British Medical Bulletin,* 62, pp. 29-44.

Montomoli, E., Piccirella, S., Khadang, B., Mennitto, E., Camerini, R., and De Rosa, A. (2011). Current adjuvants and new perspectives in vaccine formulation*, Expert Review of Vaccines,* 10, pp. 1053-1061.

Moon, J.J., Suh, H., Bershteyn, A., Stephan, M.T., Liu, H., Huang, B., Sohail, M., Luo, S., Ho Um, S., Khant, H., Goodwin, J.T., Ramos, J., Chiu, W., and Irvine, D.J. (2011). Interbilayer-crosslinked multilamellar vesicles as synthetic vaccines for potent humoral and cellular immune responses*, Nature Materials,* 10, pp. 243-251.

Morel, S., Didierlaurent, A., Bourguignon, P., Delhaye, S., Baras, B., Jacob, V., Planty, C., Elouahabi, A., Harvengt, P., Carlsen, H., Kielland, A., Chomez, P., Garçon, N., and Van Mechelen, M. (2011). Adjuvant System AS03 containing α-tocopherol modulates innate immune response and leads to improved adaptive immunity*, Vaccine,* 29, pp. 2461-2473.

Mosca, F., Tritto, E., Muzzi, A., Monaci, E., Bagnoli, F., Iavarone, C., O'Hagan, D., Rappuoli, R., and De Gregorio, E. (2008). Molecular and cellular signatures of human vaccine adjuvants*, Proceedings of the National Academy of Sciences,* 105, pp. 10501-10506.

Nagamoto, T., Hattori, Y., Takayama, K., and Maitani, Y. (2004). Novel Chitosan Particles and Chitosan-Coated Emulsions Inducing Immune Response via Intranasal Vaccine Delivery*, Pharmaceutical Research,* 21, pp. 671-674.

Nagata, T. and Koide, Y. (2010). Induction of specific CD8+ T cells against intracellular bacteria by CD8+ T-cell-oriented immunization approaches*, Journal of Biomedicine and Biotechnology,* 2010, 764542, DOI: 10.1155/2010/764542.

Nathan, C.F. and Hibbs Jr, J.B. (1991). Role of nitric oxide synthesis in macrophage antimicrobial activity*, Current Opinion in Immunology,* 3, pp. 65-70.

Neimert-Andersson, T., Hällgren, A.-C., Andersson, M., Langebäck, J., Zettergren, L., Nilsen-Nygaard, J., Draget, K.I., van Hage, M., Lindberg, A., Gafvelin, G., and Grönlund, H. (2011). Improved immune responses in mice using the novel chitosan adjuvant ViscoGel, with a Haemophilus influenzae type b glycoconjugate vaccine*, Vaccine,* 29, pp. 8965-8973.

Nie, S. (2010). Understanding and overcoming major barriers in cancer nanomedicine*, Nanomedicine,* 5, pp. 523-528.

Novavax (2013), A Study to Evaluate the Immune Response and Safety of a Seasonal Virus-Like Particle Influenza Vaccine in Healthy Young Adults, (NCT01561768), 2013 May 8, from http://www.clinicaltrials.gov.

Oussoren, C. and Storm, G. (2001). Liposomes to target the lymphatics by subcutaneous administration*, Advanced Drug Delivery Reviews,* 50, pp. 143-156.

Oyewumi, M.O., Kumar, A., and Cui, Z. (2010). Nano-microparticles as immune adjuvants: correlating particle sizes and the resultant immune responses*, Expert Review of Vaccines,* 9, pp. 1095-1107.

Parham, P. (2000) *The Immune System,* 3rd Ed. (Garland Pub., USA).

Park, J., Lim, D.-H., Lim, H.-J., Kwon, T., Choi, J.-s., Jeong, S., Choi, I.-H., and Cheon, J. (2011). Size dependent macrophage responses and toxicological effects of Ag nanoparticles*, Chemical Communications,* 47, pp. 4382-4384.

Paul, W.E. (2008) *Fundamental immunology,* 6th Ed. (Lippincott Williams & Wilkins, USA).

Pearce, R.C., Railsback, J.G., Anderson, B.D., Sarac, M.F., McKnight, T.E., Tracy, J.B., and Melechko, A.V. (2013). Transfer of Vertically Aligned Carbon Nanofibers to Polydimethylsiloxane (PDMS) While Maintaining their Alignment and Impalefection Functionality*, ACS Applied Materials and Interfaces,* 5, pp. 878-882.

Pearse, M.J. and Drane, D. (2005). ISCOMATRIX® adjuvant for antigen delivery*, Advanced Drug Delivery Reviews,* 57, pp. 465-474.

Pignataro, B. (2010) *Ideas in Chemistry and Molecular Sciences: Advances in Nanotechnology, Materials and Devices,* 1st Ed. (Wiley, Weinheim).

Plotkin, S.A., Orenstein, W.A., and Offit, P.A. (2013) *Vaccines,* 6th Ed. (Elsevier Saunders, Edinburgh).

PowderMed (2007), A Safety and Immunology Study of a DNA Trivalent Influenza Vaccine, (NCT00375206), 2013 May 6, from http://www.clinicaltrials.gov.

PowderMed (2008), Safety Study of HBV DNA Vaccine to Treat Patients With Chronic Hepatitis B Infection, (NCT00277576), 2013 May 6, from http://www.clinicaltrials.gov.

Prieur, X., Rőszer, T., and Ricote, M. (2010). Lipotoxicity in macrophages: evidence from diseases associated with the metabolic syndrome*, Biochimica et Biophysica Acta (BBA) - Molecular and Cell Biology of Lipids,* 1801, pp. 327-337.

Pusic, K., Aguilar, Z., McLoughlin, J., Kobuch, S., Xu, H., Tsang, M., Wang, A., and Hui, G. (2012). Iron oxide nanoparticles as a clinically acceptable delivery platform for a recombinant blood-stage human malaria vaccine*, The FASEB Journal,* 27, pp. 1153-1166.

Rajapaksa, T.E. and Lo, D.D. (2010). Microencapsulation of Vaccine Antigens and Adjuvants for Mucosal Targeting*, Current Immunology Reviews,* 6, pp. 29 - 37.

Reddy, S.T., Rehor, A., Schmoekel, H.G., Hubbell, J.A., and Swartz, M.A. (2006). In vivo targeting of dendritic cells in lymph nodes with poly(propylene sulfide) nanoparticles*, Journal of Controlled Release,* 112, pp. 26-34.

Reddy, S.T., van der Vlies, A.J., Simeoni, E., Angeli, V., Randolph, G.J., O'Neil, C.P., Lee, L.K., Swartz, M.A., and Hubbell, J.A. (2007). Exploiting lymphatic transport and complement activation in nanoparticle vaccines*, Nature Biotechnology,* 25, pp. 1159-1164.

Rogers, T.H. and Babensee, J.E. (2011). The role of integrins in the recognition and response of dendritic cells to biomaterials*, Biomaterials,* 32, pp. 1270-1279.

Romagnani, S. (1999). Th1/Th2 cells*, Inflammatory Bowel Diseases,* 5, pp. 285-94.

Roy, M.J., Wu, M.S., Barr, L.J., Fuller, J.T., Tussey, L.G., Speller, S., Culp, J., Burkholder, J.K., Swain, W.F., Dixon, R.M., Widera, G., Vessey, R., King, A., Ogg, G., Gallimore, A., Haynes, J.R., and Heydenburg Fuller, D. (2000). Induction of antigen-specific CD8+ T cells, T helper cells, and protective levels of antibody in humans by particle-mediated administration of a hepatitis B virus DNA vaccine*, Vaccine,* 19, pp. 764-778.

Salvador, A., Igartua, M., Hernández, R.M., and Pedraz, J.L. (2011). An Overview on the Field of Micro- and Nanotechnologies for Synthetic Peptide-Based Vaccines*, Journal of Drug Delivery,* 2011, pp. 1-23.

Samuelsen, M., Nygaard, U.C., and Løvik, M. (2009). Particle Size Determines Activation of the Innate Immune System in the Lung*, Scandinavian Journal of Immunology,* 69, pp. 421-428.

Shvedova, A.A., Fabisiak, J.P., Kisin, E.R., Murray, A.R., Roberts, J.R., Tyurina, Y.Y., Antonini, J.M., Feng, W.H., Kommineni, C., Reynolds, J., Barchowsky, A., Castranova, V., and Kagan, V.E. (2008). Sequential Exposure to Carbon Nanotubes and Bacteria Enhances Pulmonary Inflammation and Infectivity*, American Journal of Respiratory Cell and Molecular Biology,* 38, pp. 579-590.

Smith, G., Raghunandan, R., Wu, Y., Liu, Y., Massare, M., Nathan, M., Zhou, B., Lu, H., Boddapati, S., Li, J., Flyer, D., and Glenn, G. (2012). Respiratory Syncytial Virus Fusion Glycoprotein Expressed in Insect Cells Form Protein Nanoparticles That Induce Protective Immunity in Cotton Rats*, PLoS ONE,* 7, e50852, DOI: 10.1371/journal.pone.0050852.

Speiser, D.E., Li, xE, nard, D., Rufer, N., Rubio-Godoy, V., Rimoldi, D., Lejeune, F., Krieg, A.M., Cerottini, J.-C., and Romero, P. (2005). Rapid and strong human CD8+ T cell responses to vaccination with peptide, IFA, and CpG oligodeoxynucleotide 7909*, The Journal of Clinical Investigation,* 115, pp. 739-746.

Speiser, D.E., Schwarz, K., Baumgaertner, P., Manolova, V., Devevre, E., Sterry, W., Walden, P., Zippelius, A., Conzett, K.B., and Senti, G. (2010). Memory and effector CD8 T-cell responses after nanoparticle vaccination of melanoma patients*, Journal of Immunotherapy,* 33, pp. 848-858.

Springer, C., Benita, S., Sherman, Y., Gursoy, N., Gilhar, D., and Avital, A. (2005). Poly-lactic-glycolic Acid Microspheres: A Biodegradable Marker for the Diagnosis of Aspiration in Hamsters*, Pediatric Research,* 58, pp. 537-541.

Stano, A., Nembrini, C., Swartz, M.A., Hubbell, J.A., and Simeoni, E. (2012). Nanoparticle size influences the magnitude and quality of mucosal immune responses after intranasal immunization*, Vaccine,* 30, pp. 7541-7546.

Tabata, Y. and Ikada, Y. (1988). Effect of the size and surface charge of polymer microspheres on their phagocytosis by macrophage*, Biomaterials,* 9, pp. 356-362.

Thiele, L., Diederichs, J.E., Reszka, R., Merkle, H.P., and Walter, E. (2003). Competitive adsorption of serum proteins at microparticles affects phagocytosis by dendritic cells*, Biomaterials,* 24, pp. 1409-1418.

Tokura, S., Hiroshi, T., and Ichiro, A. (1999) *Chitin and chitinases* 87, eds. P. Jollès and Muzzarelli R.A.A., Exogenous chitosans “Immunological aspects of chitin and chitin derivatives administered to animals”, (Birkhäuser, Basel) pp. 279-292.

Van Zijverden, M. and Granum, B. (2000). Adjuvant activity of particulate pollutants in different mouse models*, Toxicology,* 152, pp. 69-77.

Vasir, J.K. and Labhasetwar, V. (2007) *Nanoparticulate Drug Delivery Systems* eds., Nanoparticles for Gene Delivery: Formulation Characteristics", pp. 291-304.

Verma, A. and Stellacci, F. (2010). Effect of Surface Properties on Nanoparticle–Cell Interactions*, Small,* 6, pp. 12-21.

Villemejane, J. and Mir, L.M. (2009). Physical methods of nucleic acid transfer: general concepts and applications*, British Journal of Pharmacology,* 157, pp. 207-219.

Von Andrian, U.H. and Mackay, C.R. (2000). T-Cell Function and Migration — Two Sides of the Same Coin*, New England Journal of Medicine,* 343, pp. 1020-1034.

Wilson, N.S., Yang, B., Morelli, A.B., Koernig, S., Yang, A., Loeser, S., Airey, D., Provan, L., Hass, P., Braley, H., Couto, S., Drane, D., Boyle, J., Belz, G.T., Ashkenazi, A., and Maraskovsky, E. (2012). ISCOMATRIX vaccines mediate CD8+ T-cell cross-priming by a MyD88-dependent signaling pathway*, Immunology and Cell Biology,* 90, pp. 540-552.

Xiang, S.D., Scholzen, A., Minigo, G., David, C., Apostolopoulos, V., Mottram, P.L., and Plebanski, M. (2006). Pathogen recognition and development of particulate vaccines: Does size matter?*, Methods,* 40, pp. 1-9.

Xie, Y., Bagby, T.R., Cohen, M., and Forrest, M.L. (2009). Drug delivery to the lymphatic system: importance in future cancer diagnosis and therapies*, Expert Opinion on Drug Delivery,* 6, pp. 785-792.

Yoon, K.-Y., Hoon Byeon, J., Park, J.-H., and Hwang, J. (2007). Susceptibility constants of Escherichia coli and Bacillus subtilis to silver and copper nanoparticles*, Science of the Total Environment,* 373, pp. 572-575.

Yoshida, M., Mata, J., and Babensee, J.E. (2007). Effect of poly(lactic-co-glycolic acid) contact on maturation of murine bone marrow-derived dendritic cells*, Journal of Biomedical Materials Research Part A,* 80A, pp. 7-12.

Yue, H., Wei, W., Yue, Z., Lv, P., Wang, L., Ma, G., and Su, Z. (2010). Particle size affects the cellular response in macrophages*, European Journal of Pharmaceutical Sciences,* 41, pp. 650-657.

Zahr, A.S., Davis, C.A., and Pishko, M.V. (2006). Macrophage Uptake of Core−Shell Nanoparticles Surface Modified with Poly(ethylene glycol), *Langmuir,* 22, pp. 8178-8185.

Chapter II:

Characterization of pDNA/TMC nanoparticle interaction and stability

Johanna Poecheim, Viorica Patrulea, Christian Reichert, Gerrit Borchard

School of Pharmaceutical Sciences, University of Geneva, University of Lausanne, Quai Ernest Ansermet 30, 1211 Geneva, Switzerland

Published in: Poecheim, J., Patrulea, V., Reichert, C., and Borchard, G. (2016). Characterization of pDNA/TMC nanoparticle interaction and stability, *Current Drug Delivery*, 13, pp. 1567-2018.

Abstract

Formulation of nanoparticulate DNA vaccines requires the assessment of stability and integrity of the components implicated. Stability of cationic nanoparticles made of N-trimethyl chitosan and chondroitin sulfate (TMC nanoparticles) was investigated in aqueous solution and after freeze-drying by characterization of their size, polydispersity index (PDI), and zeta potential. Furthermore, the structural integrity of plasmid DNA (pDNA) on adsorption to the nanoparticle surface was investigated. Agarose gel electrophoresis showed DNA retention when applied with the nanocarrier, suggesting that pDNA adsorption on nanoparticles took place. In circular dichroism (CD) spectra, ellipticity of pDNA decreased at 280 nm and increased at 245 nm, and the maximum wavelength shifted from 275 nm to 285 nm when nanoparticles were present. Once released from the particles, the secondary structure of the plasmid was retained in its native form. pDNA release from pDNA/TMC nanoparticles was indicated by a rise in zeta potential from initially -32 mV (pDNA adsorbed to particles) to 14 mV during one hour, and to 36 mV after 24 hours. Unloaded TMC nanoparticles remained stable in suspension for 24 hours, maintaining diameters of around 200 nm, and zeta potential values of approximately 38 mV. Freeze-drying with sucrose could ensure storage for 30 days, with minimal increase in size (291 nm) and charge (62 mV). In conclusion, TMC nanoparticles can successfully be freeze-dried in the presence of sucrose to be stored for prolonged periods of time. Furthermore, pDNA was successfully adsorbed to the cationic nanoparticles and remains intact after being released.

1. Introduction

DNA vaccination is an attractive concept for the prevention of infectious diseases through the induction of robust cytotoxic T-cell and antibody responses. However, early clinical trials with DNA vaccines targeting human immunodeficiency virus (HIV) type 1, cancer, influenza, human papillomavirus (HPV), hepatitis, and malaria showed immune response elicited to be insufficient to protect humans from infection (Ferraro *et al.*, 2011, Fuller *et al.*, 2006). An interesting approach to increase DNA vaccine potency is the improvement in vector design by formulating DNA with cationic nanoparticles, which offers an interesting potential for efficient non-viral gene delivery (Borchard, 2001).

Chitosan is a polysaccharidic copolymer of glucosamine and N-acetylclucosamine, and is obtained by partial deacetylation of chitin, a natural polymer of crustacean origin or derived from cell walls of fungi. Chitosan has been shown to be biocompatible, biodegradable, of low toxicity and is relatively easy to undergo chemical modification (Sonia and Sharma, 2011). Introducing permanent cationic charges in the polymer by trimethylation of amino groups improves the cationic properties and complexation of polyanions. Chondroitin sulfate is a naturally derived glycosaminoglycan present in the extracellular matrix of cartilage. It is an anionic polyelectrolyte, composed of sulfated N-acteylgalactosamine and glucuronic acid units, and has been shown to form complexes with chitosan of cationic net surface charge (Yeh *et al.*, 2011). All of these structures are shown in Figure 1. Upon addition of DNA, the remaining positively charged amine groups in trimethyl chitosan (TMC)/ chondroitin sulfate complexes (TMC nanoparticles) interact with DNA phosphate groups. Considerations about potential changes in the structure of DNA strands upon adsorption to cationic nanoparticles are important for their activity. As the anionic charge of the DNA phosphate backbone is neutralized when bound to cationic surfaces of nanoparticles, the conformational rigidity of the helix is relaxed and corresponding unwinding of the strands was observed (Goodman *et al.*, 2006, Minagawa *et al.*, 1991). Polymerase recognizes DNA in its helical form (Kukarin

et al., 2003, Steitz, 2004), thus, upon binding to nanoparticles, DNA helix was shown to become unrecognizable to polymerase as an appropriate substrate for transcription (Goodman *et al.*, 2006). Therefore the structural integrity of DNA in its native form on release from the nanoparticles at the target site has to be maintained for effective *in vivo* activity.

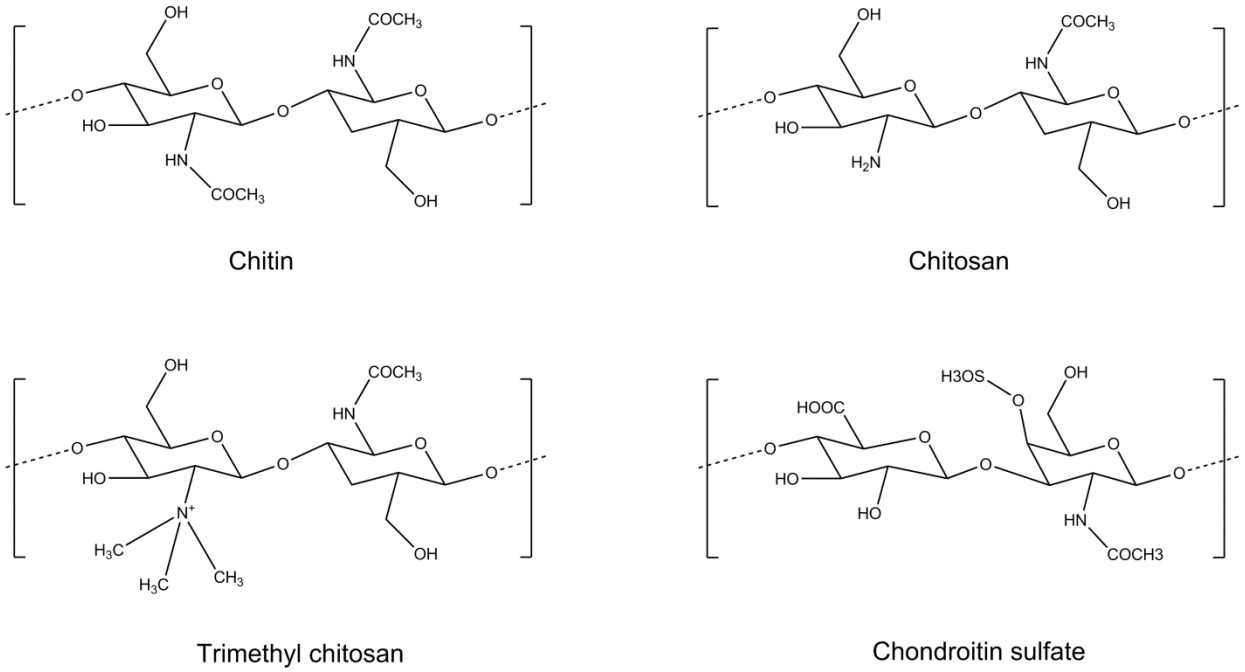

Figure 1. Chemical structures of chitin (poly (*N*-acetyl-1,4-β-D-glucopyranosamin), chitosan (N-deacetylchitin), N-trimethyl chitosan, and chondroitin-4-sulfate (β-glucuronic acid-(1-3)-N-acetyl-β-galactosamine-4-sulfate.

It is inevitable that nanoparticles made of hydrolytically degradable polymers such as chitosan will degrade over time (Szymańska and Winnicka, 2015). Polyionic polymeric gene complexes, consisting of several components, are usually prepared shortly before injection. This is thought to be required due to instability of the complexes formed, being susceptible to aggregation or increase in particle size, which can influence immunogenic features of the vaccine (Talsma *et al.*, 1997). An important aspect for further pharmaceutical development of DNA vaccines is to ensure nanoparticle stability during long time storage by maintaining critical parameters such as mean size, size

distribution, and surface charge. Freeze-drying would be a reasonable approach for stabilization and storage of standardized batches to obtain reproducible quality upon rehydration (Allison and Anchordoquy, 2001, Brus *et al.*, 2004).

In the present study the important parameters for TMC nanoparticle formulation for the delivery of plasmid DNA (pDNA) are investigated. TMC nanoparticles were prepared with chondroitin sulfate *via* complexation by a complex coacervation method. Successful pDNA adsorption onto TMC nanoparticles surface to form pDNA/TMC nanocomplexes was confirmed by gel electrophoresis as well as by circular dichroism (CD). CD was used as a valuable method to investigate structural changes of pDNA in more detail and to ascertain whether the helical structure of pDNA was present in its native form after release. Furthermore, TMC nanoparticles with or without pDNA were investigated with regard to their stability in aqueous formulations by physicochemical determination of size, surface charge, and polydispersity index (PDI). Freeze-drying is a widely used process to improve the stability of such formulations and was investigated in this study for its potential to preserve TMC nanoparticle and pDNA/TMC nanoparticle properties.

2. Material and Methods

2.1. Materials

For the synthesis of TMC, chitosan with 79 % degree of deacetylation (ChitoClear Cg10, 7–15 mPas) was purchased from Primex (Siglufjordur, Iceland). Sodium iodide, 1-methyl-2-pyrrolidinone (NMP), methyl iodide, sodium chloride as well as 3-(trimethylsilyl)propionic-2,2,3,3-d_4 acid (TSP) and chondroitin-4-sulfate were purchased from Sigma Aldrich (Buchs, Switzerland), sodium hydroxide pellets from Riedel-de Haen (Seelze, Germany) and D_2O from Armar chemicals (Doettingen, Switzerland). Dialysis was performed with Spectra/Por® Dialysis membranes (MWCO 12-14 kDa; Spectrum, USA). A 5853 base-pair (bp) double-stranded pDNA (dsDNA) encoding *Mtb*

antigene Ag85A was constructed and kindly provided by Dr. K Huygens (Institut Pasteur, Brussels, Belgium) (Tanghe *et al.*, 1999). DNA amplification and purification was performed using NovaBlue Singles Competent Cells (Novagane, Merck KGaA, Darmstadt, Germany) that were kindly provided by Prof. L. Scapozza (University of Geneva, Geneva, Switzerland) and kanamycin sulfate BioChemica (Applichem, Darmstadt, Germany). pDNA was purified by using an Endofree Plasmid Giga Kit (Qiagen, Courtaboeuf, France) according to the manufacturer's protocol. For electrophoresis Certified Molecular Biology Agarose was obtained from Bio-Rad, ethidium bromide from Life technologies (Zug, Switzerland) and a 1 kb DNA ladder from BioLabs (Hitchin, UK).

2.2. TMC synthesis

Trimethylation of chitosan was performed as previously described, with some modifications (Heuking *et al.*, 2009). The reaction scheme is depicted in Scheme 1. Briefly, chitosan (2 g) and sodium iodide (4.8 g) were suspended in NMP (80 ml). The mixture was stirred and heated at 60 °C for 30 minutes in a round bottom flask under a reflux condenser. To provide an alkaline environment throughout the reaction, 11 ml of sodium hydroxide (15 % w/v) were added while heating and stirring was maintained for another 30 minutes. Trimethylation of chitosan was achieved through nucleophilic substitution by addition of methyl iodide (12 ml). The mixture was let react at 60 °C for 70 minutes and subsequently filtered through a P3 glass filter. The resulting TMC was precipitated with a mixture of diethyl ether and ethanol (1:1 v/v) by having added 5 times the volume of the filtrate. The precipitated product was then recovered by centrifugation (2000 rpm, 15 minutes) and dissolved in 10 % sodium chloride (30 ml) to obtain counter ion replacement and to prevent iodine oxidation. The solution was stirred at 50 °C for 10 minutes until complete dissolution of TMC and purified by dialysis using a Spectra/Por 4 dialysis membrane (12-14 kDa) during 3 days before lyophilization.

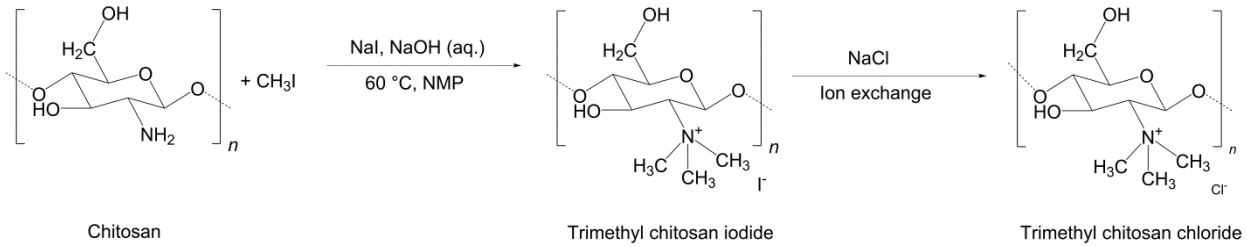

Scheme 1. Reaction scheme for the synthesis of chitosan trimethylation and counter ion replacement. Sodium iodide (NaI) acted as a catalyst. Methyl iodide (CH_3I) reacted with the primary amine groups of chitosan under alkaline conditions, provided by sodium hydroxide (NaOH). The iodide counter ion was then replaced with chloride by washing with sodium chloride.

2.3. Polymer characterization

FTIR spectra of chitosan and TMC were recorded on a Perkin-Elmer 100 FT-IR spectrometer (Perkin-Elmer, Switzerland). The degree of quaternization (DQ) and dimethylation (DM) of the resulting TMC were calculated from ^{1}H-nuclear magnetic resonance (NMR) spectra obtained with a Varian Gemini 300 MHz spectrometer (in D_2O at 80 °C; Agilent Technologies, Santa Clara, USA) as described previously using the following equations (Amidi *et al.*, 2006, Verheul *et al.*, 2008):

$$\text{Eq. 1} \quad DQ = \left[\frac{[(CH3)3]}{[H]} \times \frac{1}{9}\right] \times 100$$

$$\text{Eq. 2} \quad DM = \left[\frac{[(CH3)2]}{[H]} \times \frac{1}{6}\right] \times 100$$

$[CH_3)_3]$ and $[CH_3)_2]$ are the integrals of the ammonium group appearing at 3.3 ppm and the dimethyl amino group at 3.1 ppm, respectively. [H] is the integral of the peaks between 4.5 and 5.5 ppm, representing the hydrogen atom attached to carbon 1 of the glucopyranose ring, and taken as a reference signal with an integral of 1. The chemical shifts are given relative to trimethylsilyl propionic acid (TSP, 0.05 %) as an internal reference.

2.4. Plasmid DNA amplification and purification

The V1Jns-tPA-85A plasmid vector, shown in Figure 2, contains an antigen 85A (Ag85A) coding sequence linked to human tissue plasminogen activator (tPA) that can be expressed in eukaryotic cells under control of cytomegalovirus (CMV) promoter with intron A **(**CMV-intA) and Bovine Growth Hormone (BGH) transcription terminator (Huygen *et al.*, 1998). The kanamycin resistant plasmid was transformed into competent NovaBlue cells (Novagen, Merck KGaA, Darmstadt, Germany) and plated on Luria–Bertani (LB) agar medium containing kanamycin (50 µg/ml). Recombinant pDNA was amplified in NovaBlue cells in 3 liter kanamycin-containing LB culture for 16 h at 37 °C under agitation. pDNA was then isolated and purified by using an Endofree Plasmid Giga Kit (Qiagen, France), adjusted to a final concentration of 1 µg/µl in PBS and stored at −20 °C. Before experimental use, the integrity of the plasmid was confirmed by agarose electrophoresis.

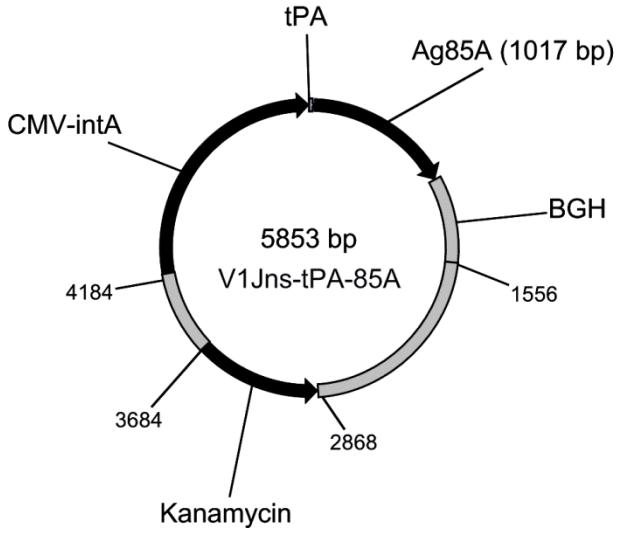

Figure 2. Gene map of recombinant DNA vaccine encoding for Ag85ADNA obtained from Institut Pasteur, Belgium. V1Jns expression vector with kanamycin resistance contains Ag85A with tPA signal sequence, under control of CMV-Intron A promoter and BGH terminator.

2.5. TMC nanoparticle preparation and DNA adsorption

TMC nanoparticles were formed spontaneously upon adding 1 ml of chondroitin-4-sulfate (1 mg/ml) aqueous solution to 1 ml of TMC aqueous solution (5 mg/ml) by one-shot addition at ambient temperature (Hansson *et al.*, 2012). The nanoparticle dispersion was vortexed for 10 seconds to allow complex formation between the polyelectrolytes. Thereafter, particles were kept at room temperature for a maximum of one hour prior to further use. For the preparation of pDNA/TMC nanoparticles, pDNA was added to the TMC nanoparticle dispersion (50 µg/ml), vortexed, and diluted 1:10 with the respective buffer according to the experiments.

2.6. Nanoparticle characterization

Z-average size, giving the hydrodynamic diameters of particles, and PDI of the nanocomplexes were determined by dynamic light scattering (DLS) using a Malvern ZetaSizer Nano ZS (Malvern Instruments, Worcestershire, UK) at a detection angle of 173°. PDI values up to 0.5 were considered to be appropriate for comparison purposes (Drogoz *et al.*, 2007). The device uses a 10 mW He/Ne laser operating at a wavelength of 633 nm and all measurements were taken at a temperature of 25 °C. The zeta potential of the particles was measured by electrophoresis and laser Doppler velocimetry using the same equipment. Before the measurement, samples were diluted at a ratio of 1:10 in 1 mM sodium chloride. Samples were prepared in duplicates and three repeat measurements of each sample were taken to check for result repeatability. For stability evaluation of the formed TMC nanoparticles and pDNA/TMC nanoparticles in aqueous dispersions, particle size distribution, PDI, and zeta potential were determined immediately after preparation, and 1 hour and 24 hours after particle formation. Furthermore, batches of TMC nanoparticles and pDNA/TMC nanoparticles were either prepared in water or a 1 % aqueous sucrose solution, frozen at -80 °C over night, and lyophilized thereafter using a Christ Alpha 2-4 LD plus freeze-drier (Kuehner AG, Birsfelden, Switzerland). Freeze-drying was carried out for 24 hours at -82 °C and

0.001 mbar. Lyophilized samples were resuspended in 1 mM sodium chloride and characterized immediately, or after storage at 4 °C for 30 days.

2.7. Electrophoretic mobility analysis

Samples were mixed with bromophenol blue as loading dye and 20 µl of each sample were placed in a 0.8 % agarose gel stained with 0.6 µg/ml of ethidium bromide. A 1 kbp pDNA ladder (BioLabs, UK) was run in parallel on each gel and pDNA in the absence of TMC nanoparticles served as controls. A voltage of 80 V was applied for 30 minutes, followed by 60 V for 1 hour (PowerPac, Bio-Rad, France) using tris-borate-EDTA buffer. pDNA migration was visualized by UV transillumination (Bio-Rad).

2.8. Circular dichroism

Samples were prepared in PBS as described above with a final pDNA concentration of 13 nM per aliquot. PBS served as a blank and unloaded TMC nanoparticles as control. pDNA was measured either alone, adsorbed to TMC nanoparticles, or after release from the nanoparticles after 24h. For pDNA release, pDNA/TMC nanoparticles were stored at 37 °C at 80 rpm in a shaking incubator (GFL, Burgwedel, Germany). After 24 h the dispersions were centrifuged for 15 min at 14000 rpm (Eppendorf 5810R, Vaudaux-Eppendorf, Basel, Switzerland) and supernatants containing the released pDNA were measured. CD data were obtained using a Jasco J-815 spectropolarimeter (Jasco, Tokyo, Japan). Spectra were taken from 240 – 300 nm at a scanning speed of 100 nm/min, with a 2 nm band width and a 2 seconds response. Sensitivity was set to standard (100 mdeg) and the scanning mode was set to continuous, in 3 accumulated runs. All spectra were taken at 20 °C in a quartz cuvette with 1 mm path length purchased from Starna (Pfungstadt, Germany). Results were obtained in millidegrees of ellipticity and converted into molar ellipticity [Θ] using Equation 3. Θ represents degrees of ellipticity, C is the molar concentration of pDNA and l the pathlength in centimeters (Woody, 2010). Eq. 3 $[\Theta] = \frac{(100 \times \Theta)}{C \times l}$

2.9. Statistical significance

To assess statistics for nanoparticles, nonparametric Kruskal-Wallis statistic with Dunn's multiple comparison test was chosen, to evaluate probability of statistical significance of mean rank differences between small sample sizes (n=3) and possible lack of normality of data.

3. Results and Discussion

3.1. TMC characterization

Chitosan was derivatized to obtain its highly water-soluble quaternary ammonium salt TMC. The FTIR spectrum of TMC, compared to the spectrum of chitosan, shows a new band at 1472 cm^{-1}, which represents the methyl group of ammonium, indicating the existence of $–N(CH_3)_2$ and $–N^+(CH_3)_3$ groups in TMC (Figure 3) (Chang *et al.*, 2009). The ^1H NMR spectra of original chitosan showed the peak of N-actelyation at δ=2.0 ppm and the N-deacetylated amino group at δ=3.2 ppm. TMC synthesis through direct trimethylation of chitosan with iodomethane led to non-selective O- and N-methylation, as shown by NMR peaks at δ=3.4 ppm ($O\text{-}CH_3$), δ=3.3 ppm ($N^+(CH_3)_3$) and δ=3.1 ppm ($N^+(CH_3)_2$) (Figure 4) (Patrulea *et al.*, 2015). The degree of N-quaternization and N-dimethylation was calculated from ^1H NMR analysis to define the substitution pattern of the synthesized TMC. A quaternization degree of 13 % and a dimethylation degree of 27 % was obtained for the TMC used in the present study. The quaternisation degree was kept low in order to avoid cytotoxic effects of the polymer caused by high cationic charge densities.

3.2. Preparation and characterization of nanoparticles

Nanoparticles were characterized for their size (Z-average), PDI and surface charge (zeta potential) in order to determine whether TMC nanoparticles, either unloaded or loaded with pDNA, remained stable under various conditions (Figure 5).

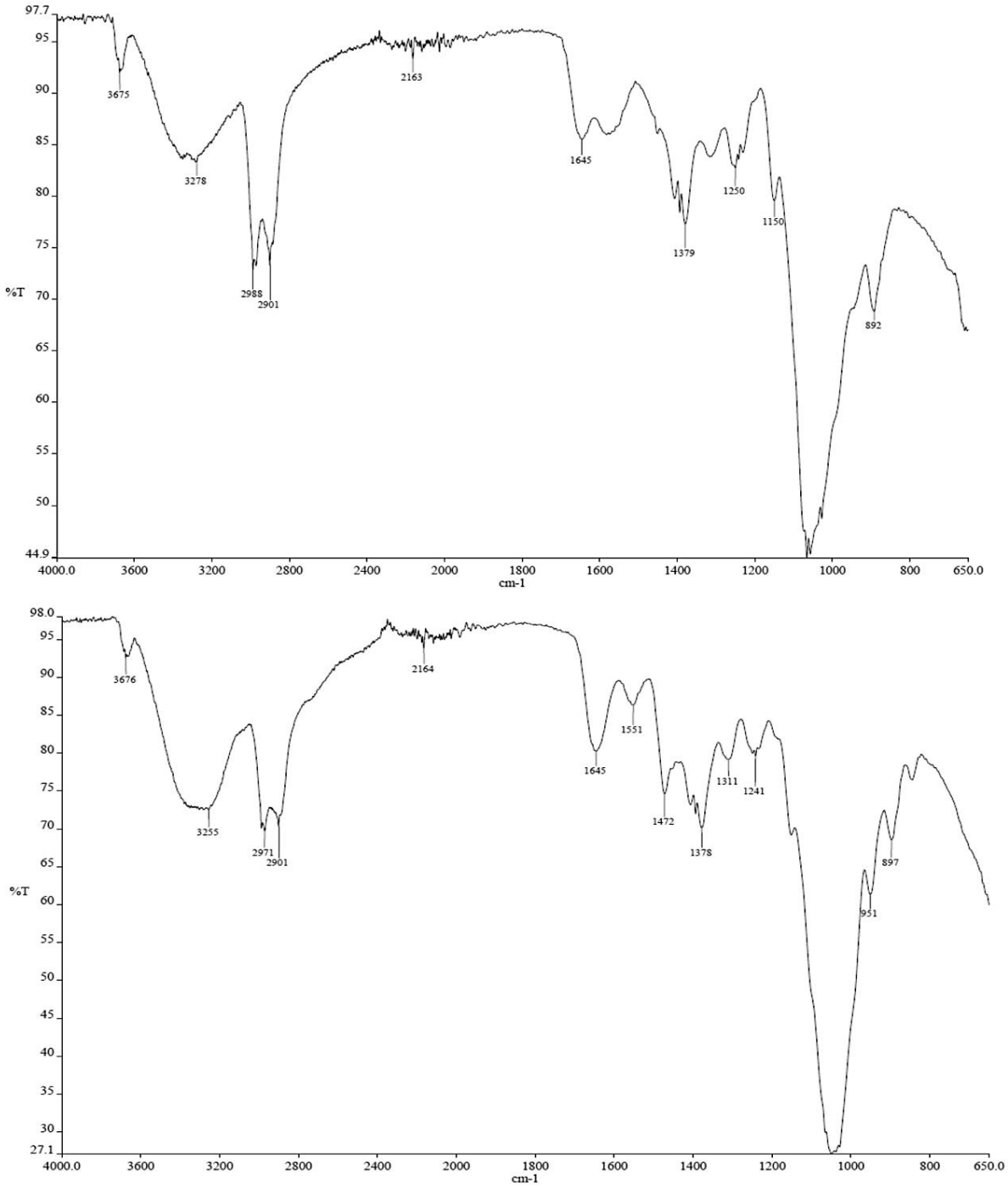

Figure 3. FTIR spectra of chitosan and N-trimethyl chitosan. The FTIR spectrum of TMC, compared to the spectrum of chitosan, shows a new band at 1472 cm^{1}, which represents the methyl group of ammonium.

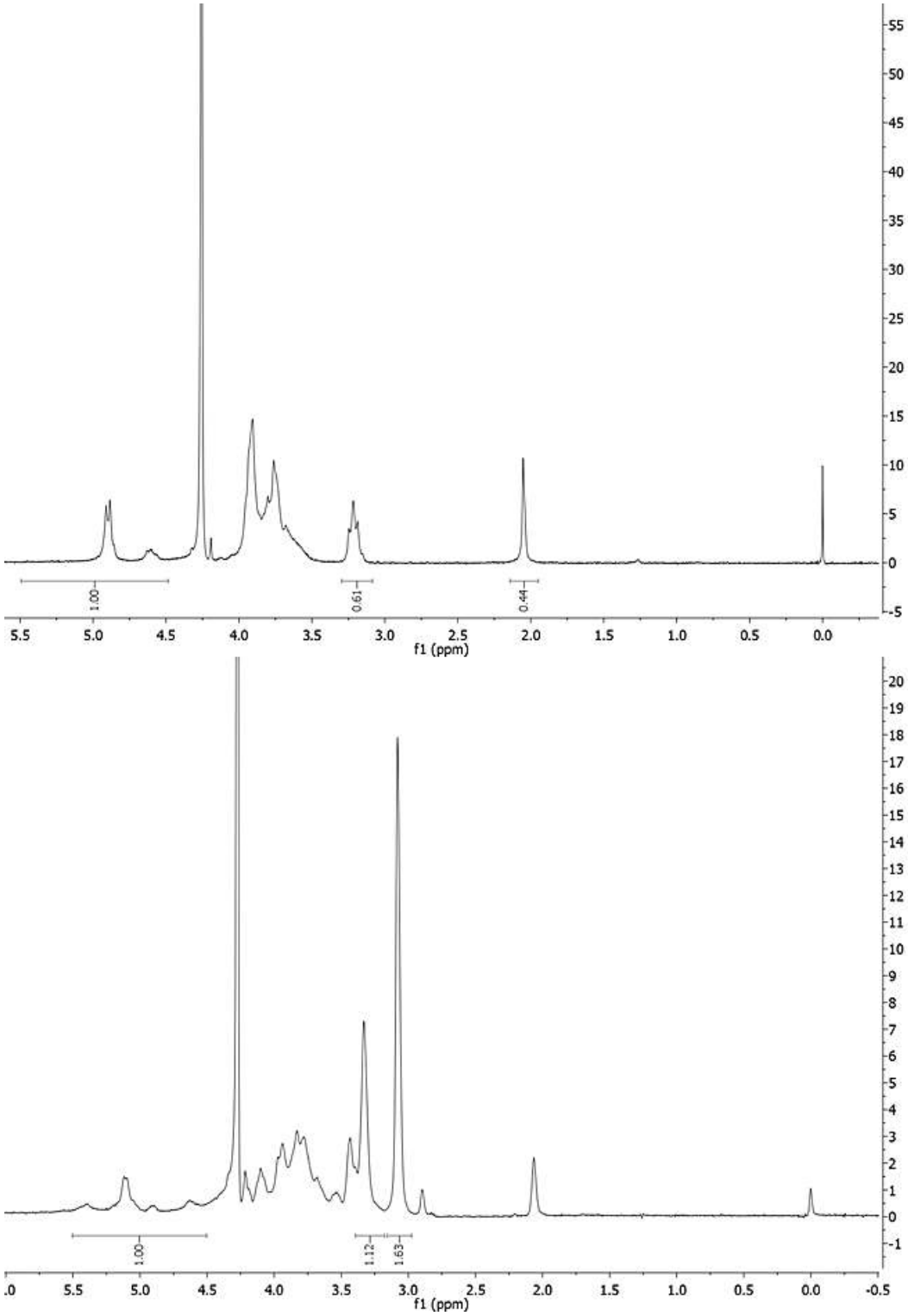

Figure 4. ^{1}H NMR spectra of chitosan and N-trimethyl chitosan showed the peak of N-actelyation at δ=2.0 ppm and the N-deacetylated amino group at δ=3.2 ppm. TMC synthesis through direct trimethylation of chitosan with iodomethane led NMR peaks at δ=3.4 ppm (O-CH_3), δ=3.3 ppm ($N^+(CH_3)_3$) and δ=3.1 ppm ($N^+(CH_3)_2$).

Having compared all groups of nanoparticles kept in suspension, TMC nanoparticles were shown to retain a constant size of approximately 200 nm for 24 hours and no significant changes in PDI (0.3) and zeta potential (36 mV) were observed ($p > 0.05$). The maintenance of a colloidal homogenous suspension is related to the small particle size in the nanometer range, allowing for Brownian motion (Aulton and Taylor, 2013). These diffusion forces are opposed to gravitational forces, and prevent particles from sedimentation. Another important factor is the effect of surface charge of the nanoparticles. The nanocomplexes carry net positive charges that eventually produce electrostatic repulsion between the particles (Derjaguin and Landau, 1993). Adsorption of pDNA to TMC nanoparticles led to size contraction from 177 nm to 159 nm. TMC nanoparticles are formed through intermolecular interactions between polycationic TMC and polyanionic chondroitin sulfate. With further application of small quantities of polyanionic pDNA to the nanoparticles it is conceivable that competition for positively charged patches on the surfaces of TMC nanoparticles leads to molecular rearrangement and tighter inter-particle bridging (Theodossiou and Thomas, 2002). A notable shift from 36 mV to negative surface charge (-32 mV) upon adsorption of pDNA to the nanoparticles was observed immediately after preparation. The change of the zeta potential to negative values can be taken as evidence for successful electrostatic binding of the nucleic acids to the surface of cationic TMC nanoparticles. After 1 hour the zeta potential increased from negative values to 14 mV, and 24 hours later to 36 mV. Presumably this increase in surface charge is due to pDNA dissociation from the nanoparticles and shows that the pDNA/TMC nanoparticle constructs are unstable in aqueous suspensions. Lower repulsion efficacy as a consequence of lower charge densities led to formation of small aggregates indicated by significantly larger hydrodynamic diameters and increased PDI values ($p < 0.01$) after one hour. After 24 hours most of the pDNA appeared to be released, resulting in positive surface charges, as well as size and PDI of the particles similar to the characteristics of unloaded TMC nanoparticles.

3.3. Freeze-drying of TMC nanoparticles

TMC nanoparticles and pDNA/TMC, lyophilized without cryoprotector, were prone to aggregation, exhibiting significantly greater hydrodynamic diameters after immediate resuspension ($p < 0.05$ and $p < 0.001$, respectively) and after storage for 30 days at 4 °C ($p < 0.001$ and $p < 0.01$, respectively), shown in Figure 5A. This can be explained by the fact that during the freeze-drying process phase separation into a cryo-concentrated nanoparticle phase and frozen suspension medium occurs (Abdelwahed *et al.*, 2006). Agglomeration and fusion of single particles could therefore be a consequence of the concentrated nanoparticles. TMC nanoparticles that were lyophilized in 1 % sucrose solution and resuspended immediately after freeze-drying, as well as after 30 days of storage at 4 °C, maintained their size with only minor increases in hydrodynamic diameters. Also their PDIs were consistent with freshly prepared particles. However, pDNA/TMC nanoparticles lyophilized with the cryoprotector did not keep their physicochemical characteristics after resuspension. Although not significant, the hydrodynamic diameters and PDI values were clearly increased compared to the freshly prepared controls. Sucrose could prevent TMC nanoparticles from aggregation, but not from changes in the zeta potential, suggesting alterations in the complex composition of TMC nanoparticles after freeze-drying that also take place in the presence of a cryoprotector. The surface charge of TMC nanoparticles was still positive but increased during the freeze-drying process, and was shown to be even higher after one month of storage ($p < 0.01$), as shown in Figure 5B. Changes in the zeta potential were reported previously for different non-viral vector formulations induced by freeze- drying (Brus *et al.*, 2004). Weakly bound components, namely chondroitin sulfate and pDNA, might have been set free due to mechanical stress (Abdelwahed *et al.*, 2006). The resulting higher zeta potential could therefore derive from a lower number of neutralized charges within the TMC nanoparticles after lyophilization. Another explanation could be the presence of residual TMC molecules in suspension that were not complexed during nanoparticle formation, but instead

incorporated during formation of the cryo-concentrated nanoparticle phase (Brus *et al.*, 2004).

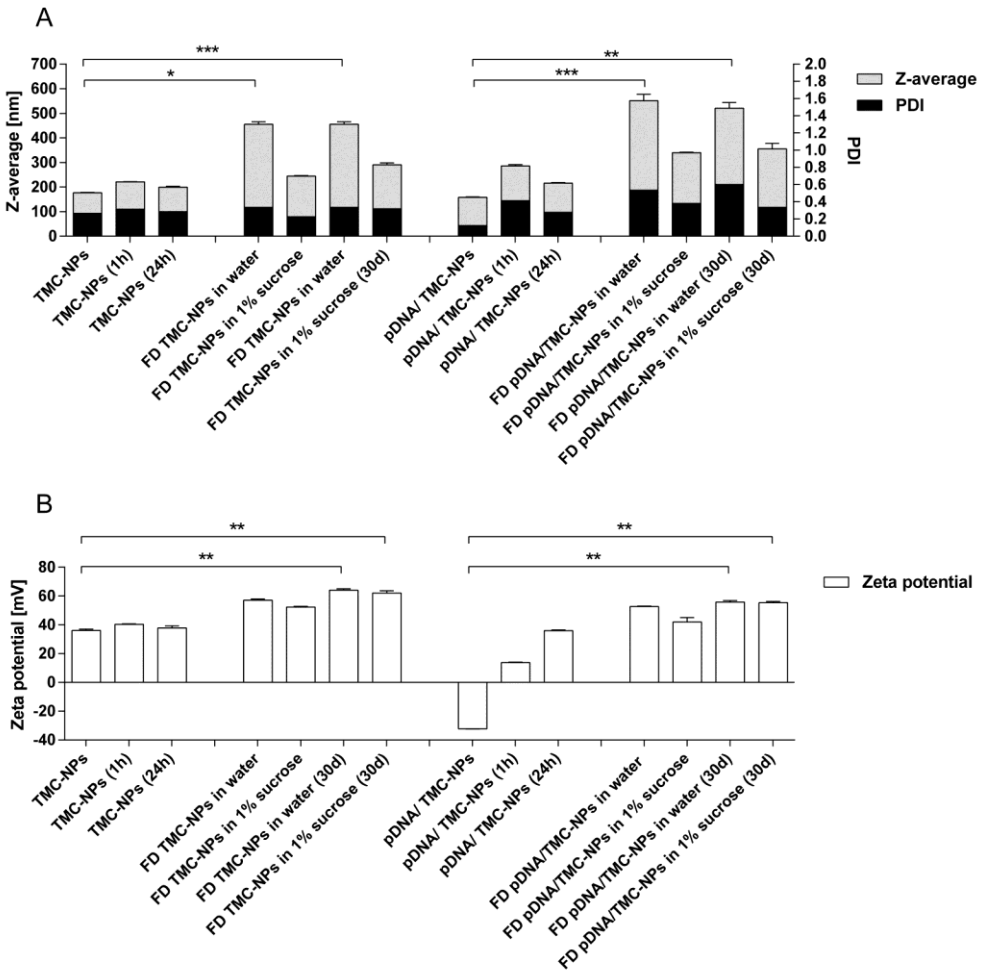

Figure 5. Stability of nanoparticles formed from TMC through complexation with chondroitin sulfate (TMC-NPs) with or without pDNA adsorbed on their outer surface. The size and PDI (A) and zeta potential (B) was measured in aqueous suspension after preparation, after 1 h and after 24 h. Particles were also characterized after freeze-drying (FD) either in water or in 1 % sucrose (w/v), resuspended immediately after freeze-drying or after 30 days of storage at 4°C

Charge increase does not imply that freeze-drying is not a successful method for TMC nanoparticles. On the contrary, higher surface charges may be even more advantageous for gene delivery and cellular uptake. However, if these freeze-dried nanoparticles are introduced for standardized use, they must be tested on their toxicity potential, due to higher charge densities present on their surface. Freeze-drying of pDNA/TMC nanoparticles, with and without cryoprotector led to highly positive charges similar to those of freeze-dried unloaded TMC nanoparticles. A complete loss of pDNA from nanoparticle surfaces has therefore to be assumed, which could also not be prevented by addition of sucrose. Therefore the freeze-drying of the complete formulation with pDNA containing TMC nanoparticles cannot be a method of choice for future formulation design. However, for large scale production, it is suggested to lyophilize unloaded TMC nanoparticles with 1 % sucrose solution, to be reconstituted with pDNA containing buffer solution prior to use. This way, standardization of batches can be achieved and optimal pDNA adsorption assured.

3.4. Electrophoretic mobility

Electrophoretic mobility of pDNA confirmed the integrity of the plasmid after purification, after storage in PBS until use, and after release from TMC nanoparticles (data not shown). Free pDNA remained in supercoiled form, which indicates that the physical integrity of pDNA was not altered. Similar observations were reported previously for chitosan pDNA polyplexes (Heuking and Borchard, 2012, Köping-Höggård *et al.*, 2004). Furthermore, agarose gel electrophoresis demonstrated the capacity of TMC nanoparticles to retain pDNA (Figure 6). The retention effect has also been previously observed for other nanoparticles (Railsback *et al.*, 2012, Zanchet *et al.*, 2001). This indicates that adsorption of the plasmid on the positively charged surface of the nanocarrier takes place. However, it has to be considered that the discrete change in mobility might be due to denaturation of dsDNA upon binding to cationic nanoparticles (Railsback *et al.*, 2012).

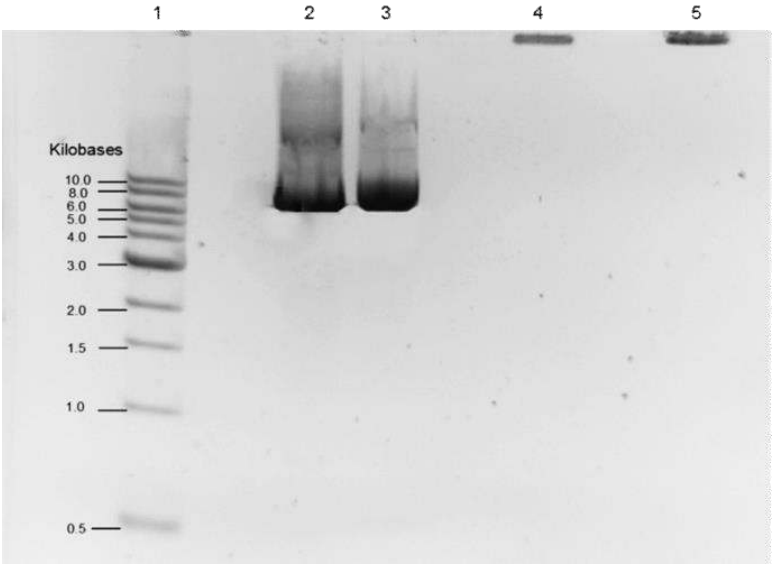

Figure 6. Agarose gel electrophoresis of 1 kbp DNA ladder (lane 1), pDNA (lane 2 and 3), and pDNA adsorbed to TMC nanoparticles (TMC-NPs; lane 4 and 5).

3.5. Secondary structure of pDNA

Information regarding the secondary structure of pDNA and its behavior upon interaction with TMC nanoparticles was obtained using CD (Figure 7). The CD spectrum of pDNA alone shows a maximum at approximately 280 nm, indicative of the B-form duplex (Goodman *et al.*, 2006). Upon adsorption to TMC nanoparticles a significant change in the DNA conformation could be observed. The decrease in ellipticity at approximately 280 nm, and increases at approximately 245 nm, together with a shift in the maximum wavelength is indicative of conversion to a denatured double strand. The conformational change of DNA upon interacting with nanoparticles has also been investigated by others (Ghosh *et al.*, 2007, Goodman *et al.*, 2006, Railsback *et al.*, 2012) Presumably, pDNA behavior in our study may be comparable to molecular dynamics simulations by Railsback et al., who demonstrated groove specific interaction of cationic gold nanoparticles with DNA, that bend and separate dsDNA strands upon binding (Railsback *et al.*, 2012). Highly charged nanoparticle binding to dsDNA appears to be mediated by a combination of electrostatic and van der Waals force interactions (Goodman *et al.*, 2006). Van der-Waals component of interaction

involves disruption of Watson-Crick base pairing, while charged groups bind to the phosphate backbone of DNA and induce significant bending along the helical curve of the DNA strands (Railsback *et al.*, 2012). It has been shown that thermal denaturation and enzymatic degradation of DNA is significantly inhibited in the presence of cationic nanoparticles (Kamata *et al.*, 2011, Oster *et al.*, 2005). However, it was shown elsewhere that maintenance of the helical structure is required for the recognition of its promoter sequence and subsequent RNA transcript synthesis (Goodman *et al.*, 2006). Therefore studying the recovery of DNA secondary structure is an essential aspect when using cationic nanoparticles as delivery vectors. We further evaluated if the secondary structure of the plasmid was recovered after desorption from the TMC nanoparticles. Indeed, CD showed the release of pDNA in its native form from the particle surface by an increase in ellipticity at 280 nm and a DNA conformation which is identical to the helical CD spectrum of the DNA control sample.

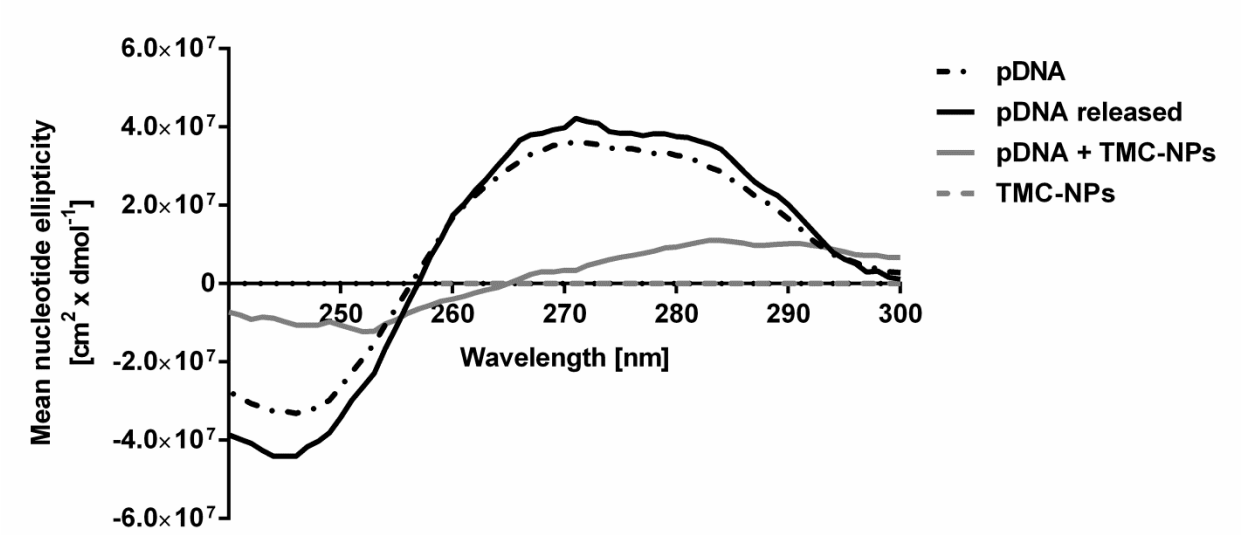

Figure 7. Effect of adsorption to TMC nanoparticles (TMC-NPs) on the secondary structure of pDNA. Circular dichroism of PBS and TMC-NPs (controls), pDNA in PBS, pDNA adsorbed to TMC-NPs, and pDNA after release from TMC-NPs.

4. Conclusion

The purpose of this study was to clarify the effects of cationic TMC nanoparticles on the denaturation and renaturation of DNA and its colloidal stability in aqueous solutions and after freeze-drying. The stability study to assess the formulations' behavior in suspension to proceed to further experiments showed that TMC nanoparticles remained suspended for 24 hours without changes in their physicochemical properties. For further pharmaceutical development, freeze-drying and storage in the presence of 1 % sucrose solution was proven to be appropriate to preserve TMC nanoparticle characteristics during long-term storage. Changes in the secondary structure of pDNA upon adsorption to TMC nanoparticles were observed that were shown to be reversible, suggesting an intact double strand after release from the carriers.

References

Abdelwahed, W., Degobert, G., Stainmesse, S., and Fessi, H. (2006). Freeze-drying of nanoparticles: formulation, process and storage considerations*, Advanced Drug Delivery Reviews,* 58, pp. 1688-1713.

Allison, S.D. and Anchordoquy, T.J. (2001). Maintenance of nonviral vector particle size during the freezing step of the lyophilization process is insufficient for preservation of activity: insight from other structural indicators*, Journal of Pharmaceutical Sciences,* 90, pp. 1445-1455.

Amidi, M., Romeijn, S.G., Borchard, G., Junginger, H.E., Hennink, W.E., and Jiskoot, W. (2006). Preparation and characterization of protein-loaded N-trimethyl chitosan nanoparticles as nasal delivery system*, Journal of Controlled Release,* 111, pp. 107-116.

Aulton, M.E. and Taylor, K.M. (2013) *Aulton's pharmaceutics: the design and manufacture of medicines,* 4th Ed. (Elsevier Health Sciences, UK).

Borchard, G. (2001). Chitosans for gene delivery*, Advanced Drug Delivery Reviews,* 52, pp. 145-150.

Brus, C., Kleemann, E., Aigner, A., Czubayko, F., and Kissel, T. (2004). Stabilization of oligonucleotide–polyethylenimine complexes by freeze-drying: physicochemical and biological characterization*, Journal of Controlled Release,* 95, pp. 119-131.

Chang, Y., Xiao, L., and Du, Y. (2009). Preparation and properties of a novel thermosensitive N-trimethyl chitosan hydrogel*, Polymer Bulletin,* 63, pp. 531-545.

Derjaguin, B. and Landau, L. (1993). Theory of the stability of strongly charged lyophobic sols and of the adhesion of strongly charged particles in solutions of electrolytes*, Progress in Surface Science,* 43, pp. 30-59.

Drogoz, A., David, L., Rochas, C., Domard, A., and Delair, T. (2007). Polyelectrolyte complexes from polysaccharides: formation and stoichiometry monitoring*, Langmuir,* 23, pp. 10950-10958.

Ferraro, B., Morrow, M.P., Hutnick, N.A., Shin, T.H., Lucke, C.E., and Weiner, D.B. (2011). Clinical applications of DNA vaccines: current progress*, Clinical Infectious Diseases,* 53, pp. 296-302.

Fuller, D.H., Loudon, P., and Schmaljohn, C. (2006). Preclinical and clinical progress of particle-mediated DNA vaccines for infectious diseases*, Methods,* 40, pp. 86-97.

Ghosh, P.S., Han, G., Erdogan, B., Rosado, O., Krovi, S.A., and Rotello, V.M. (2007). Nanoparticles Featuring Amino Acid-functionalized Side Chains as DNA Receptors*, Chemical biology & drug design,* 70, pp. 13-18.

Goodman, C.M., Chari, N.S., Han, G., Hong, R., Ghosh, P., and Rotello, V.M. (2006). DNA-binding by Functionalized Gold Nanoparticles: Mechanism and Structural Requirements*, Chemical biology & drug design,* 67, pp. 297-304.

Hansson, A., Di Francesco, T., Falson, F., Rousselle, P., Jordan, O., and Borchard, G. (2012). Preparation and evaluation of nanoparticles for directed tissue engineering*, International Journal of Pharmaceutics,* 439, pp. 73-80.

Heuking, S. and Borchard, G. (2012). Toll-like receptor-7 agonist decoration enhances the adjuvanticity of chitosan–DNA nanoparticles*, Journal of Pharmaceutical Sciences,* 101, pp. 1166-1177.

Heuking, S., Iannitelli, A., Di Stefano, A., and Borchard, G. (2009). Toll-like receptor-2 agonist functionalized biopolymer for mucosal vaccination*, International Journal of Pharmaceutics,* 381, pp. 97-105.

Huygen, K., Liu, M.A., Montgomery, D., and Ulmer, J. (1998). Polynucleotide tuberculosis vaccine, U.S. Patent No. 5,736,524.

Kamata, H., Zinchenko, A., and Murata, S. (2011). Effects of cationic and anionic nanoparticles on the stability of the secondary structure of DNA*, Colloid and Polymer Science,* 289, pp. 1329-1335.

Köping-Höggård, M., Vårum, K., Issa, M., Danielsen, S., Christensen, B., Stokke, B., and Artursson, P. (2004). Improved chitosan-mediated gene delivery based on easily dissociated chitosan polyplexes of highly defined chitosan oligomers*, Gene therapy,* 11, pp. 1441-1452.

Kukarin, A., Rong, M., and McAllister, W.T. (2003). Exposure of T7 RNA polymerase to the isolated binding region of the promoter allows transcription from a single-stranded template*, Journal of Biological Chemistry,* 278, pp. 2419-2424.

Minagawa, K., Matsuzawa, Y., Yoshikawa, K., Matsumoto, M., and Doi, M. (1991). Direct observation of the biphasic conformational change of DNA induced by cationic polymers*, FEBS letters,* 295, pp. 67-69.

Oster, C.G., Kim, N., Grode, L., Barbu-Tudoran, L., Schaper, A.K., Kaufmann, S.H.E., and Kissel, T. (2005). Cationic microparticles consisting of poly(lactide-co-glycolide) and polyethylenimine as carriers systems for parental DNA vaccination*, Journal of Controlled Release,* 104, pp. 359-377.

Patrulea, V., Applegate, L.A., Ostafe, V., Jordan, O., and Borchard, G. (2015). Optimized synthesis of O-carboxymethyl-N, N, N-trimethyl chitosan*, Carbohydrate Polymers,* 122, pp. 46-52.

Railsback, J.G., Singh, A., Pearce, R.C., McKnight, T.E., Collazo, R., Sitar, Z., Yingling, Y.G., and Melechko, A.V. (2012). Weakly charged cationic nanoparticles induce DNA bending and strand separation*, Advanced materials,* 24, pp. 4261-4265.

Sonia, T. and Sharma, C.P. (2011) *Chitosan for Biomaterials I* eds. R. Jayakumar, M. Prabaharan, and Muzzarelli R. A. A., 243 “Chitosan and its derivatives for drug delivery perspective", (Springer Verlag, Germany) pp. 23-53.

Steitz, T.A. (2004). The structural basis of the transition from initiation to elongation phases of transcription, as well as translocation and strand separation, by T7 RNA polymerase*, Current opinion in structural biology,* 14, pp. 4-9.

Szymańska, E. and Winnicka, K. (2015). Stability of Chitosan—A Challenge for Pharmaceutical and Biomedical Applications*, Marine Drugs,* 13, pp. 1819-1846.

Talsma, H., Cherng, J.-Y., Lehrmann, H., Kursa, M., Ogris, M., Hennink, W.E., Cotten, M., and Wagner, E. (1997). Stabilization of gene delivery systems by freeze-drying*, International Journal of Pharmaceutics,* 157, pp. 233-238.

Tanghe, A., Lefèvre, P., Denis, O., D’Souza, S., Braibant, M., Lozes, E., Singh, M., Montgomery, D., Content, J., and Huygen, K. (1999). Immunogenicity and Protective Efficacy of Tuberculosis DNA Vaccines Encoding Putative Phosphate Transport Receptors*, The Journal of Immunology,* 162, pp. 1113-1119.

Theodossiou, I. and Thomas, O.R. (2002). DNA-induced inter-particle cross-linking during expanded bed adsorption chromatography: Impact on future support design*, Journal of Chromatography A,* 971, pp. 73-86.

Verheul, R.J., Amidi, M., van der Wal, S., van Riet, E., Jiskoot, W., and Hennink, W.E. (2008). Synthesis, characterization and in vitro biological properties of O-methyl free N,N,N-trimethylated chitosan*, Biomaterials,* 29, pp. 3642-3649.

Woody, R.W. (2010). *Instrumental analysis of intrinsically disordered proteins: Assessing structure and conformation,* eds. V.N. Uversky and Longhi S., Chapter 10 “Circular dichroism of intrinsically disordered proteins”, (Wiley, US) pp. 303-321.

Yeh, M.-K., Cheng, K.-M., Hu, C.-S., Huang, Y.-C., and Young, J.-J. (2011). Novel protein-loaded chondroitin sulfate–chitosan nanoparticles: preparation and characterization*, Acta Biomaterialia,* 7, pp. 3804-3812.

Zanchet, D., Micheel, C.M., Parak, W.J., Gerion, D., and Alivisatos, A.P. (2001). Electrophoretic isolation of discrete Au nanocrystal/DNA conjugates*, Nano Letters,* 1, pp. 32-35.

Chapter III:

Nanocarriers for DNA vaccines: co-delivery of TLR-9 and NLR-2 leads to synergistic enhancement of proinflammatory cytokine release

Johanna Poecheim[a], Simon Heuking[b], Livia Brunner[b], Christophe Barnier-Quer[b], Nicolas Collin[b], Gerrit Borchard[a]

[a] *School of Pharmaceutical Sciences, University of Geneva, University of Lausanne, Quai Ernest Ansermet 30, 1211 Geneva, Switzerland*

[b] *Vaccine Formulation Laboratory, Department of Biochemistry, University of Lausanne, Chemin des Boveresses 155, 1066 Epalinges, Switzerland*

Published in: Poecheim, J., Heuking, S., Brunner, L., Barnier-Quer, C., Collin, N., and Borchard, G. (2015). Nanocarriers for DNA vaccines: co-delivery of TLR-9 and NLR-2 ligands leads to synergistic enhancement of proinflammatory cytokine release, *Nanomaterials*, *5*, pp. 2317-2334.

Abstract

Three cationic nanoparticle formulations were evaluated for their potential as carriers for plasmid DNA (pDNA) encoding antigen 85A of *Mycobacterium tuberculosis (Mtb)*. The formulations included (1) nanoparticles prepared from trimethyl chitosan (TMC), (2) a cationic squalene-in-water nanoemulsion prepared with DOTAP and (3) the commercially available cationic oil-in-water nanoemulsion Cationorm®. The adjuvant effect of the different pDNA-nanoparticle complexes was evaluated and compared *in vivo* by serum antibody analysis of immunized mice. pDNA as applied in these formulations naturally contain immunostimulatory unmethylated CpG motifs that are recognized by Toll-like receptor 9 (TLR-9). In mechanistic *in vitro* studies, activation of TLR-9 was investigated along with MDP as second immunostimulator for nuclear-binding domain (NOD)-like receptor 2 (NLR-2) targeting. The ability to enhance immunogenicity of the pDNA-nanoparticle complexes by simultaneous targeting of TLR-9 and NLR-2 was determined by pro-inflammatory cytokine release in RAW264.7 macrophages. Blocking of RIP-2 kinase of the NLR-2 pathway was accomplished to show dependency of NOD2 activation on synergistic enhancement of innate immune responses during co-stimulation of pDNA with MDP. In conclusion, it could be demonstrated that all carriers display a strong adjuvant effect *in vivo*, however, only TMC nanoparticles were capable to bias immune responses towards Th1 dependent cellular immune responses. In the *in vitro* model, pDNA in combination with MDP, delivered with all three cationic nanocomplexes was shown to significantly increase pro-inflammatory cytokine release in a synergistic manner, dependent on NLR-2 activation. In summary, we could develop pDNA loaded nanoparticle formulations to induce cell-mediated immune responses in mice and demonstrated *in vitro* how sophisticated combinations of TLR and NLR agonists can lead to increase of the carriers' adjuvanticity.

1. Introduction

Vaccination by direct injection of plasmid DNA (pDNA) encoding bacterial and viral antigens has been tested against various infectious diseases. Several preclinical studies were promising, showing that these so-called DNA vaccines can trigger not only humoral but also cell-mediated immunity in animals (Kutzler and Weiner, 2008). Generally, DNA vaccines consist of a bacterial plasmid vector that is genetically modified to express selected antigens of the pathogen in the absence of the other bacterial components present in traditional attenuated and live vaccines. Therefore genetic vaccines are considered to be advantageous over traditional vaccines in terms of safety and specificity (Shedlock and Weiner, 2000). However, although proven to be safe and well tolerated, clinical trials demonstrated that first-generation DNA vaccines failed to demonstrate sufficient vaccine-specific immunity in humans (Le *et al.*, 2000, MacGregor *et al.*, 2002, Wang *et al.*, 1998). The low immunogenicity of these DNA vaccines is hypothesized to be due to suboptimal delivery of the plasmids to antigen presenting cells. Current research attempts to focus on developing novel strategies to improve immunogenicity by formulating pDNA with delivery systems and immunologic adjuvants (Rottinghaus *et al.*, 2003, Sasaki *et al.*, 1998). Particle based adjuvants are known to offer high carrier capacity acting as delivery vehicles for pDNA to enhance plasmid stability and uptake into cells (Giljohann *et al.*, 2007, Lee, 2013). Moreover, versatility of particulate carriers in terms of size, surface charge, and material, enables tailoring according to the desired outcome of immune responses (Cui and Mumper, 2003, Poecheim and Borchard, 2015, O'Hagan *et al.*, 2001). Another advantage of nano- and microparticles might be the induction of local chemotaxis to the immunization site due to the promotion of a depot effect (Denis-Mize *et al.*, 2003). Our approach was to adsorb pDNA at the outer surface of diverse cationic nanoparticles, to avoid steric shielding effects by encapsulating pDNA, while still making use of the potential adjuvant effects of nanoparticles as delivery systems.

Among various existing particle-based formulations, three cationic nanocomplexes, offering different structural characteristics, were chosen for this study, to evaluate the most suitable formulation to improve DNA vaccination. Accordingly, N-trimethyl chitosan (TMC) nanoparticles, a cationic squalene-in-water nanoemulsion (named SWE06) and the commercially available cationic nanoemulsion Cationorm® were compared for their adjuvant potential to increase immunogenicity of pDNA. Chitosan-based particles have been used previously as DNA delivery systems, with pDNA entrapped inside the nanoparticles, to maintain the cationic surface charge, which can be beneficial for mucosal application of DNA vaccines (Heuking and Borchard, 2012, Kumar *et al.*, 2002). However, preliminary *in vivo* studies from our lab with such formulations could not demonstrate higher immunogenicity over non-adjuvanted pDNA, when administered intramuscularly. The strong electrostatic charge interaction of condensed pDNA with the cationic polymer may have led to difficulties of DNA release once the polyplex is taken up by the cell, at the site of action. Squalene based oil-in-water emulsions have already been approved for human use in influenza vaccines (Egli *et al.*, 2014, FDA, 2013). The cationic phospholipid 1,2-dioleoyl-3-trimethylammonium-propane (DOTAP) was added to the hydrophobic phase of the squalene-in-water nanoemulsion (SWE06) to obtain positively charged oil droplets. Cationorm® was chosen as a third type of nanoformulation, as it is known to be safe in ophthalmic applications (Lallemand *et al.*, 2012). Therefore it was expected to be a non-toxic example for inert mineral oil-in-water nanoemulsions, with cetalkonium chloride accounting for the positive charge. The rational of using Cationorm® as an adjuvant for parenteral delivery of pDNA was to achieve a similar effect as the potent mineral oil based Freund's adjuvant, without safety concerns (Coffman *et al.*, 2010).

DNA vaccines promote exogenous major histocompatibility complex (MHC) class II-restricted, as well as endogenous (MHC class I-restricted) antigen presentation, which mimics antigen processing induced by intracellular pathogens such as *Mycobacterium tuberculosis (Mtb)* (Bruffaerts *et al.*, 2014). Protection against *Mtb* is known to be

mediated by cellular immunity, in which proinflammatory cytokines and Th1 cells play a pivotal role. Among Th1 cytokines, IFN-γ and TNF-α were identified as the most important agents in mycobacterial control, acting synergistically in the activation of macrophages (Appelberg, 1994, Cavalcanti *et al.*, 2012). The cellular immune system can specifically be targeted by immunostimulatory adjuvants resembling certain antigenic structures of the pathogen. The innate immune system has evolved to recognize conserved pathogen-associated molecular structures by pattern recognition receptors (PRRs), mainly represented by Toll-like receptors (TLRs) and NOD-like receptors (NLRs). Recognition of bacteria, as well as vaccination with live attenuated vaccines, induces activation of multiple PRRs, triggering different signaling pathways, which has been shown to be more effective in establishing immune responses than activation of a single pathway alone (Querec *et al.*, 2006). Unmethylated CpG sequences present on bacterial pDNA are recognized by endosomal membrane-bound TLR-9, whereas muramyl dipeptide, a bacterial cell wall component, stimulates cytosolic NLR-2. TLR-9 activates the MyD88-dependent pathway, while NLR-2 activation leads to recruitment of receptor-interacting protein 2 (RIP-2) kinase (Coulombe, 2009, West). There is documentation on cross-talk of TLR and NLR signaling through RIP-2, demonstrating extensive activation of immune cells in a synergistic manner by simultaneous co-activation of these two pathways (Archer *et al.*, 2010, Chin *et al.*, 2002, Kobayashi *et al.*, 2002, Uehara *et al.*, 2005).

To our knowledge the adsorption of *Mtb* antigen 85A (Ag85A) encoding pDNA to TMC nanoparticles, SWE06, and Cationorm® is a novel approach to increase immunogenicity of this DNA vaccine. The aim was to compare these cationic nanoparticle formulations as pDNA delivery systems to increase Th1 related immune responses against Ag85A in a preliminary proof of concept study in mice. Following *in vivo* screening, the second objective was to exploit the potential of concurrent activation of two non-redundant PRR pathways to potentially optimize and further enhance cell-mediated immunity by innate immune activation. Therefore, mechanistic

investigations of TLR-9 targeting by unmethylated CpG sequences present on pDNA, together with MDP as a second immunostimulatory agent for NLR-2 activation were performed in RAW264.7 murine macrophages as an *in vitro* model. Hence, RIP-2 kinase of the NLR-2 pathway was blocked to show dependency of NOD2 activation on synergistic enhancement of innate immune responses during co-stimulation of pDNA with MDP.

2. Materials and methods

2.1 Materials

Chitosan (79 % degree of deacetylation, ChitoClear Cg10, 7 – 15 mPa s) was purchased from Primex (Siglufjordur, Iceland). Methyl iodide and chondroitin sulfate and bovine serum albumin (BSA, endotoxin <0.1 ng/mg) were obtained from Sigma-Aldrich (Buchs, Switzerland). DOTAP was purchased from Avanti Polar Lipids (Alabaster, AL, USA) and Cationorm® (Novagali Pharma, Evry, France) was purchased at a local pharmacy (Collonges-sous-salève, France). Double stranded 5853 bp pDNA encoding Ag85A was provided by the Institute Pasteur (Brussels, Belgium), propagated in NovaBlue competent cells (Novagene, Merck, Darmstadt Gernamy) that were kindly provided by Prof. L. Scapozza (University of Geneva, Geneva, Switzerland). The plasmid was then purified by using an Endofree Plasmid Giga Kit (Quiagen, France) according to the manufacturer's protocol and suspended in PBS. Goat anti-mouse total IgG, IgG1, IgG2b and IgG2c conjugated to horseradish peroxidase (HRP) was obtained from Southern Biotech (Birmingham, AL, USA) and 3,3',5,5'-Tetramethylbenzidine (TMB) substrate from (Becton Dickinson, CA, USA). Recombinant Ag85A protein (rAg85A) was obtained through BEI Resources, National Institute of Allergy and Infectious Diseases (NIAID), National Institute of Health (NIH), Bethesda, MD, USA. All cell culture reagents were provided by Life technologies (Zug, Switzerland) and Sigma-Aldrich (Buchs, Switzerland) and XTT-cell proliferation kit II was bought from Roche (Basel, Switzerland). MDP, as well as LPS-EB, CpG-free pDNA (pCpGfree-giant) and

inactive MDP (D-MDP) as controls, and RIP-2 tyrosin kinase inhibitor gefitinib were purchased from Invivogen (San Diego, CA, USA). For proinflammatory cytokine detection in cell supernatants, mouse TNF-α ELISA Ready-SET-Go! Kit was obtained from eBioscience (Paris, France).

2.2 Preparation of nanoparticle formulations

TMC nanoparticles: TMC was synthesized from chitosan by quaternisation of the amino groups based on the method first published by Domard et al. (Domard *et al.*, 1986), and later modified by Heuking et al. (Heuking *et al.*, 2009). In this study only one methylation step was employed for the synthesis procedure of TMC. Briefly, 2 g of high molecular weight chitosan of crustacean origin were trimethylated through nucleophilic substitution by addition of 12 ml methyl iodide for 70 min at 60 °C under reflux. TMC nanoparticles were prepared by polyelectrolyte complexation with chondroitin sulfate according to Schatz et al (Schatz *et al.*, 2004). (Schatz *et al.*, 2004). TMC (5 mg/ml) and chondroitin sulfate (1 mg/ml) were solubilized separately in water at room temperature and filtered through 0.22 µm syringe filters (Millipore AG, Zug, Switzerland). Equal volumes of each polymer solution were mixed, briefly vortexed at maximum speed, and the resulting nanoparticle suspension diluted 1:10 with the appropriate media. In case of nanoparticles containing MDP the dipeptide was mixed with the TMC solution before particle formation. The final MDP concentration per ml nanoparticle suspension was 30 µg. For pDNA adsorption, 50 µg/ml of the plasmid were incubated for 15 minutes at 4 °C with the TMC nanoparticle suspensions.

Nanoemulsions SWE06 and Cationorm®: Cationic SWE06 was manufactured by the Vaccine Formulation Laboratory at the University of Lausanne (Epalinges, Switzerland) and contained 0.1 % DOTAP, 3.9 % (w/v) squalene, 0.5 % (w/v) Tween® 80 and 0.5 % (w/v) Span® 85 in saline. The third nanoparticle formulation investigated was Cationorm® developed by Novagali Pharma (now Santen), an oil-in-water nanoemulsion composed of 0.1 % poloxamer 188, 0.3 % tyloxapol, 0.002 % cetalkonium chloride, 1 % mineral oils and 1.6 % glycerol in Tris hydrochloride buffer as

indicated in the decision report of the French National Authority for Health (HAS, 2013). Cationorm® obtained a marketing authorization in Europe for the treatment of dry eye symptoms (Lallemand et al., 2012). Both nanoemulsion formulations were diluted at a ratio of 1:100 with the appropriate media prior to each experiment. pDNA was incubated for 15 minutes at 4 °C with the nanoemulsions to obtain electrostatic binding of pDNA to the cationic nanodroplets and a final pDNA concentration of 50 ug/ml. For the MDP containing nanoemulsion formulations, the dipeptide was simply mixed with the emulsion to obtain a final concentration of 30 µg/ml, then vortexed at high speed, and immediately applied in the experiments. According to Endosafe® Test Record all three nanoparticle suspensions showed an endotoxin level < 1 EU/ml.

2.3 Particle size, zeta potential and morphology of nanocarriers

Hydrodynamic diameters and polydispersity index (PDI) were determined by dynamic light scattering measurements and zeta potential by electrophoresis and laser light scattering using a Zetasizer Nano ZS (Malvern Instruments, Worcestershire, U.K.). Samples were diluted ten times in 1 mM NaCl to achieve a constant ionic background and measured at 25 °C in clear disposable zeta cells. The morphology of dried TMC nanoparticles was imaged with scanning electron microscopy (SEM; Jeol JSM-7001FA, Tokyo, Japan) at an accelerating voltage of 15 kV. The samples were 1000-fold diluted with water, placed on a grid, and air-dried overnight under vacuum. The grids were sputter coated with 10 nm gold under vacuum before imaging (Leica EM SCD 500). SWE06 and Cationorm® nanoemulsions were stained with uranyl acetate and their morphology examined by transmission electron microscopy at 200 kV (TEM; Tecnai G2 T20 Sphera, FEI, Hillsboro, OR, USA).

To assess the particle area and radius, microscopic images were analyzed using ImageJ 1.46r software (National Institute of Health, Bethesda, MD, USA). Assuming that the nanostructures are roughly spherical their radius was calculated from the particle areas, and subsequently their diameters, according to the following equations:

Eq. 1 $r = \sqrt{\frac{A}{\pi}}$

Eq. 2 $d = 2\,r$

2.4 Loading efficiency

The adsorption rate of pDNA (50 µg/ml) onto nanoparticles was evaluated. Nanoparticle suspensions were centrifuged at 14,000 rpm for 15 min (Eppendorf 5810R, Vaudaux-Eppendorf, Basel, Switzerland) and unloaded pDNA in the supernatant was quantified by PicoGreen assay according to the manufacturer's protocol. A calibration curve was established by plotting the fluorescence intensity of each standard over the concentration series. The samples were excited at a wavelength of 480 nm and the fluorescence emission intensity was measured at 520 nm using a fluorescence microplate reader (Tecan Group Ltd., Männedorf, Switzerland). The amount of pDNA adsorbed on TMC nanoparticles or nanoemulsions was calculated by subtracting the pDNA quantity found in the supernatants or in the oil phase after centrifugation, from the amount of pDNA initially added.

2.5 *In vivo* immunogenicity of pDNA-nanoformulations

Female C57BL/6 mice (Harlan, Itingen, Switzerland) were maintained under standardized conditions in the animal facility of the Department of Biochemistry (University of Lausanne, Epalinges, Switzerland). The study was done according to the guidelines of the authorization N° 2475 of the Service de la consommation et des affaires vétérinaires (SCAV, Lausanne, Switzerland). The formulations were prepared as described above, diluted with phosphate buffered saline (PBS) and pDNA at a final concentration of 50 µg per dose was applied. Eight week old mice (n = 4 per group) were immunized on days 0, 21, and 42 with a dose of 50 µl by intramuscular administration in the hind limb. The mice were bled 1 week after the second boost immunization by cardiac puncture and sera were stored at -20 °C. Anti-Ag85A-specific serum IgG titers and IgG isotypes 1, 2b, and 2c were determined by ELISA at the

endpoint of the optical density-log dilution curves. Non-responding mice were given an arbitrary titer of 1. Briefly, the antibody ELISA involved coating of 96-well microtiter plates (Nunc, Roskilde, Denmark) with 1 µg/ml rAg85A in PBS over night at 4 °C, followed by blocking of the wells with 1% (w/v) BSA in PBS for 2 h at room temperature (RT) to reduce nonspecific binding and subsequent addition of serial dilutions of serum ranging from 100 to 2.2 x 10^5 for 1 h at RT. Ag85A specific antibodies were detected by incubating HRP conjugated goat anti-mouse IgG, IgG1, IgG2b or IgG2c (1h, RT) and by developing plates with TMB for 5 min at RT in the dark. The reaction was stopped with 1 N sulfuric acid and absorbance was determined at 450 nm with an iMARK micro plate reader (Bio-Rad Laboratories, Hercules, CA, USA).

2.6 Cell culture

The murine macrophage cell line RAW264.7 was obtained from American Type Culture Collection (ATCC, Rockville, MD, USA) and used for the following *in vitro* cell studies. The cells were cultured in full cell culture medium based on DMEM, supplemented with 10 % heat-inactivated fetal calf serum (FCS) and 1 % penicillin/streptomycin, at 37 °C in an atmosphere containing 5% CO_2. Cells were seeded at an initial density of 3 x 10^4 cells per well in a 96-well plate, if not indicated otherwise.

2.7 *In vitro* cytotoxicity and cytokine release assays

Potential cytotoxic effects of the nanoparticle formulations were evaluated by XTT assay to determine cell viability following nanoparticle exposure. RAW264.7 cells were cultured with the nanoformulations for 24 h. Additionally, positive controls were run in parallel, *SDS* 0.2% for cytotoxicity and LPS (5 ug/ml) for proinflammatory cytokine release. The cell supernatants were withdrawn for cytokine analysis, replaced by XTT reagent and incubated for another 5 h at 37 °C. The mean OD value of the wells was determined by measuring at a wavelength of 490 nm using a microplate spectrophotometer reader (Power Wave XS, Biotek, France) and corrected by the

blank value. The relative cell viability was expressed as a *percentage* relative to untreated control cells cultured under the same conditions.

Cell supernatants from the cell viability assay as described above were centrifuged at 300 x g for 5 min and frozen at -80 °C prior to analysis. TLR-9 and NLR-2 control samples included nanoparticle complexes, formed with pCpGfree and D-MDP. Both control ligands were applied at the same concentrations as pDNA and MDP, respectively. For NLR-2 pathway inhibition, cells were pretreated with 100 nM gefitinib for 1 h before stimulation with the nanoparticle formulations. Cell supernatants of all cytokine release experiments were diluted 1:10 and TNF-alpha (TNF-α) induction determined by mouse TNF-α sandwich ELISA, according to the manufacturer's instruction. Cytokine concentrations were calculated against a standard curve prepared in duplicates.

2.8 Statistical analysis

The statistical significance for all *in vitro* experiments, measuring TNF-α release, was assessed by Student's t-test for two samples, assuming equal variance. Experiments were repeated at least once and data evaluated are mean values of triplicate samples. Antibody titers were logarithmically transformed before statistical analysis. All *in vivo* data, measuring IgG antibody titers, were analyzed by a two-tailed Mann-Whitney test to demonstrate significant differences between the experimental groups (n=4). The statistical analysis was carried out using *GraphPad Prism 6* software (GraphPad, San Diego, CA, USA) and p values less than 0.05 were considered to be significant.

3. Results and Discussion

3.1 Nanoparticle characterization

The formulations were characterized for their size expressed in Z-average (nm), PDI, and the charge as Zeta-potential (mV), as shown in Table 1. The mean hydrodynamic

diameter of the mere unloaded polymer complexes and nanodroplets was between 133 - 216 nm (PDI ≤ 0.2) and their surface charge was positive, ranging between +18 and +31 mV. After adsorption of pDNA the size increased for all formulations, while the Zeta-potential decreased drastically to negative values. While addition of MDP did not have any influence on size and zeta potential, PDI values for TMC nanoparticles increased slightly. PDIs between 0.1 and 0.5 were observed for all nanoparticle formulations, corresponding to systems of mid-range polydispersity (Gadad et al.). Only small amounts of pDNA were found in the supernatant, indicating pDNA adsorption of 99.8 % to TMC nanoaprticles, 95 % to SWE06, and 93 % to Cationorm® of initially added 50 µg/ml pDNA to the cationic nanocomplexes.

Table 2. Physicochemical properties of TMC nanoparticles, SWE06 and Cationorm®, either unloaded or loaded with pDNA, MDP, or both.

	TMC nanoparticles			SWE06			Cationorm®		
Loaded with:	Size (nm)	PDI	ζ (mV)	Size (nm)	PDI	ζ (mV)	Size (nm)	PDI	ζ (mV)
- (blank)	216 ± 2	0.1	31 ± 2	133 ± 2	0.1	27 ± 1	157 ± 3	0.2	18 ± 1
pDNA	252 ± 5	0.2	7 ± 5	188 ± 3	0.1	-14 ± 1	205 ± 2	0.3	-39 ± 0.5
MDP	215 ± 0.5	0.2	32 ± 4	134 ± 2	0.2	26 ± 1	156 ± 2	0.2	14 ± 0.2
pDNA and MDP	259 ± 3	0.2	4± 5	189 ± 3	0.2	-16 ± 1	267 ± 12	0.5	-41± 1

Electron microscopy of empty nanocarriers and associated particle size calculations revealed a size distribution that confirmed size measurements by DLS (Figure 1). Mean diameters determined by electron microscopy were slightly smaller than for DLS (192 ± 28 nm for TMC nanoparticles, 114 ± 37 nm for SWE06 and 126 ± 21 nm, respectively). This might be due to shrinking during preparation, which can affect the measurements of particle diameters (Bootz et al., 2004). TMC nanoparticles were of circular shape (Figure 1a), whereas the emulsions droplets were of subangular shape (Figure 1b and 1c). Upon pDNA adsorption TMC nanoparticles appeared to deform by loosening the electrostatically formed structure (Figure 1A). pDNA at the external site of nanoemulsion droplets make them distract due to charge repulsion and single droplets

and small groups of droplets appear (Figure 1B). Repulsion was also observed within pDNA loaded Cationorm®, however to a lesser extent (Figure 1C).

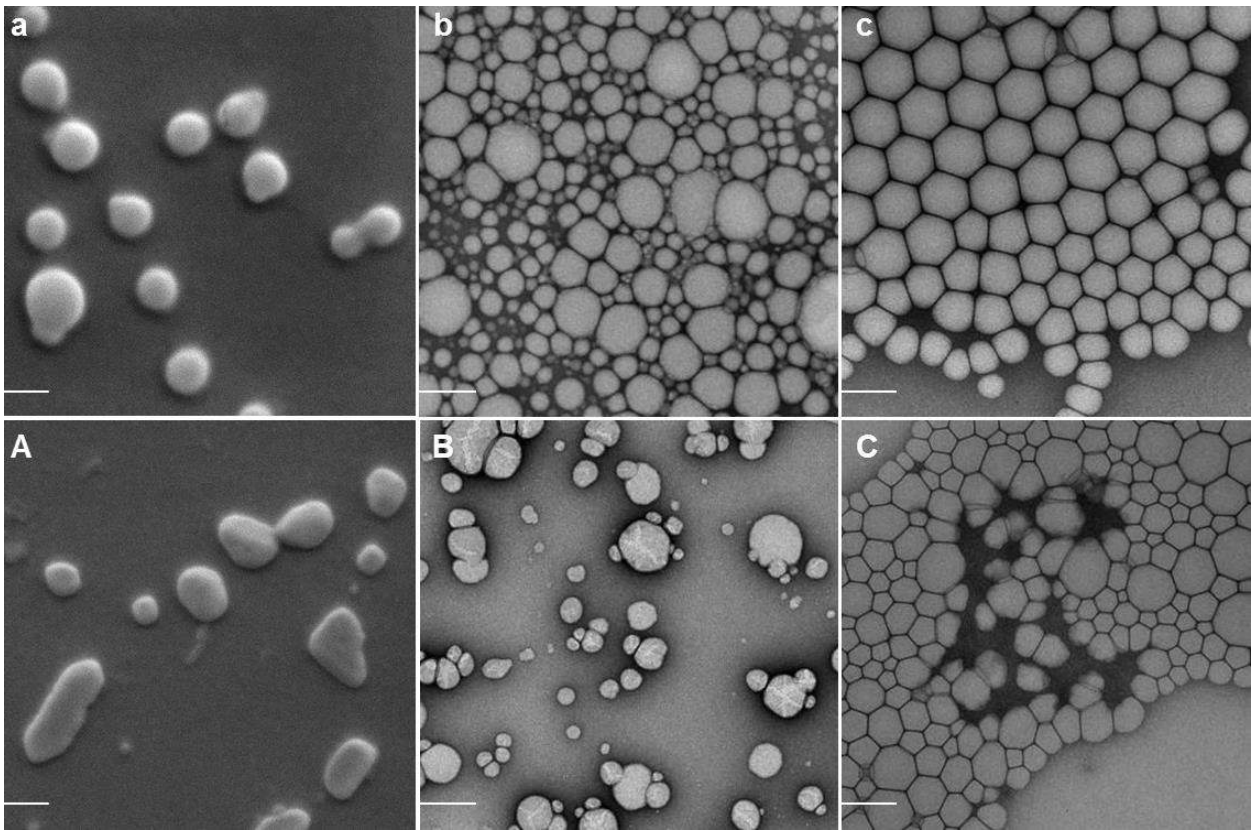

Figure 1. SEM images of plain TMC nanoparticles (a) and pDNA loaded TMC nanoparticles (A), TEM images of plain SWE06 (b) and SWE06 + pDNA (B), and TEM images of plain Cationorm® (c) and Cationorm® + pDNA (C). The scale bars represent a size of 200 nm.

3.2 Adjuvant effect of pDNA-nanoformulations *in vivo*

In a preliminary *in vivo* experiment TMC nanoparticles, SWE06 and Cationorm® applied with pDNA were sought to be evaluated for their potential to increase *Mtb* antigen-specific Th1 related immune responses of a tuberculosis DNA vaccine. A higher amount of pDNA was applied to achieve a detectable magnitude of antigen-specific antibodies and influence of the nanocomplexes on the outcome of these

immune responses in mice, dependent on the nature of the delivery systems. The adsorption rate of pDNA within these formulations was 43 to 44 %. Generally, antigen specific total IgG responses to pDNA in the adjuvanted groups were higher than those seen to naked pDNA. However, only in TMC nanoparticle vaccinated mice significantly increased titers of total IgG were observed in comparison with pDNA alone (Figure 2A). Oil-in-water emulsions based on squalene or mineral oils reportedly induce Th2 responses in protein vaccines (Fang and Hora, 2000, Ioannou *et al.*, 2002). Formulated with DNA both nanoemulsions promoted increase in Ag85A specific antibodies to pDNA without altering the balanced Th1/Th2 responses observed with naked pDNA (Figure 2). TMC nanoparticle adjuvanted pDNA delivery induced a clear bias of Th activation towards type 1. Th1 polarization of immune responses by TMC nanoparticle complexes with pDNA was indicated by detection of ratios of serum IgG2b/IgG1 (Figure 2B) and IgG2c/IgG1 (Figure 2C) titers above unity. According to the literature the adjuvant effect of TMC and chitosan on Th1/Th2 balance seems to be very dependent on the antigen applied, route of administration, or formulation as particles(Li *et al.*, 2013). Chitosan itself reveals Th2 adjuvant effects (Borchard *et al.*, 2012, Tokura *et al.*, 1999), whereas formulated as particles immune response are shifted towards Th1 (Slütter *et al.*, 2009, Strong *et al.*, 2002). Moreover, although we did not investigate the physical interaction between CpG containing pDNA, a TLR-9 ligand, and TMC, the physicochemical properties of chitin derivatives, known to activate PRRs such as TRL-2, Dectin-1, and the mannose receptor could mediate such interactions (Bueter *et al.*, 2013). It is tempting to speculate that the observed increase in Th1 type responses is dependent upon the triggering of distinct intracellular signals, which then merge to activate NF-kB, as has been demonstrated following stimulation of mannose receptors and TLR-2 in parallel to TLR-9 stimulation (Dan *et al.*, 2008). Whether this Th1 polarization results from the physical association of pDNA with TMC or the effect of enhanced uptake of pDNA through particle mediated delivery, remains to be determined.

These screening experiments suggest that physical or chemical association between pDNA and adjuvants may be necessary to impart Th1 adjuvanticity. In subsequent mechanistic experiments the inherent adjuvant effect of unmethylated CpG containing pDNA in combination with MDP as an additional immunostimulator, delivered with all three cationic nanocomplexes, was investigated to potentially further optimize cell-mediated immunity by simultaneous innate immune activation.

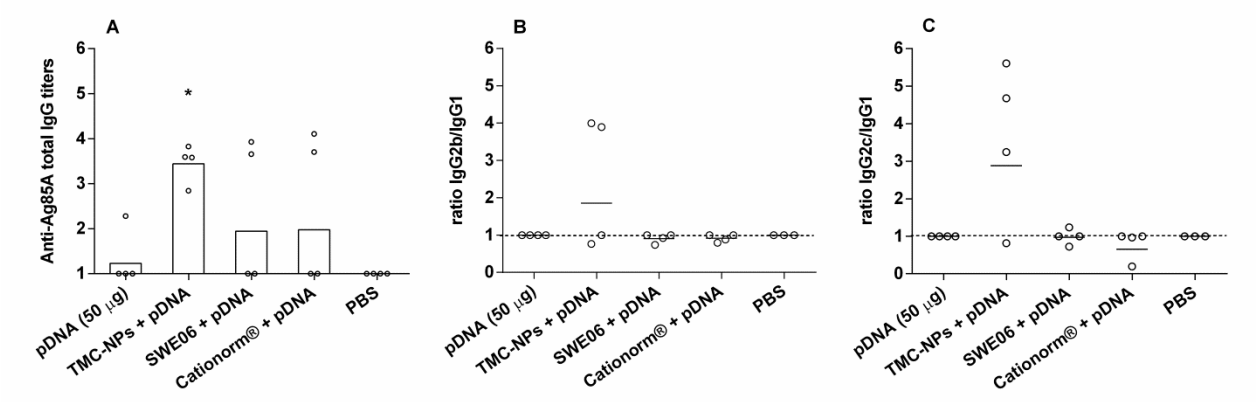

Figure 2. Immune responses in mice to pDNA (50 µg per dose) with/ without TMC nanoparticles one week after the 2nd booster injection (i.m.). Ag85A-specific serum IgG titers were analyzed by endpoint ELISA. Each ∘ symbol represents the log serum titer of an individual mouse (non-responding mice were given an arbitrary titer of 1). (A): Bars represent mean n=4 ± SEM, *p < 0.05, compared to pDNA alone. (B; C): Corresponding average Log IgG2b/ Log IgG1 and Log IgG2c/ Log IgG1 ratios are indicative for the quality of the immune response, where values higher than 1 (dotted line) characterize Th1 biased immune responses.

3.3 Cell viability

Cell viability after exposure to the different particle formulations for 24 h in culture were confirmed with XTT assays including Trypan blue dye exclusion, as shown in Figure 3. It is proposed that cationic nanoparticles interact with the cell membrane and may cause damage by membrane disruption, leading to cell death (Hwang *et al.*, 2015). Therefore investigation of the potential toxicity of the cationic nanoformulations was

needed, to exclude biological responses due to cell death and to assess safety concerns for *in vivo* applications. When uncomplexed TMC polymer was applied to the cells, reduced cell viability was observed (data not shown). Chondroitin sulfate partially balanced the cationic charge of TMC and cell viability to the resulting nanoparticles increased. This is in accordance with other studies that showed less toxicity by charge neutralization with anionic agents or pDNA (Heuking *et al.*, 2009, Kean *et al.*, 2005). No significant toxicity was detected for all nanoformulations, either unloaded, pDNA and/or MDP loaded, compared to the untreated control cells (viability >80 % in all cases). For TMC nanoparticles and SWE06 emulsions cell viability was slightly increased with pDNA loading compared to the unloaded formulations, which is probably due to neutralization of cationic surface charges known to be linked to better biocompatibility (Goodman *et al.*, 2004).

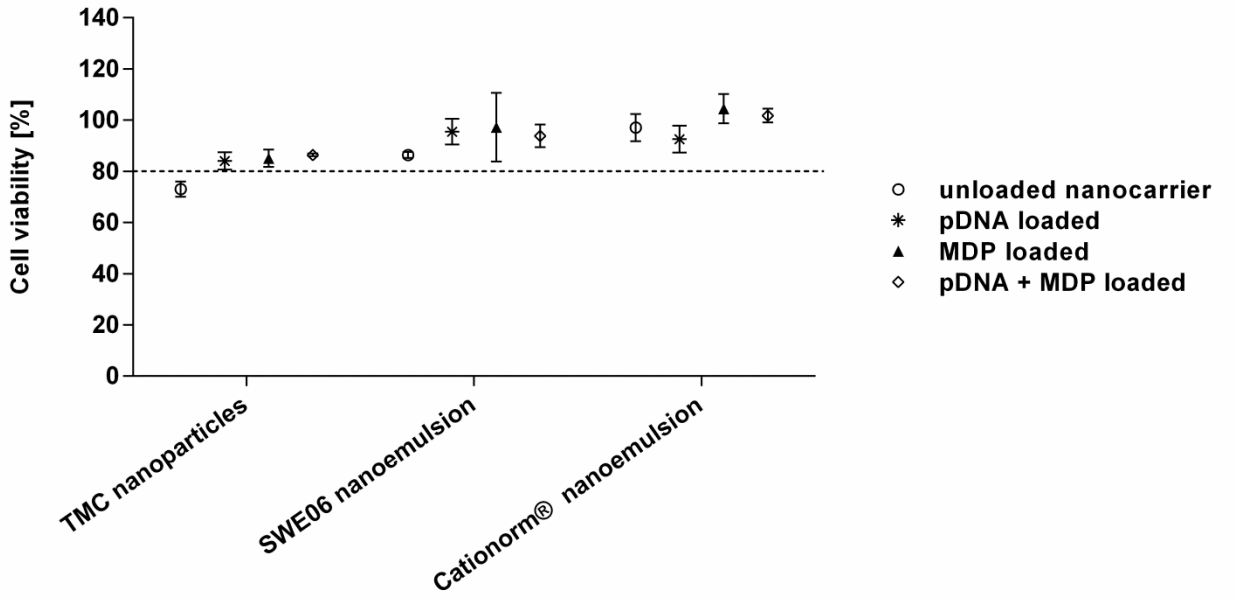

Figure 3. Cell viability of RAW264.7 macrophages, detected with XTT reagent, after 24h of incubation with the following formulations: unloaded TMC nanoparticles, SWE06 and Cationorm® (∘) and each nanoformulation loaded either with pDNA (∗), MDP (▲), or pDNA + MDP (⋄).

3.4 *In vitro* activation of TLR-9 and NLR-2

Optimization of adjuvanted pDNA with muramyl dipeptide was accomplished and tested on proinflammatory cytokine release *in vitro*. More precisely, synergistic enhancement of immune response by two PRR ligands was investigated using CpG islet containing pDNA for TLR-9 stimulation, and MDP as a NOD2 ligand. Emerging evidence suggests cooperative effects of PRRs (Petterson *et al.*, 2011). Consequently we also investigated the outcome of combined stimulation *via* the TLR and NLR systems. Neither pDNA nor MDP alone could substantially activate macrophages as shown in Figure 4. TMC nanoparticles loaded with pDNA were shown to significantly increase cytokine release, compared to pDNA alone ($p < 0.001$).

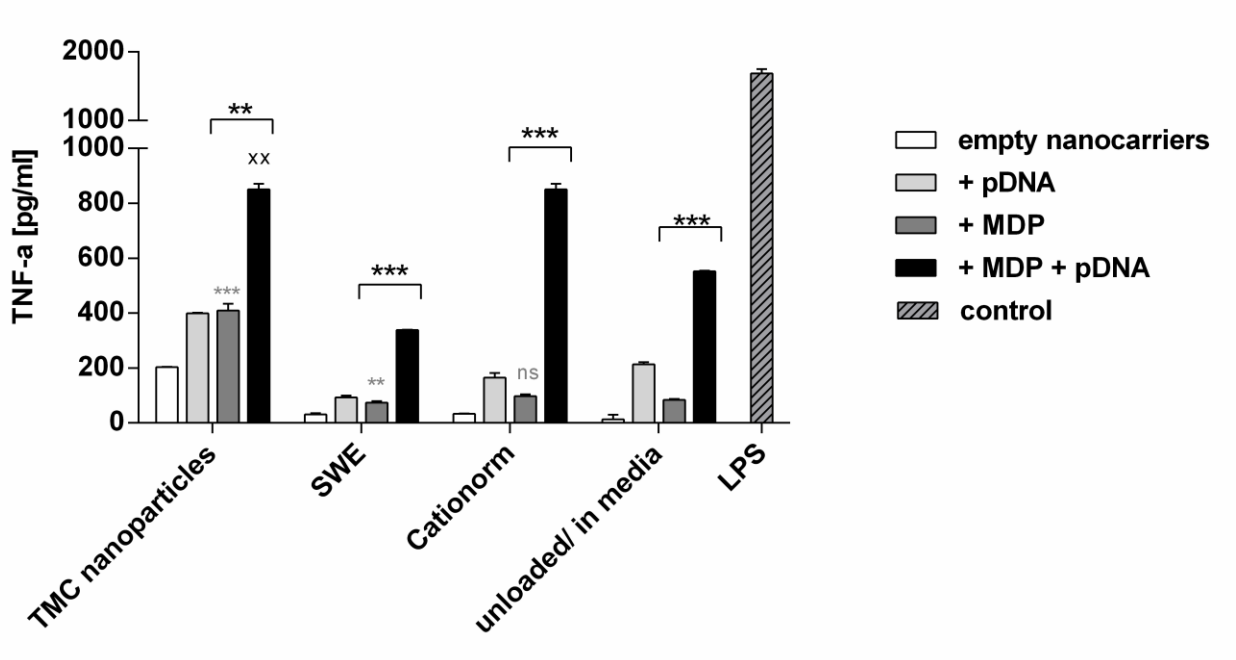

Figure 4. TNF-α release from RAW264.7 murine macrophages on exposure to different stimulating agents: pDNA and MDP applied either alone or in combination in solution, or with TMC nanoparticles (TMC-NP), SWE06, and Cationorm®, respectively. Bars represent mean values (n=3) ± SEM. pDNA loaded nanoformulations were compared with either pDNA alone (*) or with [pDNA + MDP] loaded nanoformulations (*), and [pDNA + MDP] in solution with [nanocarrier + pDNA + MDP] (x). Significant differences were indicated with ** ($p < 0.01$), *** ($p < 0.001$), and ns (not significant).

Carrier function for Cationorm® seemed to be less important and SWE06 even decreased TNF-α release induced by pDNA alone ($p < 0.01$). When having combined both ligands in one formulation, the NOD2 ligand MDP augmented pDNA-induced activation of murine macrophages *in vitro* up to 4-fold, having observed a significant increase, compared to naked pDNA ($p < 0.001$) or pDNA adsorbed to nanocarriers (TMC nanoparticle $p < 0.01$, SWE06 $p < 0.001$, Cationorm® $p < 0.01$). This might indicate that MDP has an influence on enhancing immune responses in a synergistic manner, as cytokine production by the combination of immune receptor ligands was higher than production of each of the single stimulations and, moreover, as the sum of the two.

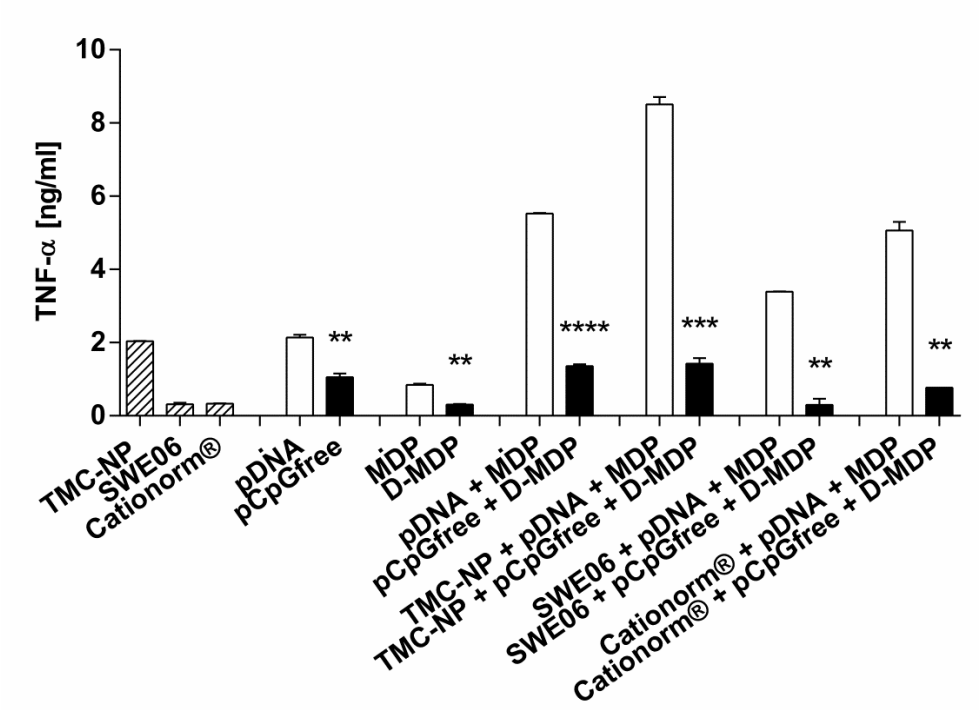

Figure 5. TNF- α release from RAW264.7 murine macrophages treated with pDNA and/or MDP and their inactive controls pCpGfree and/ or D-MDP, respectively. The ligands were applied either in solution, as single components, or combined with TMC nanoparticles (TMC-NP), SWE06, or Cationorm®, respectively. Significantly reduced activity by control ligands compared to their active ligands are indicated with **($p < 0.01$), ($p < 0.001$)***, and **** ($p < 0.0001$).

TLR-9 specifically recognizes unmethylated or hypomethylated CpG islets, prevalent in bacterial and many viral DNAs (Krieg, 2002). To confirm that TNF-α response is dependent on TLR-9 activation, macrophages were stimulated with pDNA, either containing or lacking CpG motifs. To further assure that the cytokine response is also dependent on NLR-2 activation the inactive D-isoform of MDP was applied in the same experiment. The dependency on PRR activation to induce a distinct TNF-α response towards TLR-9 and NLR-2 ligands implemented in the experiments is shown in Figure 5. Nanoparticles loaded with control ligands were found to not induce cytokine release, compared to the unloaded nanocarriers. Significant decrease of cytokine release was observed for control ligands transported by TMC nanoparticles, SWE06 and Cationorm®, compared to their active forms. Chitosan has the ability to stimulate innate immunity (Gafvelin and Grönlund, 2014). Due to inherent adjuvant effects of TMC, that possibly derive from its precursors' molecular features to activate PRRs, and potential contributions to immune activation by pDNA by other elements than TLR-9 activation, such as cytosolic TANK-binding kinase-1 activation by the double stranded B-form of pDNA, cells were also minimally stimulated with TMC and pCpGfree containing control samples (Ishii *et al.*, 2008). Mineral oil based incomplete Freund's adjuvant as well as squalene based formulations have been shown to polarize the immune response toward the production of anti-inflammatory cytokines, which may mask the TNF-α increasing effect by the double stranded nature of pCpGfree, as well as of the active ligands, applied with SWE06 and Cationorm®, respectively (Hart *et al.*, 1989, Mantile *et al.*, 2011).

3.5 NLR-2 dependent synergistic enhancement of TNF-α release

NLR-2 activation was inhibited to show its influence during co-stimulation with TLR-9 ligand on the synergistic enhancement of immune responses. Cells incubated with pDNA and MDP were treated with or without RIP-2 tyrosin kinase inhibitor gefitinib, to study NOD2 synergy with pDNA. The mechanism of the cross-talk between the pathways for PRRs is not yet fully understood, but it has been shown that there are

functional links between protein RIP2 and both pathways of TLR and NLR (Chin 2002, Kobayashi 2002). If synergistic enhancement is dependent on interaction between RIP2, activated by NOD2, and MyD88 of the TLR pathway, then inhibition of RIP2 kinase may serve to correct the excessive activation seen with combination of pDNA + MDP (Tigno-Aranjuez *et al*., 2010). Indeed, RIP2 blocking led to significant reduction of cytokine release, showing reduced cytokine release for ligands applied in solution ($p < 0.05$), for TMC nanoparticle-conjugates ($p < 0.01$) and for ligands applied with SWE06 ($p < 0.001$) and Cationorm® ($p < 0.01$) nanoemulsions, respectively, compared to untreated cells (Figure 6). The diminished macrophage activation, was shown to be similar to that induced by pDNA alone or pDNA applied with the nanocarriers without MDP.

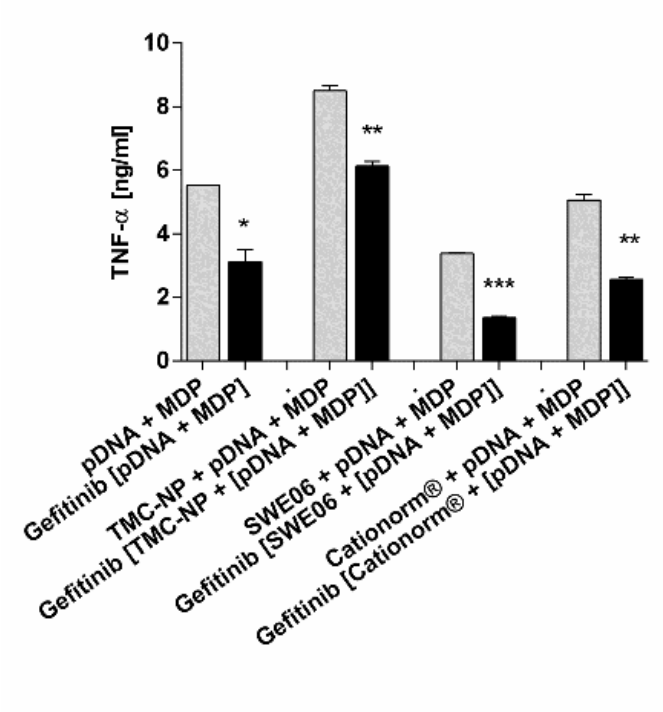

Figure 6. TNF-α release from RAW264.7 murine macrophages treated with or without RIP2 tyrosine kinase blocker gefitinib. Stimulants were pDNA and MDP in combination, applied either in solution or with TMC nanoparticles, SWE06, or Cationorm®, respectively. Significantly reduced activity by RIP2 tyrosine kinase blocking compared to unblocked NLR-2 pathway are indicated with *($p < 0.05$), **($p < 0.01$), and *** ($p < 0.001$).

4. Conclusion

In the present study, we compared cationic polymeric TMC nanoparticles with the cationic oil-in-water nanoemulsions SWE06 and Cationorm®, with regards to their ability to increase immune responses to pDNA *in vitro* and *in vivo*. Among the three nanoformulations evaluated, TMC nanoparticles were identified as the most successful carrier for DNA vaccines, by not only having increased immunogenicity of pDNA *in vivo* and *in vitro*, but also by having directed the outcome to cell-mediated immune responses. In mechanistic *in vitro* studies it was demonstrated that immune responses to pDNA can be substantially increased by MDP, showing significantly increased pro-inflammatory cytokine release in a synergistic manner. pDNA loaded TMC nanoparticles were shown to be promising candidates for further vaccine development to be investigated in future *in vivo* studies for immunopotentiating effects by simultaneous targeting of TLR-9 and NLR-2 with MDP.

References

Appelberg, R. (1994). Protective Role of Interferon Gamma, Tumor Necrosis Factor Alpha and Interleukin-6 in Mycobacterium tuberculosis and M. avium Infections*, Immunobiology,* 191, pp. 520-525.

Archer, K.A., Ader, F., Kobayashi, K.S., Flavell, R.A., and Roy, C.R. (2010). Cooperation between multiple microbial pattern recognition systems is important for host protection against the intracellular pathogen Legionella pneumophila*, Infection and Immunity,* 78, pp. 2477-2487.

Bootz, A., Vogel, V., Schubert, D., and Kreuter, J. (2004). Comparison of scanning electron microscopy, dynamic light scattering and analytical ultracentrifugation for the sizing of poly(butyl cyanoacrylate) nanoparticles*, European Journal of Pharmaceutics and Biopharmaceutics,* 57, pp. 369-375.

Borchard, G., Esmaeili, F., and Heuking, S. (2012) *Chitosan-Based Systems for Biopharmaceuticals* eds. B. Sarmento and Neves, J.d., Chapter 12 "Chitosan-Based Delivery Systems for Mucosal Vaccination", (Wiley, UK) pp. 211-224.

Bruffaerts, N., Huygen, K., and Romano, M. (2014). DNA vaccines against tuberculosis*, Expert Opinion on Biological Therapy,* 14, pp. 1801-1813.

Bueter, C.L., Specht, C.A., and Levitz, S.M. (2013). Innate Sensing of Chitin and Chitosan*, PLoS Pathogens,* 9, pp. e1003080. DOI: 10.1371/journal.ppat.1003080.

Cavalcanti, Y.V.N., Brelaz, M.C.A., Neves, J.K.d.A.L., Ferraz, J.C., and Pereira, V.R.A. (2012). Role of TNF-alpha, IFN-gamma, and IL-10 in the development of pulmonary tuberculosis*, Pulmonary medicine,* 2012,

Chin, A.I., Dempsey, P.W., Bruhn, K., Miller, J.F., Xu, Y., and Cheng, G. (2002). Involvement of receptor-interacting protein 2 in innate and adaptive immune responses*, Nature,* 416, pp. 190-194.

Coffman, R.L., Sher, A., and Seder, R.A. (2010). Vaccine Adjuvants: Putting Innate Immunity to Work*, Immunity,* 33, pp. 492-503.

Coulombe, F. (2009), NOD2 and Mycobacteria, McGill University (Departement of Microbiology & Immunology, Montreal, Canada), 2011 February 23, from http://digitool.library.mcgill.ca/R/

Cui, Z. and Mumper, R.J. (2003). The effect of co-administration of adjuvants with a nanoparticle-based genetic vaccine delivery system on the resulting immune responses*, European Journal of Pharmaceutics and Biopharmaceutics,* 55, pp. 11-18.

Dan, J.M., Wang, J.P., Lee, C.K., and Levitz, S.M. (2008). Cooperative Stimulation of Dendritic Cells by Cryptococcus neoformans Mannoproteins and CpG Oligodeoxynucleotides*, PLoS ONE,* 3, pp. e2046. DOI: 10.1371/journal.pone.0002046.

Denis-Mize, K.S., Dupuis, M., Singh, M., Woo, C., Ugozzoli, M., O'Hagan, D.T., Donnelly Iii, J.J., Ott, G., and McDonald, D.M. (2003). Mechanisms of increased immunogenicity for DNA-based vaccines adsorbed onto cationic microparticles*, Cellular Immunology,* 225, pp. 12-20.

Domard, A., Rinaudo, M., and Terrassin, C. (1986). New method for the quaternization of chitosan*, International Journal of Biological Macromolecules,* 8, pp. 105-107.

Egli, A., Santer, D., Barakat, K., Zand, M., Levin, A., Vollmer, M., Weisser, M., Khanna, N., Kumar, D., and Tyrrell, L. (2014). Vaccine adjuvants-understanding molecular mechanisms to improve vaccines*, Swiss Med Wkly,* 144, w13940. DOI: 10.4414/smw.2014.13940.

Fang, J.-H. and Hora, M. (2000) *Vaccine Adjuvants* 42, eds. D. O'Hagan, 12 "The Adjuvant MF59: A 10-Year Perspective Gary Ott, Ramachandran Radhakrishnan", (Springer New York, USA) pp. 211-228.

FDA (2013). *FDA approves first adjuvanted vaccine for prevention of H5N1 avian influenza*, 2015 March 26, from: http://www.fda.gov/NewsEvents/Newsroom/PressAnnouncements/ucm376444.htm.

Gadad, A., Chandra, P.S., Dandagi, P., and Mastiholimath, V. (2012). Moxifloxacin Loaded Polymeric Nanoparticles for Sustained Ocular Drug Delivery, *International Journal of Pharmaceutical Sciences and Nanotechnology*, *5*, pp. 1727-34.

Gafvelin, G. and Grönlund, H. (2014). *Molecular Vaccines* eds. M. Giese, 13 "Chitosan-Based Adjuvants", (Springer International Publishing, Switzerland) pp. 623-631.

Giljohann, D.A., Seferos, D.S., Patel, P.C., Millstone, J.E., Rosi, N.L., and Mirkin, C.A. (2007). Oligonucleotide Loading Determines Cellular Uptake of DNA-Modified Gold Nanoparticles*, Nano Letters,* 7, pp. 3818-3821.

Goodman, C.M., McCusker, C.D., Yilmaz, T., and Rotello, V.M. (2004). Toxicity of Gold Nanoparticles Functionalized with Cationic and Anionic Side Chains*, Bioconjugate Chemistry,* 15, pp. 897-900.

Hart, P.H., Vitti, G.F., Burgess, D.R., Whitty, G.A., Piccoli, D.S., and Hamilton, J.A. (1989). Potential antiinflammatory effects of interleukin 4: suppression of human monocyte tumor necrosis factor alpha, interleukin 1, and prostaglandin E2*, Proceedings of the National Academy of Sciences,* 86, pp. 3803-3807.

HAS (2013), Decision by the national committee for the evaluation of medical devices and health technologies., 2015 May 21, from http://www.has-sante.fr/portail/jcms/c_1696520/fr/cationorm.

Heuking, S., Adam-Malpel, S., Sublet, E., Iannitelli, A., Stefano, A.d., and Borchard, G. (2009). Stimulation of human macrophages (THP-1) using Toll-like receptor-2 (TLR-2) agonist decorated nanocarriers*, Journal of drug targeting,* 17, pp. 662-670.

Heuking, S. and Borchard, G. (2012). Toll-like receptor-7 agonist decoration enhances the adjuvanticity of chitosan–DNA nanoparticles*, Journal of Pharmaceutical Sciences,* 101, pp. 1166-1177.

Heuking, S., Iannitelli, A., Di Stefano, A., and Borchard, G. (2009). Toll-like receptor-2 agonist functionalized biopolymer for mucosal vaccination*, International Journal of Pharmaceutics,* 381, pp. 97-105.

Hwang, T.-L., Aljuffali, I.A., Lin, C.-F., Chang, Y.-T., and Fang, J.-Y. (2015). Cationic additives in nanosystems activate cytotoxicity and inflammatory response of human neutrophils: lipid nanoparticles versus polymeric nanoparticles*, International Journal of Nanomedicine,* 10, pp. 371.

Ioannou, X.P., Gomis, S.M., Karvonen, B., Hecker, R., Babiuk, L.A., and van Drunen Littel-van den Hurk, S. (2002). CpG-containing oligodeoxynucleotides, in combination with conventional adjuvants, enhance the magnitude and change the bias of the immune responses to a herpesvirus glycoprotein*, Vaccine,* 21, pp. 127-137.

Ishii, K.J., Kawagoe, T., Koyama, S., Matsui, K., Kumar, H., Kawai, T., Uematsu, S., Takeuchi, O., Takeshita, F., Coban, C., and Akira, S. (2008). TANK-binding kinase-1 delineates innate and adaptive immune responses to DNA vaccines*, Nature,* 451, pp. 725-729.

Kean, T., Roth, S., and Thanou, M. (2005). Trimethylated chitosans as non-viral gene delivery vectors: Cytotoxicity and transfection efficiency*, Journal of Controlled Release,* 103, pp. 643-653.

Kobayashi, K., Inohara, N., Hernandez, L.D., Galán, J.E., Núñez, G., Janeway, C.A., Medzhitov, R., and Flavell, R.A. (2002). RICK/Rip2/CARDIAK mediates signalling for receptors of the innate and adaptive immune systems*, Nature,* 416, pp. 194-199.

Krieg, A.M. (2002). CpG motifs in bacterial DNA and their immune effects*, Annual Review of Immunology,* 20, pp. 709-760.

Kumar, M., Behera, A.K., Lockey, R.F., Zhang, J., Bhullar, G., de la Cruz, C.P., Chen, L.-C., Leong, K.W., Huang, S.-K., and Mohapatra, S.S. (2002). Intranasal Gene Transfer by Chitosan–DNA Nanospheres Protects BALB/c Mice Against Acute Respiratory Syncytial Virus Infection*, Human Gene Therapy,* 13, pp. 1415-1425.

Kutzler, M.A. and Weiner, D.B. (2008). DNA vaccines: ready for prime time?*, Nat Rev Genet,* 9, pp. 776-788.

Lallemand, F., Daull, P., Benita, S., Buggage, R., and Garrigue, J.-S. (2012). Successfully Improving Ocular Drug Delivery Using the Cationic Nanoemulsion, Novasorb*, Journal of Drug Delivery,* 604204. DOI:10.1155/2012/604204.

Le, T.P., Coonan, K.M., Hedstrom, R.C., Charoenvit, Y., Sedegah, M., Epstein, J.E., Kumar, S., Wang, R., Doolan, D.L., Maguire, J.D., Parker, S.E., Hobart, P., Norman, J., and Hoffman, S.L. (2000). Safety, tolerability and humoral immune responses after intramuscular administration of a malaria DNA vaccine to healthy adult volunteers*, Vaccine,* 18, pp. 1893-1901.

Lee, S.H. (2013). Topological conformational changes of human papillomavirus (HPV) DNA bound to an insoluble aluminum salt—A study by low temperature PCR*, Advances in Biological Chemistry*, 3, pp. 76-85.

Li, X., Min, M., Du, N., Gu, Y., Hode, T., Naylor, M., Chen, D., Nordquist, R.E., and Chen, W.R. (2013). Chitin, Chitosan, and Glycated Chitosan Regulate Immune Responses: The Novel Adjuvants for Cancer Vaccine*, Clinical and Developmental Immunology,* 387023. DOI: 10.1155/2013/387023

MacGregor, R.R., Ginsberg, R., Ugen, K.E., Baine, Y., Kang, C.U., Tu, X.M., Higgins, T., Weiner, D.B., and Boyer, J.D. (2002). T-cell responses induced in normal volunteers immunized with a DNA-based vaccine containing HIV-1 env and rev*, AIDS,* 16, pp. 2137-2143.

Mantile, F., Basile, C., Cicatiello, V., De Falco, D., Caivano, A., De Berardinis, P., and Prisco, A. (2011). A multimeric immunogen for the induction of immune memory to beta-amyloid*, Immunology and cell biology,* 89, pp. 604-609.

O'Hagan, D., Singh, M., Ugozzoli, M., Wild, C., Barnett, S., Chen, M., Schaefer, M., Doe, B., Otten, G.R., and Ulmer, J.B. (2001). Induction of potent immune responses by cationic microparticles with adsorbed human immunodeficiency virus DNA vaccines*, Journal of Virology,* 75, pp. 9037-9043.

Petterson, T., Jendholm, J., Månsson, A., Bjartell, A., Riesbeck, K., and Cardell, L.-O. (2011). Effects of NOD-like receptors in human B lymphocytes and crosstalk between NOD1/NOD2 and Toll-like receptors*, Journal of Leukocyte Biology,* 89, pp. 177-187.

Poecheim, J. and Borchard, G. (2015) *Controlled Release Systems: Advances in Nanobottles and Active Nanoparticles* eds. J. Forcada, A. v. Herk, and Pastorin, G., 17 "Immunotherapie and Vaccines", (Pan Stanford Publishing, Singapore) pp. 523-551.

Querec, T., Bennouna, S., Alkan, S., Laouar, Y., Gorden, K., Flavell, R., Akira, S., Ahmed, R., and Pulendran, B. (2006). Yellow fever vaccine YF-17D activates multiple dendritic cell subsets via TLR2, 7, 8, and 9 to stimulate polyvalent immunity*, The Journal of experimental medicine,* 203, pp. 413-424.

Rottinghaus, S.T., Poland, G.A., Jacobson, R.M., Barr, L.J., and Roy, M.J. (2003). Hepatitis B DNA vaccine induces protective antibody responses in human non-responders to conventional vaccination*, Vaccine,* 21, pp. 4604-4608.

Sasaki, S., Sumino, K., Hamajima, K., Fukushima, J., Ishii, N., Kawamoto, S., Mohri, H., Kensil, C.R., and Okuda, K. (1998). Induction of systemic and mucosal immune responses to human immunodeficiency virus type 1 by a DNA vaccine formulated with QS-21 saponin adjuvant via intramuscular and intranasal routes*, Journal of Virology,* 72, pp. 4931-4939.

Schatz, C., Domard, A., Viton, C., Pichot, C., and Delair, T. (2004). Versatile and Efficient Formation of Colloids of Biopolymer-Based Polyelectrolyte Complexes*, Biomacromolecules,* 5, pp. 1882-1892.

Shedlock, D.J. and Weiner, D.B. (2000). DNA vaccination: antigen presentation and the induction of immunity*, Journal of Leukocyte Biology,* 68, pp. 793-806.

Slütter, B., Plapied, L., Fievez, V., Alonso Sande, M., des Rieux, A., Schneider, Y.-J., Van Riet, E., Jiskoot, W., and Préat, V. (2009). Mechanistic study of the adjuvant effect of biodegradable nanoparticles in mucosal vaccination*, Journal of Controlled Release,* 138, pp. 113-121.

Strong, P., Clark, H., and Reid, K. (2002). Intranasal application of chitin microparticles down-regulates symptoms of allergic hypersensitivity to Dermatophagoides pteronyssinus and Aspergillus fumigatus in murine models of allergy*, Clinical & Experimental Allergy,* 32, pp. 1794-1800.

Tigno-Aranjuez, J.T., Asara, J.M., and Abbott, D.W. (2010). Inhibition of RIP2's tyrosine kinase activity limits NOD2-driven cytokine responses*, Genes & development,* 24, pp. 2666-2677.

Tokura, S., Hiroshi, T., and Ichiro, A. (1999) *Chitin and chitinases* 87, eds. P. Jollès, Immunological aspects of chitin and chitin derivatives administered to animals", (Birkhäuser, Switzerland) pp. 279-292.

Uehara, A., Yang, S., Fujimoto, Y., Fukase, K., Kusumoto, S., Shibata, K., Sugawara, S., and Takada, H. (2005). Muramyldipeptide and diaminopimelic acid-containing desmuramylpeptides in combination with chemically synthesized Toll-like receptor agonists synergistically induced production of interleukin-8 in a NOD2-and NOD1-dependent manner, respectively, in human monocytic cells in culture*, Cellular Microbiology,* 7, pp. 53-61.

Wang, R., Doolan, D.L., Le, T.P., Hedstrom, R.C., Coonan, K.M., Charoenvit, Y., Jones, T.R., Hobart, P., Margalith, M., Ng, J., Weiss, W.R., Sedegah, M., de Taisne, C., A. Norman, J., and Hoffman, S.L. (1998). Induction of Antigen-Specific Cytotoxic T Lymphocytes in Humans by a Malaria DNA Vaccine*, Science,* 282, pp. 476-480.

West, A.P. Recognition and Signaling by Toll-Like Receptors*, Annual Review of Cell and Developmental Biology,* 22, pp. 409-437.

Chapter IV:

Ag85A DNA vaccine delivery by nanoparticles: Influence of the formulation characteristics on immune responses

Johanna Poecheim[a], Christophe Barnier-Quer[b], Nicolas Collin[b], Gerrit Borchard[a]

[a] *School of Pharmaceutical Sciences, University of Geneva, University of Lausanne, Quai Ernest Ansermet 30, 1211 Geneva, Switzerland*

[b] *Vaccine Formulation Laboratory, Department of Biochemistry, University of Lausanne, Chemin des Boveresses 155, 1066 Epalinges, Switzerland*

In submission.

Abstract

The influence of DNA vaccine formulations on immune responses in combination with adjuvants was investigated with the aim to increase cell-mediated immunity against plasmid DNA (pDNA) as a model tuberculosis vaccine, encoding *Mycobacterium tuberculosis* antigen 85A. To accomplish this goal the historical empirical approach to formulation development *in vivo* was sought to be extended with a systematic approach of detailed physicochemical and biophysical characterization of DNA nanoparticle formulations. Different ratios of pDNA with cationic trimethyl chitosan (TMC) nanoparticles were characterized for their morphology and physicochemical characteristics (size, zeta potential, loading efficiency and pDNA release profile) applied *in vitro* for cellular uptake studies and *in vivo*, to determine dose-dependent effects of pDNA on immune responses. Finally, a selected pDNA/TMC nanoparticle formulation was optimized by incorporation of muramyl dipeptide as an immunostimulatory agent. Cellular uptake investigations *in vitro* showed saturation to a maximum level upon increase in pDNA/TMC nanoparticle ratios, correlating with increasing Th1 related antibody responses up to a definite pDNA dose applied. Moreover, TMC nanoparticles induced clear polarization towards a Th1 response, indicated by IgG2c/IgG1 ratios above unity and enhanced numbers of antigen-specific IFN-γ producing T-cells in the spleen. Remarkably, the incorporation of MDP in TMC nanoparticles provoked a significant additional increase in T-cell mediated responses induced by pDNA. In conclusion, pDNA loaded TMC nanoparticles are capable of provoking strong Th1 type cellular and humoral immune responses, with the potential to be further optimized by incorporation of MDP.

1. Introduction

Tuberculosis was declared a ‘‘global health emergency’’ by the World Health Organization in 1993, and continues to be a leading cause of deaths worldwide with nearly 1.5 million lethal cases per year (WHO, 2014). Prevalence of tuberculosis infections is the highest in developing countries, where the concomitant HIV infections as well as malnutrition lead to immunodepression and therefore poor efficacy of bacillus Calmette–Guérin (BCG), the only vaccine currently licensed against tuberculosis (Russell, 2007). BCG has several limitations, including a variable efficacy in different populations and a lack of protection against pulmonary tuberculosis in adults. Also, BCG-induced protection wanes with time and BCG boosters have not been found to be effective, nor considered to be safe in immunocompromised patients, as it is a live vaccine (Andersen and Kaufmann, 2014). Moreover, exposure to non-tuberculous environmental mycobacteria can cause antagonistic influence on BCG vaccination and exposure to parasitic infections lead to Th2 dominance in humans, which diminishes protective cellular responses and facilitates *Mycobacterium tuberculosis (Mtb)* evasion from the immune system (Bentwich *et al.*, 1999, Brandt *et al.*, 2002). It is anticipated that all these problems might be overcome by developing more effective, safe, and reliable vaccines that are not dependent on mycobacterial replication.

The acquisition of protective immunity during latent tuberculosis in healthy individuals, as well as by BCG vaccination, mainly depends on the induction of IFN-γ-producing type 1 T helper (Th1) cells. Activation of potent Th1 responses have been shown to prevent *Mtb* infection and reactivation and is used as a strategy for developing an effective vaccine against tuberculosis (Hoft *et al.*, 1999, Lindblad *et al.*, 1997, Tameris *et al.*, 2014). DNA vaccines offer an interesting approach to replace BCG. *In situ* expression of antigenic proteins encoded by plasmid DNA (pDNA) induce specific immune responses against the pathogen, without the risk of reversion into virulence associated with live-attenuated vaccines (Ingolotti *et al.*, 2010). Moreover, DNA

vaccines have the ability to induce both, humoral and cellular immune responses, including cytotoxic T-cell responses, which is crucial to prevent reactivation of latent tuberculosis infection and to mediate elimination of intracellular *Mtb (Kutzler and Weiner, 2008).*

Antigen Ag85A is among the major *Mtb* secretory proteins and display key immunoprotective activities against tuberculosis infection (Yuk and Jo, 2014). DNA encoding Ag85A is among the most investigated DNA vaccines against *Mtb* and demonstrated promise due to its ability to stimulate strong humoral and cell-mediated immune responses, as well as protective effects in mice (Huygen *et al.*, 1996). However, it has been found that biodistribution and *cellular uptake* present significant limitations to *DNA vaccine* potency and the amount of actual protein synthesized (Dupuis *et al.*, 2000). Therefore current research on DNA vaccines is focused on the use of appropriate adjuvants as delivery vectors. Furthermore, immunostimulatory adjuvants can enhance immune responses against the encoded antigen and modulate the outcome towards a Th1 bias and CD4+ T-cells activation (Kim *et al.*, 1999). Nanoparticles composed of cationic polymers like trimethyl chitosan (TMC), a chitosan derivative characterized by its permanent positive charges, can be loaded with pDNA by electrostatic interactions (Amidi *et al.*, 2006, Thanou *et al.*, 1999). TMC nanoparticles have previously been shown to promote enhanced cellular uptake of nucleic acids and model antigens, as well as to induce dendritic cell maturation, which makes them an interesting adjuvant system for DNA vaccines (Slütter *et al.*, 2009, Thanou *et al.*, 2002).

Immune responses can be modulated by activation of pattern recognition receptors of the innate immune system, such as Toll-like receptors (TLR) and NOD-like receptors. pDNA naturally contains unmethylated CpG islets for TLR-9 targeting that activate proinflammatory cytokine release upon receptor binding. Muramyl dipeptide (MDP), a ligand of NOD-like receptor 2 (NOD2), has been shown to enhance Th1 responses against leishmania, AIDS/HIV, and malaria in different animal models (Bomford *et al.*,

1992, Lemesre *et al.*, 2007, Pye *et al.*, 1997). Co-delivery of pDNA with MDP by TMC nanoparticle transport, allows simultaneous targeting of immune cells in order to potentiate Th1 immune responses in a synergistic fashion (Abbott *et al.*, 2007, Higgins and Mills, 2010).

The aim of the present work is to investigate the influence of formulating a DNA vaccine with polymeric nanoparticles on its immune responses. pDNA was adsorbed at the outer surface of cationic TMC nanoparticles and the impact on cell-mediated immune activation of different pDNA/TMC nanoparticle ratios was investigated. In this approach, DNA vaccine investigations were initiated with physicochemical characterization to better understand the adjuvant mechanism of TMC nanoparticles towards pDNA delivery, followed up by *in vitro* uptake studies, with the goal to explore the correlation of the results to the outcome of *in vivo* immunization studies. Finally, we aimed to optimize a selected pDNA/TMC nanoparticle formulation by co-delivery of MDP to further enhance cell-mediated immune responses in mice.

2. Materials and methods

2.1 Materials

N-trimethyl chitosan with a degree of quaternisation of 20% was synthesized from chitosan (ChitoClear cg10; Primex, Siglufjordur, IC). The methodology for the synthesis was adapted from Heuking et al., employing a one-step reductive methylation with methyl iodide for 70 minutes at 60 °C, in the presence of sodium hydroxide (Heuking *et al.*, 2009). Chondroitin sulfate and bovine serum albumin (BSA, endotoxin <0.1 ng/mg) were obtained from Sigma-Aldrich (Buchs, CH); UltraPure DNase/RNase free distilled water and OptiMEM reduced serum medium were purchased from Life Technologies (Zug, CH); Muramyl dipeptide (MDP, Invivogen) and LabelIT Cy5 Nucleic Acid Labeling Kit (Mirus Bio LLC) were obtained from Labforce (Muttenz, CH), and paraformaldehyde (Alfa Aesar, Ward Hill, USA), Triton X-100, phalloidin conjugated to Alexa 488 (Lonza,

Basel, CH), 4′,6-diamidino-2-phenylindole (DAPI; AppliChem, Axon Lab AG, Baden, CH) used for cell staining. pDNA encoding for the Ag85A antigenic epitope of *Mtb* (V1Jns.*tPA-85A*, 5853bp) was a kind gift from Institut Pasteur (Brussels, BE) and was amplified using the Endofree Qiagen plasmid Giga kit (Hombrechtikon, CH). A549 cells (American Type Culture Collection, Rockville, MD), a cell line derived from human carcinoma, were cultured in Ham's F12 medium with 10% FCS, both from PAN Biotech GmbH (Aidenbach, DE), and 1 % Penicillin/Streptomycin (PS; Life Technologies). Mouse spleen cells were cultured in DMEM (Gibco), containing 10% fetal calf serum (FCS, Gibco), 1% PS, all obtained from Life Technologies, and 0.01% β-Mercaptoethanol and 2mM Glutamine, both from Sigma-Aldrich. Recombinant Ag85A protein (rAg85A) was obtained through BEI Resources, National Institute of Allergy and Infectious Diseases (NIAID), National Institute of Health (NIH), Bethesda, MD, USA.

2.2 Nanoparticle preparation

Nanoparticles were formed according to the procedure described by Hansson et al. with some modifications (Hansson *et al.*, 2012). Briefly, TMC and chondroitin sulfate were dissolved separately in water with 5 mg/ml TMC and 1 mg/ml chondroitin sulfate and equal volumes of the two polymer solutions were mixed. The intermolecular linkages created between the positively charged amino groups of TMC and the negatively charged sulfate and carboxylate groups of chondroitin sulfate are responsible for the success of the nanoparticle formation process. The resulting nanoparticle dispersion were diluted 1:10 in phosphate buffered saline (PBS). According to Endosafe® Test Record nanoparticle suspensions showed an endotoxin level < 1 EU/ml. In case of MDP containing nanoparticle formulations in the *in vivo* immunogenicity studies, 10 µg of the dipeptide per injection volume (50 µl) was added to the TMC solution before particle formation. If not stated otherwise, pDNA/TMC nanocomplexes were prepared according to the following procedure: pDNA in PBS, at four different concentrations, was added to the diluted nanoparticle suspension (15 µg TMC nanoparticles per 50 µl) while shaking, at concentrations of 1 µg, 10 µg, 50 µg,

and 100 µg per 50 µl, yielding pDNA to TMC nanoparticle weight ratios of 0.07 (pDNA/TMC-NPs-0.07), 0.7 (pDNA/TMC-NPs-0.7), 3 (pDNA/TMC-NPs-3), and 7 (pDNA/TMC-NPs-7), respectively. The formed nanocomplexes with adsorbed pDNA were kept at room temperature for a maximum of 1 hour prior to experimental use.

2.3 Nanoparticle characterization

2.3.1 Size and zeta potential

Particle size distribution was determined by means of dynamic light scattering (DLS) using a Malvern ZetaSizer Nano ZS (Malvern Instruments, Worcestershire, UK). The zeta potential (ζ) of the particles was measured by electrophoresis and laser Doppler velocimetry using the same equipment. Before the measurement samples were diluted at a ratio of 1:10 in 1mM sodium chloride.

2.3.2 Loading efficiency

The loading capacity of pDNA in different concentrations on a fixed amount of TMC nanoparticles was quantified by separation of the nanoparticles from unloaded pDNA using centrifugal ultrafiltration devices (Vivaspin, Sartorius, Göttingen, DE). Samples were centrifuged through 300 kDa polyethersulfone (PES) membranes at 3220 x g for 20 min and non-adsorbed pDNA in the filtrate was determined by measuring the absorption at a wavelength of 260 nm with a ND-1000 NanoDrop spectrophotometer (Thermo Scientific, France). Loading efficiency was expressed in percentage as the amount of adsorbed pDNA compared to the amount of pDNA initially used to form the nanocomplexes.

2.3.3 Scanning electron microscopy

To examine the surface characteristics of nanoparticles the particles were washed 3 times with filtered water by centrifugation at 14000 x g for 15 min before pDNA adsorption. pDNA/TMC nanoparticles were diluted 1:100 in water, placed on a grid (Ted Pella Inc., Redding, CA, USA), dried under vacuum and sputter coated with a 10

nm gold layer. Images were viewed with a scanning electron microscope (SEM; Jeol JSM-7001FA, Tokyo, JP) at 5 kV and 10 mm working distance.

2.3.4 pDNA release profile

Nanoparticles with a pDNA/TMC nanoparticle ratio of 0.7, representing 100% pDNA adsorbed at the surface, were either diluted 1:10 in PBS (pH 7.4) or in 0.1 M phosphate buffer solution (pH 4.5) and stored in several aliquots at 37 °C at 80 rpm in a shaking incubator (GFL, Burgwedel, DE). At different time points after 1 h, 2 h, 3 h, 6 h, 8 h, 12 h and 24 h, the dispersions were placed in Vivaspin 300 kDa PES membrane tubes and centrifuged for 20 min at 3220 x g. Released pDNA was measured spectrophotometrically in the filtrate at 260 nm. The absorption values for the filtrate of plain nanoparticles were used as a blank and centrifugation of pDNA alone served as a positive control for 100% release. pDNA release was calculated using Equation 1.

Eq. 1 $$\text{pDNA release [\%]} = \frac{(OD_{pDNA\text{-}NPs} - OD_{blank})}{OD_{pDNA}} \times 100$$

2.4 Nanoparticle uptake *in vitro*

Cellular uptake of pDNA, covalently labeled with Cy5 (pDNA-Cy5), was imaged with an automated fluorescence microscope (ImageXpress Micro XL, Molecular Devices). A549 cells (10^5 cells/ ml) were seeded in a 96-well clear-bottom black BD Falcon plate (Becton Dickinson, Allschwil, Switzerland) with 100 µl per well and cultured at 37 °C and 5 % CO_2 for 24h. Culture medium was replaced by PBS containing either pDNA, pDNA applied with Lipofectamine2000 3:1 (v/w), or the pDNA/TMC nanoparticle formulations. Exclusively in this study, pDNA was applied in the same concentration in all wells, to allow comparability of uptake abilities between pDNA alone and the pDNA/TMC nanoparticle formulations of different ratios, meaning different pDNA densities on nanoparticle surfaces. Therefore 2 µg of pDNA-Cy5 in PBS was added to varying concentrations of TMC nanoparticles while shaking, yielding pDNA to TMC nanoparticle weight ratios of 0.07 (pDNA-Cy5/TMC-NPs-0.07), 0.7 (pDNA-Cy5/TMC-

NPs-0.7), 3 (pDNA-Cy5/TMC-NPs-3), and 7 (pDNA-Cy5/TMC-NPs-7). All samples, studied in triplicates in two separate experiments, were incubated with cells for 2h followed by extensive washing (5 times with PBS) to remove material that remained at the external side of the cell membranes. The cells were fixed with 4% paraformaldehyde, permeabilized with 0.1% Triton X-100 for 3 min, re-incubated with 1% BSA for 20 min, before being stained with 6.6 µM phalloidin conjugated to Alexa 488 and 1 µg/ml DAPI for 15 minutes, respectively. Acquisition setup and image analysis was performed with MetaXpress software. Nine positions in the center of each 96-well sample were collected, and the data were averaged across three biological replicates. Following imaging analysis with MetaXpress software, data were evaluated by multiwavelength scoring to calculate the percentage of Cy5 positive cells for each site within a well using Equation 2.

Eq. 2 Cells with pDNA-Cy5 uptake [%] = $\frac{\text{Number of Cy5 positive cells}}{\text{Number of nuclei count}} \times 100$

To evaluate the effect of the pDNA/TMC nanoparticle formulations on cell viability and survival of A549 cells during the uptake experiment the XTT cell proliferation method was applied (Roche, Switzerland). Cells were seeded in a 24-well plate (Costar, Corning, Amsterdam, NL) at a concentration of 10^5 cells per ml the day prior to the experiment ensuring non-confluent state, so healthy cells can proliferate and false-positive results are excluded. The pDNA/TMC nanoparticle formulations were prepared as described above in the *in vitro* uptake experiment, with a fixed amount of unlabeled pDNA to obtain pDNA/TMC nanoparticle ratios of 0.07, 0.7, 3, and 7. Samples were diluted with culture medium and distributed on cells (0.5 ml per well) for 24 h, before replacing the medium with XTT-reagent. The absorbance was measured at 490 nm after 5 h using a Tecan plate reader (Tecan Group Ltd., Männedorf, Switzerland). Cell viability was expressed as a percentage relative to the control with medium alone.

2.5 Immunogenicity studies

2.5.1 Immunization with pDNA loaded nanoparticles

All animal studies were approved by the cantonal veterinary authority of Geneva, Switzerland (SCAV; authorization number 2475). Female C57BL/6 mice (Harlan, Itingen, Switzerland), 8 weeks old at the beginning of the experiment, were vaccinated 3 times by i.m. injection (50 µl) in the thigh muscle, on days 0, 21, and 42. To study the influence of pDNA dose on the outcome of immune responses, mice (n=5) received increasing concentrations of pDNA adsorbed to a constant concentration of nanoparticles to obtain pDNA/TMC nanoparticle formulations of the ratios 0.07, 0.7, 3, and 7. In a follow-up experiment, each group of mice (n=8) received pDNA/TMC-NPs-0.7, or pDNA/TMC-NPs-0.7 with 10 µg MDP per injection as an additional adjuvant. In each experiment groups of mice were also vaccinated with pDNA alone in equivalent concentrations as in the TMC nanoparticle formulations, and PBS, respectively, as controls. Blood samples were collected through terminal cardiac puncture one week after the last injection. Sera, isolated by centrifugation, were stored at -20 °C before analysis. After sacrificing the animals, spleens were collected and immediately prepared for immunological assays.

2.5.2 Antibody ELISA

Maxisorp Nunc-immunoplates (Nunc, Roskilde, Denmark) were coated with 1 µg/ml rAg85A in PBS overnight at 4 °C. To reduce unspecific binding, wells were blocked with 1 % BSA (w/v) in PBS for 2 h at room temperature (RT). After extensive washing with PBS serial dilutions of serum ranging from 100 to $2.2x10^5$ were applied in duplicates. After incubation for 1 h at RT and extensive washing, Ag85A specific antibodies were detected using goat anti-mouse total IgG, IgG1, or IgG2c conjugated to horseradish peroxidase (Southern Biotech, Birmingham, AL, USA) for 1h at ambient temperature and by developing plates with TMB substrate (3,3',5,5'-Tetramethylbenzidine substrate; Becton Dickinson, USA) for 5 min in the dark. reactions were stopped by adding an

equal volume of 1N sulfuric acid and the optical density (OD) was measured at 450 nm using an iMARK microplate absorbance reader (Bio-Rad Laboratories, Hercules, CA, USA). IgG2c/IgG1 ratios above unity, calculated from serum antibody titers, were associated with Th1 related immune response profiles.

2.5.3 IFN-γ ELISPOT

MultiScreen HTS-HA filter plates (Merck Millipore, Saint Quentin en Yvelines*, France)* were coated overnight at 4 °C with anti-mouse IFN-γ antibody (BD Pharmingen, Basel, Switzerland), carefully washed five times with PBS and blocked for 2 h at 37 °C with DMEM medium containing 10% FCS. Single cell suspensions were prepared by passing the freshly isolated spleens through 100 µm cell strainers and by treating the cells with ammonium chloride 0.84% for 1.5 min to lyse red blood cells. Splenocytes were plated in duplicates at 10^6 cells, $5x10^5$ cells, and $2.5x10^5$ cells per well and stimulated with 5 µg/ml rAg85A, 5 µg/ml ConA, or media for 72 h at 37 °C. The plates were then washed with 0.05% PBS-Tween20 and incubated for 2 h at RT with biotinylated anti-mouse IFN-γ antibody (BD Pharmingen) diluted 1:100 in 0.05% PBS-Tween20 1% BSA. After washing the plates, streptavidin-alkaline phosphatase (Roche, Basel, Switzerland) was added to each well at 1 U/ml and incubated for 2 h at RT, washed, and filters developed using bromo-chloro-indolyl-phosphate/nitro blue tetrazolium ready-to-use (Sigma-Aldrich) until spots appeared. The reaction was stopped by washing the plates with deionized water. Plates were dried in the dark for several days and spots were counted on an automated ELISPOT reader (Bioreader 2000; BioSys GmbH, Karben, *Germany*). Results were expressed as the number of IFN γ-secreting cells (spots forming cells; SFC) per million cells, taking the cell dilution factor into consideration.

2.5 Statistical methods

Antibody titers were logarithmically transformed before statistical analysis. All data were analyzed by a two-tailed Mann-Whitney test to demonstrate significant differences

between the experimental groups. The statistical analysis was carried out using Prism (Graphpad) and p values lower than 0.05 were considered to be significant.

3. Results and Discussion

3.1 Particle characterization

Hydrodynamic diameters, PDI values and zeta potential were assessed for the pDNA/TMC nanoparticle formulations prepared in PBS as applied in our in vivo immunogenicity study and in vitro cellular-uptake experiments, respectively, to ensure comparability of the results for both preparation methods. Data are consistent between the preparation with constant TMC nanoparticles and varying pDNA concentrations and the preparation with fixed pDNA concentration and variable amounts of TMC nanoparticles (Table 1) Other than the final amount of each component used in the formulation composition, no differences in physicochemical characteristics of the final product of pDNA/TMC nanoparticle formulations were observed. Hence, this allows us to draw correlations between *in vitro* uptake and *in vivo* immunogenicity studies. Particle size measurements in PBS of unloaded TMC nanoparticles revealed hydrodynamic diameters of 527 nm, a PDI of 0.3, and zeta potentials of 10 mV. Upon pDNA adsorption, nanoparticles with pDNA/TMC nanoparticle ratios of 0.07 represented a size increase to approximately 700 nm, with stable polydispersity index (PDI) values of 0.3. However, surface charge dropped to near neutral values, indicative for charge neutralization through electrostatic interaction of pDNA with the cationic nanoparticles. Formulation of pDNA/TMC-NPs-0.7 led to size contraction (406 - 436 nm) and zeta potential values below zero, of around -24 mV. By having further increased pDNA concentrations, forming pDNA/TMC-NPs-3, particle diameters remained at 401 nm to 485 nm, whereas surface charges decreased again to approximately -30 mV. For nanoparticles with the highest pDNA/TMC nanoparticle ratio (ratio of 7) higher hydrodynamic diameters were observed (519 – 652 nm), however, the zeta potential remained in a range between -22 and -36 mV. Different doses of

pDNA in the TMC nanoparticle formulation presumably lead to variable packing densities of pDNA at the surface of the nanoparticles. The zeta potential of the particles with the lowest pDNA concentration was neutral, whereas all the other pDNA/TMC nanoparticle formulations showed a negative zeta potential. Uptake and immunostimulating mechanisms of particle based vaccines may be related to mimic pathogens by their size, surface display of antigens and adjuvant activity of the bacterial components in the particle formulations. The pDNA/TMC nanoparticles formulated in this study were of a size range between 400 and 700 nm. Particles used in vaccine formulations offering comparable size to pathogens are recognized during evolution by the immune system (< 5 um) and consequently represent a favorable dimension for cellular uptake and promotion of immune responses (Poecheim and Borchard, 2015). 100 % adsorption of pDNA at nanoparticles' surfaces was observed for pDNA/TMC-NPS-0.07 and pDNA/TMC-NPS-0.7 (Table 1).

Table 1. Particle Size (Z-av), Polydispersity Index (PDI), Zeta Potential (ζ) and Loading Efficiency (LE) of TMC nanoparticles (NPs) with or without (n=3). pDNA/TMC-NPs were either prepared with constant TMC nanoparticles and varying pDNA concentrations or with fixed pDNA concentration and variable amounts of TMC nanoparticles.

	Fixed TMC-NP concentration			Fixed pDNA concentration		
	Z-av (nm)	PDI	ζ (mV)	Z-av (nm)	PDI	ζ (mV)
TMC-NPs unloaded	527 ± 17	0.3	10 ± 1			
pDNA/TMC-NPs-0.07	684 ± 107	0.3	2 ± 0.4	712 ± 58	0.3	1 ± 1
pDNA/TMC-0.7	406 ± 3	0.3	-24 ± 2	436 ± 14	0.3	-23 ± 3
pDNA/TMC-3	485 ± 8	0.4	-28 ± 2	401 ± 20	0.3	-30 ± 3
pDNA/TMC-7	652 ± 26	0.4	-36 ± 1	519 ± 8	0.4	-22 ± 4

While increasing the pDNA/TMC-NPs ratio induced lower adsorption rate within pDNA/TMC-NPS-3 and pDNA/TMC-NPS-7 only 31 % and 15 % pDNA, respectively, of the initially added pDNA was adsorbed. By extrapolating the quantity of pDNA from

these percentages it can be assumed that maximally 15 µg of pDNA is strongly adsorbed on these nanoparticles. Surplus pDNA may be easily dissociated due to repulsion as a consequence of higher pDNA densities on the nanoparticle surfaces, or may partly stay in suspension.

Unloaded nanoparticles were of spherical shape, as seen by SEM imaging (Figure 1A). pDNA/TMC-NPs-0.07 formulations appeared to form clusters of single spherical particles (Figure 1B). Higher pDNA concentrations in the ternary polyplexes (ratios from 0.7 to 7), led to deformation of the formerly spherical particles as seen in Figure 1C-1E (Wang *et al.*, 2012).

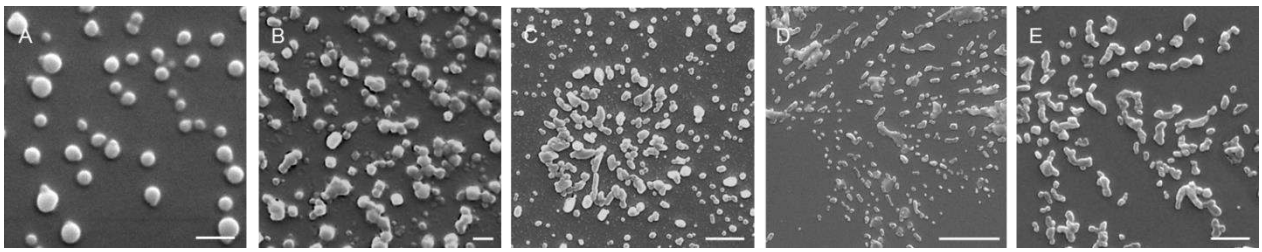

Figure 1. Scanning electron microscopy images of plain TMC nanoparticles (TMC-NPs) (A), pDNA/TMC-NPs-0.07 (B), pDNA/TMC-NPs-0.7 (C), pDNA/TMC-NPs-3 (D) and pDNA/TMC-NPs-7 (E), prepared in deionized water and dried and dried under vacuum. The scale bars represent 500 nm.

3.2 Kinetics of pDNA release

The *in vitro* release studies demonstrated highly pH dependent release of pDNA from TMC nanoparticles. Significantly faster DNA release was observed at acidic pH of 4.5 compared to physiological pH. The kinetics of pDNA release from TMC nanoparticles showed an initial burst release within 1h at pH 4.5 (lysosomal pH) with 80% release, followed by 88% after 12 h and 100% release after 24h (Figure 2). On the contrary, at physiological pH, pDNA/TMC nanoparticles remained stable for 8 hours with only 14% pDNA release and dissociated slowly with only 50% pDNA being released after 24h. These pH sensitive pDNA/TMC nanoparticle complexes are particularly appealing for targeted intracellular release. While maintaining their electrostatically conjugated

structure in the physiological environment after injection, to efficiently transfer pDNA into the host cell, pDNA can be liberated from the nanoparticles inside lysosomes at pH 4 to 5 after endocytosis to allow entrance into the nucleus for gene transcription.

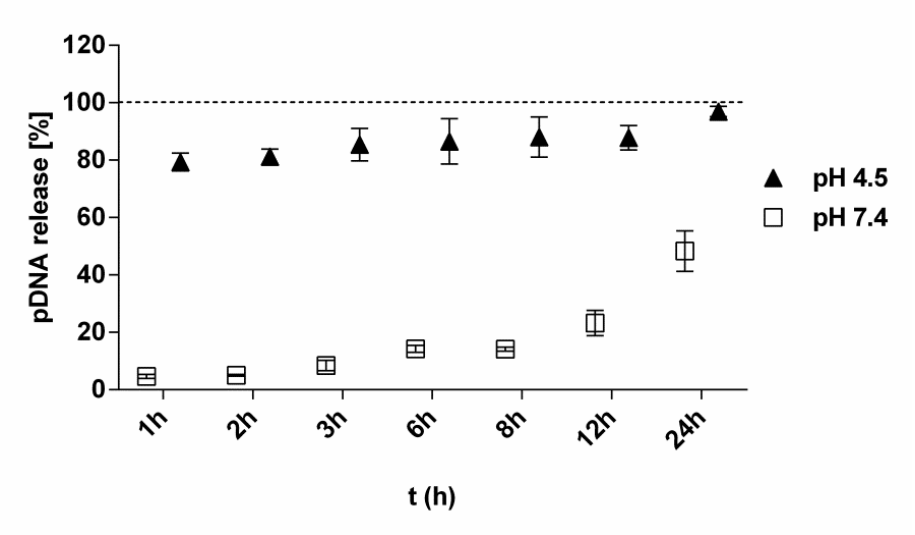

Figure 2. Release profiles of pDNA (10 µg) from pDNA/TMC-NPs-0.7 at pH 4.5 (▲) and pH 7.4 (□) at 37 °C for 24 h, calculated in percent in relation to 100 % pDNA in solution (dotted line). All measurement points are expressed as means for a minimum of 3 measurements ± SEM.

3.3 *In vitro* evaluation of cytotoxicity and cellular uptake

The formulations for *in vitro* uptake were prepared with fixed pDNA-Cy5 quantities and decreasing concentrations of TMC nanoparticles, in order to obtain the same ratios of labeled pDNA in relation to TMC nanoparticles as in our in vivo experiments, rising from 0.07, 0.7, 3 to 7. This was necessary, to allow comparability and quantification of pDNA-Cy5 uptake for the different formulations applied. It was found that the level of uptake was the highest for pDNA-Cy5/TMC-NPs-3 and pDNA-Cy5/TMC-NPs-7 (Figure 3 A-F and a-f). As presented in Figure 4, 87% Cy5 positive cells were detected after incubation with pDNA-Cy5/TMC-NPs-7 and 83% with pDNA-Cy5/TMC-NPs-3. Cellular uptake of pDNA-Cy5/TMC-NPs-0.7 was notably reduced to 45% and for

pDNA-Cy5/TMC-NPs-0.07 only 1% of Cy5 positive cells were found. No pDNA-Cy5 uptake was observed for pDNA-Cy5 in the absence of nanoparticle delivery.

The TMC nanoparticle concentration varied and was the highest for pDNA/TMC-NPs-0.07, however, DNA uptake was shown to be the lowest for this formulation. pDNA-Cy5/TMC-NPs-0.07 display neutral surface charges and consequently seem to resist interaction with cells showing minimal internalization. It is well-known that cationic particles interact with negatively charged cell membranes and are very efficient in cell-membrane penetration. Yet we could show that despite their negative surface coating pDNA-Cy5/TMC nanoparticles of ratios 0.7, 3, and 7 were readily taken up by cells and there has been evidence of uptake of negatively charged particles as reported by others (Limbach *et al.*, 2005, Patil *et al.*, 2007). Giljohann et al. quantified cellular uptake of oligonucleotide loaded nanoparticles, having observed that higher densities of DNA on the surface lead to greater uptake, which is in accordance with our studies (Giljohann *et al.*, 2007). Their investigations revealed that the nanoparticles adsorbed serum proteins on the surface through electrostatic and hydrophobic interactions. The amount of proteins increased with the amount of oligonucleotides on the particle surface and their uptake into cells might be due to the amount and nature of the proteins that are bound to the DNA strands. These investigations let us assume that the amount of pDNA present on the nanoparticle surface might influence uptake of our pDNA-Cy5/TMC nanoparticle formulations, rather than the quantity of nanoparticles. Cell viability for the same preparations of pDNA/TMC nanoparticle formulations using unlabeled pDNA was shown to be above 80% and the particles were therefore considered to be safe to be used in successive *in vivo* studies (Figure 4).

3.4 *In vivo* investigations of pDNA/TMC nanoparticles

To study the influence of pDNA dose on the outcome of immune responses, mice received increasing concentrations of pDNA (1 µg, 10 µg, 50 µg and 100 µg) adsorbed to a constant concentration of nanoparticles to obtain pDNA/TMC nanoparticle

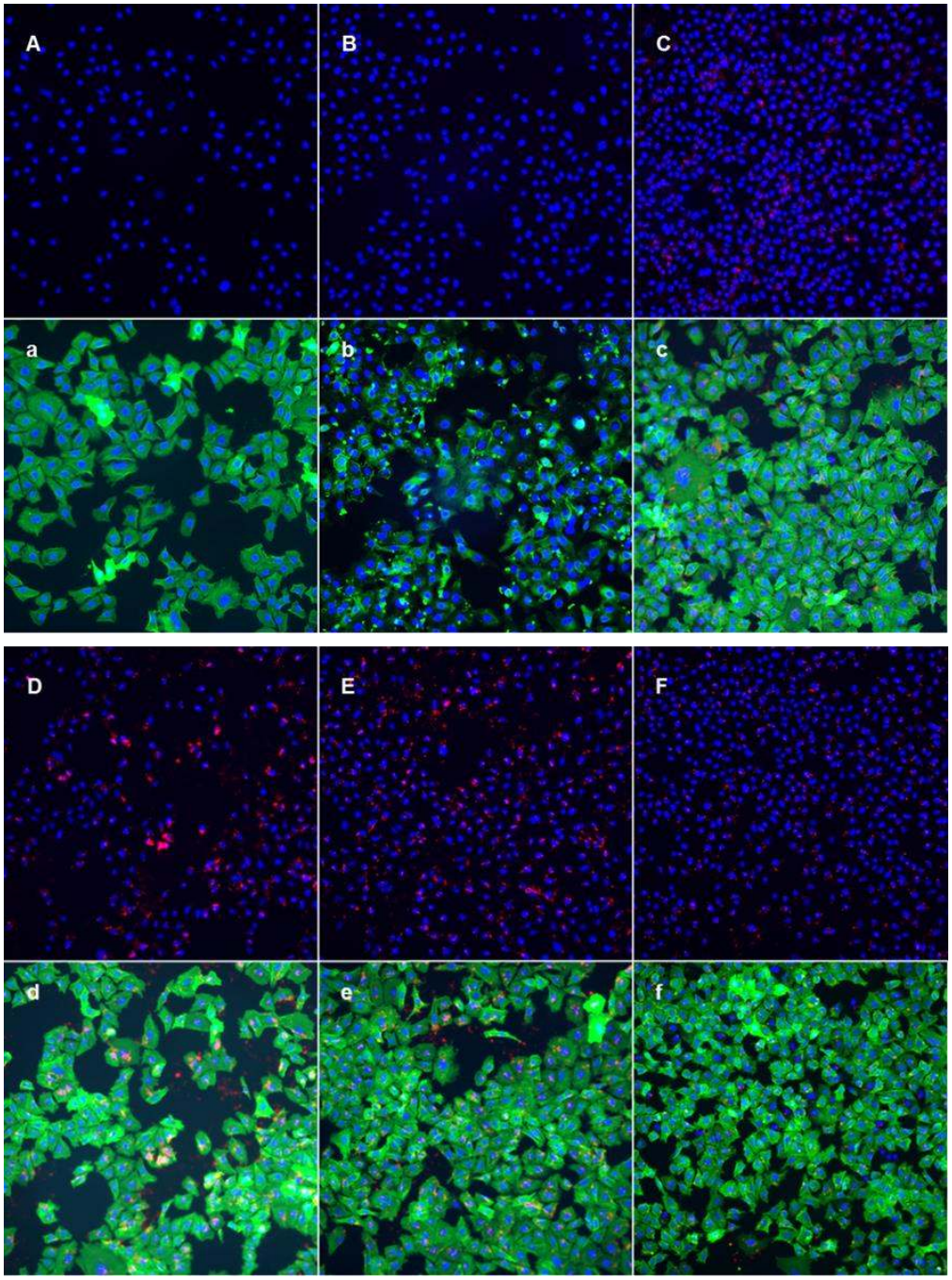

Figure 3. Representative widefield high content microscopy images of A549 cells, incubated for 2 h with formulations of pDNA-Cy5 alone (A), pDNA-Cy5/TMC-NPs-0.07 (B), pDNA-Cy5/TMC-NPs-0.7 (C), pDNA-Cy5/TMC-NPs-3 (D), pDNA-Cy5/TMC-NPs-7 (E), pDNA-Cy5-Lipofectamine2000 (F) and were taken at 20x magnification and the scale bar represents 500 µm. Identical images (a-f) of images A-F are presented to visually distinguish pDNA-Cy5 within cells, marked by the cytoskeleton (phalloidin-Alexa488; green) around nuclei, from pDNA-Cy5 not taken up by cells.

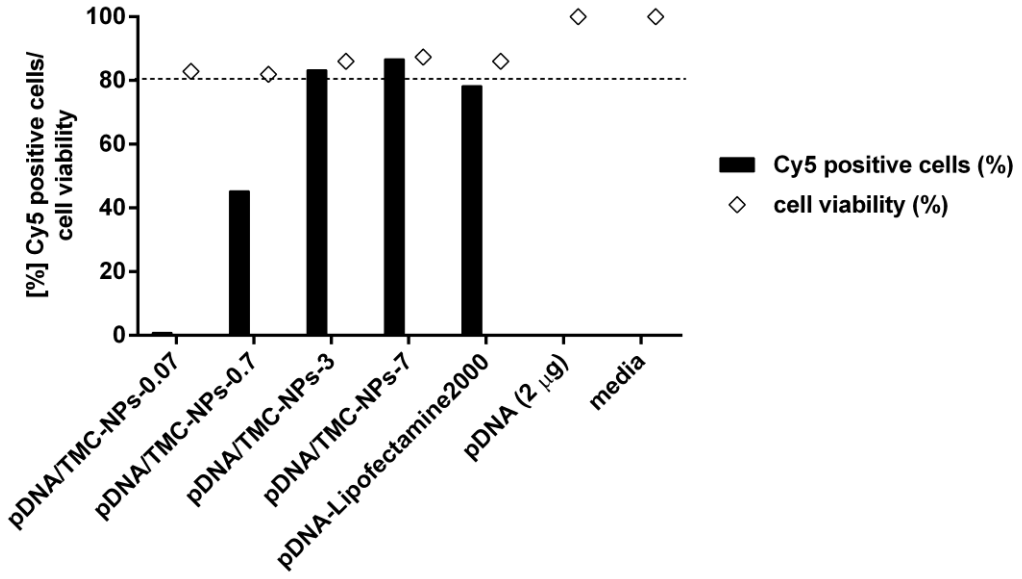

Figure 4. Cellular uptake was calculated for each well by having set Cy5 positive cells (red) in relations to the number of nuclei (DAPI; blue). The formulations with unlabeled pDNA were shown to maintain cell viability >80% after 24 h in relation to cells cultured in media (XTT assay).

formulations of the ratios 0.07, 0.7, 3, and 7. As shown in Figure 5, IgG2c/IgG1 ratios of the lowest dose of pDNA applied were below unity, indicating Th2 bias induced by pDNA alone that was altered by TMC nanoparticles (pDNA/TMC-NPs-0.07) to mixed Th1/Th2 responses, seen in increase of IgG2c titers and decrease of IgG1 titers (Figure 6). With higher pDNA/TMC nanoparticle ratios (ratios of 0.7, 3, and 7), which implies higher pDNA content adsorbed to TMC nanoparticles, a clear shift to Th1 type immune responses could be provoked. An increase of Th1 biased immune responses dependent on increase of pDNA/TMC nanoparticle ratios was observed with a maximum effect for pDNA/TMC-NPs-3. Interestingly, when having further increased pDNA concentrations and hence having further increased the ratio of pDNA to TMC nanoparticles to 7, the Th1 biased immune responses unanticipatedly waned. According to the loading efficiency studies described above, 15 µg of pDNA is the maximum amount strongly bound to the nanoparticles. pDNA/TMC-NPs-3 with 50 µg

pDNA and pDNA/TMC-NPs-7 with 100 µg pDNA per injection dose, contain excess amounts of pDNA that is either loosely bound (conceivably in pDNA/TMC-NPs-3) or remains as free unbound pDNA in suspension (pDNA/TMC-NPs-7).

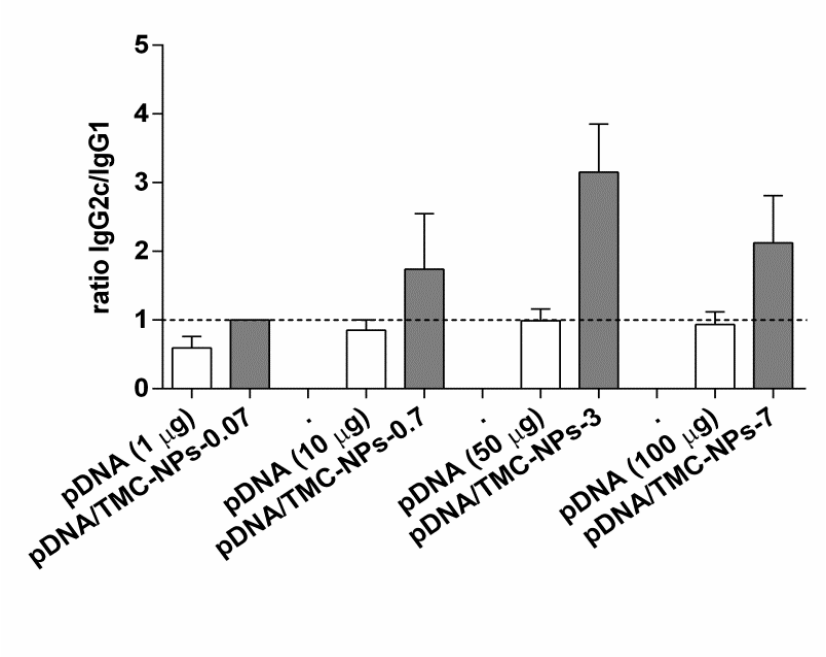

Figure 5. Influence of different pDNA doses on Th1 and Th2 polarization, either alone or adsorbed to TMC nanoparticles. Mice were immunized three times at 3-week intervals and sera were analyzed by ELISA at week 7. Bars represent mean n=5 ± SEM. Ratios of IgG2c and IgG1 antibodies specific to Ag85A were determined and values higher than 1 (dotted line) characterize Th1 biased immune responses.

Looking closer at the serum IgG antibody subclasses, free pDNA in all concentrations generally induced high titers of Th2 related IgG1 antibodies (Figure 6). The non-adsorbed pDNA may provoke induction of humoral immunity, and suppress IgG2c formation associated with cell-mediated Th1 responses. The high IgG1 titers, as well as high total IgG levels detected in mice immunized with naked pDNA may be caused by the presence of DNA that remains at the outside of cells after i.m. injection. It has been suggested that the presence of extracellular host DNA, released from necrotic cells exposed to alum, acts as a damage-associated molecular pattern and is linked to alum adjuvant activity, inducing a Th2-bias of the subsequent adaptive response (Marichal *et*

al., 2011). Extracellular DNA represents a condition not to be found in healthy subjects and thus may stimulate the immune system offering a “danger signal” and strongly boost the response in a similar way as proposed for alum adjuvant activity. TMC nanoparticles evidently changed the impact of pDNA on serum IgG antibody responses towards Th1 related immunity. This might be partly caused by the nanoparticles themselves, as chitosan and trimethyl chitosan particles reportedly provoke dendritic cell maturation and proinflammatory cytokine production by phagocytosis-dependent mechanisms (Babensee, 2008, Bal *et al.*, 2010). Furthermore, higher quantities of ingested pDNA due to TMC nanoparticle delivery may lead to stronger intracellular stimulation of endosomal TLR9 *via* unmethylated CpG sequences found in pDNA as well as cytosolic TANK-binding kinase-1 activation by the double stranded B-form of pDNA. Both incitements activate NF-κB to promote proinflammatory gene transcription and thus Th1 cell differentiation (Cui and Mumper, 2003).

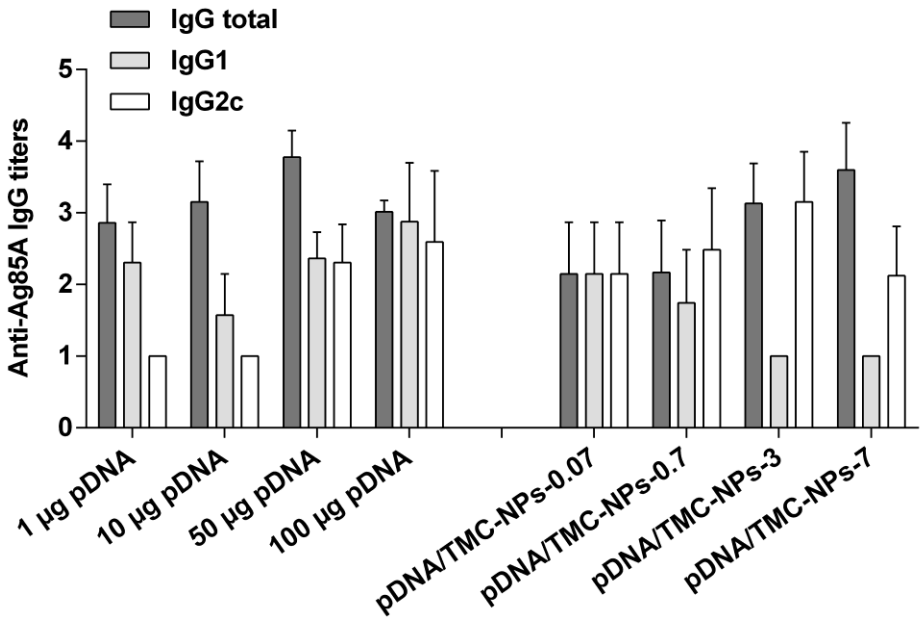

Figure 6. Anti-Ag85A antibody responses (IgG, IgG1, IgG2c) in mice vaccinated with different pDNA doses, applied either alone or adsorbed to TMC nanoparticles. Mice (n=5) were immunized intramuscularly three times at 3-week intervals and sera were analyzed by ELISA at week 7.

3.5 Impact of MDP on pDNA/TMC-NPs-0.7 formulation

The formulation with the lowest ratio (pDNA/TMC-NPs-0.7) capable to polarize immune responses to a Th1 bias, as shown in Figure 5, was chosen to investigate the impact of MDP on enhancing cell-mediated immune responses. 10 µg of MDP per dose was applied such that it was administered at a weight ratio to pDNA of 1:1 per formulation. This complies with previously published MDP dosages in adjuvant combination studies already tested *in vivo* (Cheng *et al.*, 2011, Moschos *et al.*, 2005).

pDNA was adsorbed onto TMC particles (pDNA/TMC-NPs-0.7) or applied with MDP containing TMC particles (pDNA/TMC-NPs-0.7 + MDP). An immunopotentiating effect *in vivo* was sought to be investigated, as we have reported on synergistic enhancement of proinflammatory cytokine release *in vitro* by co-delivery of pDNA with MDP

(Poecheim *et al.*, submitted). These previous *in vitro* investigations didn't show macrophage activation with only MDP (Poecheim *et al.*, submitted), therefore we excluded this group from the animal experiments. As shown in Figure 7A significantly lower Ag85A-specific total IgG antibody production was detected following vaccination with both adjuvanted pDNA formulations ($p < 0.001$), when compared to vaccination with naked pDNA. Similar results were observed for the IgG1 isotype (Figure 8), indicating that the Th2 immune response profile induced by pDNA is reduced by the adjuvanted formulations. However, IgG2c isotype levels were significantly increased by pDNA delivered with TMC nanoparticles ($p < 0.05$) and were even more enhanced with MDP ($p < 0.01$), compared to the non-adjuvanted pDNA. To characterize the polarization of immune responses induced by the different vaccine formulations, ratios of IgG2c/IgG1 titers were calculated from the measurements in mouse sera, as shown in Figure 7B. The major important difference between the effects of adjuvanted and non-adjuvanted pDNA appeared to be the type of immune response elicited. Mice vaccinated with naked pDNA developed marked Th2 immune responses with high IgG1 titers. IgG2c/IgG1 ratios were shifted to a value above unity for the pDNA/TMC

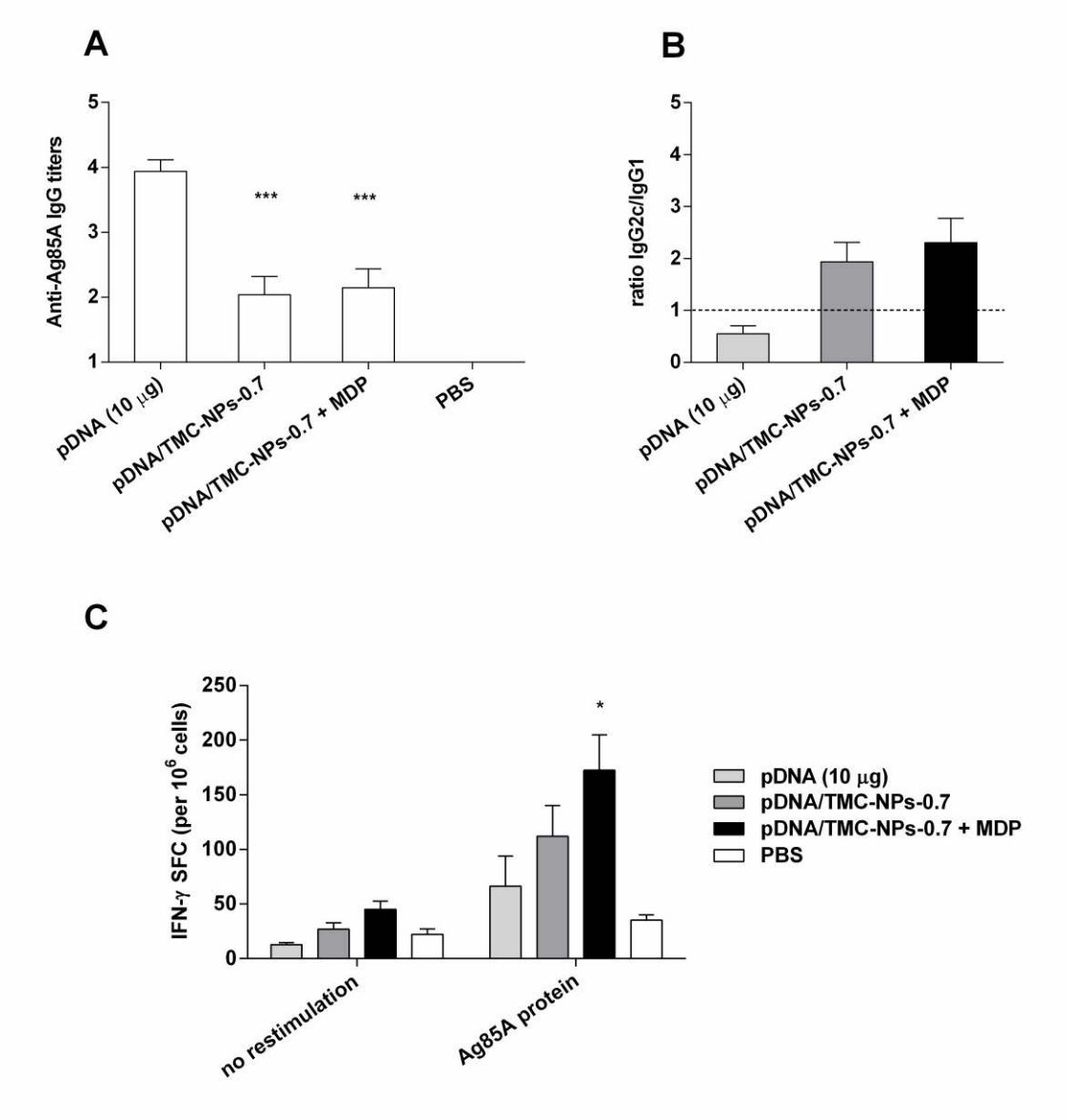

Figure 7. Immune responses in mice one week after the 2nd booster injection (i.m.); (A-C): pDNA (10 µg) formulations +/- MDP (10 µg) and/or TMC nanoparticles per dose. Bars represent mean n=8 ± SEM, *p < 0.05, ***p < 0.001 compared to pDNA alone. (A): Ag85A-specific serum IgG titers, analyzed by endpoint ELISA; (B): Corresponding average Log IgG2c/ Log IgG1 ratios, indicative for the quality of the immune response; (C): IFN-γ secretion in mouse splenocytes analyzed by ELISPOT and data expressed as spot-forming cell (SFC) responses to media (no restimulation) and Ag85A protein. nanoparticles as well as for the pDNA/TMC-MDP nanoparticles, which is associated with a Th1 type immune response.

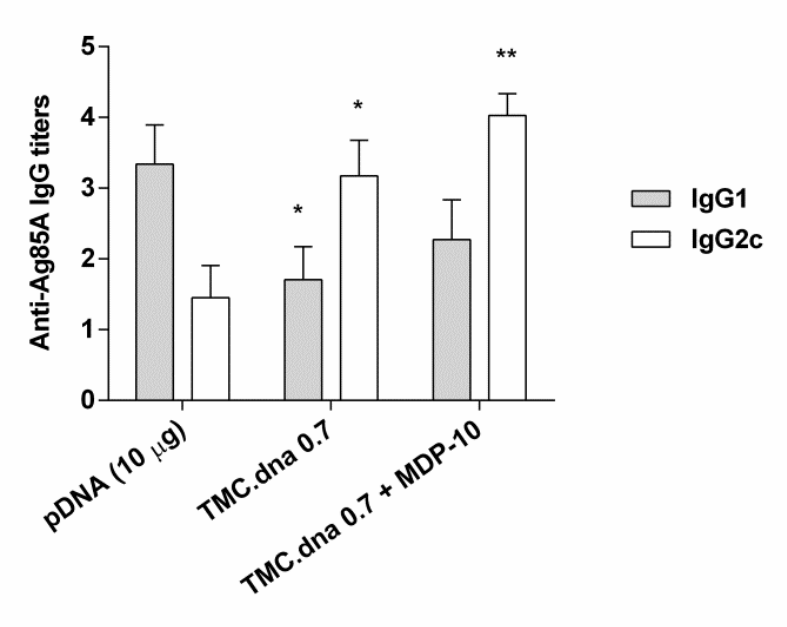

Figure 8. IgG1 and IgG2c isotypes from sera were determined by ELISA. Bars represent mean n=5 to 8 mice ± SEM, *$p < 0.05$, **$p < 0.01$ compared to pDNA alone.

Finally, the number of IFN-γ producing spleen cells after restimulation with the antigen was determined by ELISPOT (Figure 7C) and confirm the Th1 polarizing effect of the adjuvanted pDNA formulations. The numbers of IFN-γ producing T-cells were shown to be enhanced by TMC nanoparticles. MDP in the pDNA/TMC nanoparticle formulation further increased the Th1 increasing effect of pDNA/TMC nanoparticles, resulting in significant higher cell-mediated responses compared to non-adjuvanted pDNA ($p < 0.05$). The adjuvant activity of MDP in combination with pDNA may be attributed to NOD2 to cross-talk with TLR-9 receptor pathways activating NF-κB in a synergistic fashion (Abbott *et al.*, 2007). Most bacteria simultaneously expose a variety of different pathogen-associated molecular patterns (PAMPs) to the immune system of the host, recognized by PRRs. Several studies reported a synergistic outcome on inflammatory cytokine expression in different cells stimulated with NLR and TLR agonist in parallel, having observed synergy between TLR-2, TLR-4 and TLR-9 agonists and both Nod1 and Nod2 elicitors in macrophages and epithelial cells (Tada *et al.*, 2005, Uehara *et al.*, 2005, van Heel *et al.*, 2005). According to biochemical screens RIP2 predominantly interacting with NLRs also binds to TRAF6 of the TLR signaling pathway upon co-

stimulation of both receptors (Kufer and Sansonetti, 2007). In terms of biological relevance, activation of both TLRs and NLRs might be important for the fine-tuning of the inflammatory response and was successfully applied in this study in co-delivery of those ligands with TMC nanoparticles.

4. Conclusion

Our studies provided evidence that the strategy to deliver Ag85A encoding pDNA and adjuvants in a single nanoparticle formulation allows an effective targeting of the cellular immune system and developed profound Th1 cell mediated immune responses.

The information gained from investigation of physicochemical properties and *in vitro* characterization of nanoparticle-based pDNA formulations is valuable in forming the base of knowledge for the design of an effective DNA vaccine. Cellular uptake investigations of pDNA *in vitro* showed saturation to a maximum level upon increase in pDNA/TMC nanoparticle ratios, correlating with increasing Th1 related antibody responses up to a definite ratio. Variations in pDNA doses changed the outcome of immune responses and indicate that dose investigation is crucial for the desired outcome of Th1 biased immune responses. Hence, a potential context for the interpretation of the effects of formulation parameters on the type and extent of immune response elicited *in vivo* can be provided. An adjuvant effect of MDP co-delivered with pDNA/TMC nanoparticles was demonstrated in further increase in Th1-associated antibody levels as well as in numbers of IFN-γ producing T-cells. Such responses, which correlate with cell-mediated immune responses, are critical for the control of intracellular pathogens and may render pDNA/TMC nanoparticles a potential candidate for further investigations of protective efficacy against *Mtb* infections in a challenge model.

References

Abbott, D.W., Yang, Y., Hutti, J.E., Madhavarapu, S., Kelliher, M.A., and Cantley, L.C. (2007). Coordinated regulation of Toll-like receptor and NOD2 signaling by K63-linked polyubiquitin chains*, Molecular and cellular biology,* 27, pp. 6012-6025.

Amidi, M., Romeijn, S.G., Borchard, G., Junginger, H.E., Hennink, W.E., and Jiskoot, W. (2006). Preparation and characterization of protein-loaded N-trimethyl chitosan nanoparticles as nasal delivery system*, Journal of Controlled Release,* 111, pp. 107-116.

Andersen, P. and Kaufmann, S.H. (2014). Novel Vaccination Strategies against Tuberculosis*, Cold Spring Harbor Perspectives in Medicine,* a018523. DOI: 10.1101/ cshperspect.a018523

Babensee, J.E. (2008). Interaction of dendritic cells with biomaterials*, Seminars in Immunology,* 20, pp. 101-108.

Bal, S.M., Slütter, B., van Riet, E., Kruithof, A.C., Ding, Z., Kersten, G.F.A., Jiskoot, W., and Bouwstra, J.A. (2010). Efficient induction of immune responses through intradermal vaccination with N-trimethyl chitosan containing antigen formulations*, Journal of Controlled Release,* 142, pp. 374-383.

Bentwich, Z., Kalinkovich, A., Weisman, Z., Borkow, G., Beyers, N., and Beyers, A.D. (1999). Can eradication of helminthic infections change the face of AIDS and tuberculosis?*, Immunology today,* 20, pp. 485-487.

Bomford, R., Stapleton, M., Winsor, S., McKnight, A., and Andronova, T. (1992). The control of the antibody isotype response to recombinant human immunodeficiency virus gp120 antigen by adjuvants*, AIDS research and human retroviruses,* 8, pp. 1765-1771.

Brandt, L., Feino Cunha, J., Weinreich Olsen, A., Chilima, B., Hirsch, P., Appelberg, R., and Andersen, P. (2002). Failure of the Mycobacterium bovis BCG Vaccine: Some Species of Environmental Mycobacteria Block Multiplication of BCG and Induction of Protective Immunity to Tuberculosis*, Infection and Immunity,* 70, pp. 672-678.

Cheng, C., Jain, P., Bettahi, I., Pal, S., Tifrea, D., and Luis, M. (2011). A TLR2 agonist is a more effective adjuvant for a Chlamydia major outer membrane protein vaccine than ligands to other TLR and NOD receptors*, Vaccine,* 29, pp. 6641-6649.

Cui, Z. and Mumper, R.J. (2003). Microparticles and nanoparticles as delivery systems for DNA vaccines*, Critical Reviews™ in Therapeutic Drug Carrier Systems,* 20,

Dupuis, M., Denis-Mize, K., Woo, C., Goldbeck, C., Selby, M.J., Chen, M., Otten, G.R., Ulmer, J.B., Donnelly, J.J., and Ott, G. (2000). Distribution of DNA vaccines determines their immunogenicity after intramuscular injection in mice*, The Journal of Immunology,* 165, pp. 2850-2858.

Giljohann, D.A., Seferos, D.S., Patel, P.C., Millstone, J.E., Rosi, N.L., and Mirkin, C.A. (2007). Oligonucleotide Loading Determines Cellular Uptake of DNA-Modified Gold Nanoparticles*, Nano Letters,* 7, pp. 3818-3821.

Hansson, A., Di Francesco, T., Falson, F., Rousselle, P., Jordan, O., and Borchard, G. (2012). Preparation and evaluation of nanoparticles for directed tissue engineering*, International Journal of Pharmaceutics,* 439, pp. 73-80.

Heuking, S., Adam-Malpel, S., Sublet, E., Iannitelli, A., Stefano, A.d., and Borchard, G. (2009). Stimulation of human macrophages (THP-1) using Toll-like receptor-2 (TLR-2) agonist decorated nanocarriers*, Journal of drug targeting,* 17, pp. 662-670.

Higgins, S.C. and Mills, K.H. (2010). TLR, NLR agonists, and other immune modulators as infectious disease vaccine adjuvants*, Current infectious disease reports,* 12, pp. 4-12.

Hoft, D.F., Kemp, E.B., Marinaro, M., Cruz, O., Kiyono, H., McGhee, J.R., Belisle, J.T., Milligan, T.W., Miller, J.P., and Belshe, R.B. (1999). A double-blind, placebo-controlled study of Mycobacterium-specific human immune responses induced by intradermal bacille Calmette-Guérin vaccination*, Journal of Laboratory and Clinical Medicine,* 134, pp. 244-252.

Huygen, K., Denis, O., Montgomery, D.L., Yawman, A.M., Deck, R.R., DeWitt, C.M., Orme, I.M., Baldwin, S., D'Souza, C., and Drowart, A. (1996). Immunogenicity and protective efficacy of a tuberculosis DNA vaccine*, Nature Medicine,* 2, pp. 893-898.

Ingolotti, M., Kawalekar, O., Shedlock, D.J., Muthumani, K., and Weiner, D.B. (2010). DNA vaccines for targeting bacterial infections*, Expert Review of Vaccines,* 9, pp. 747-763.

Kim, J.J., Simbiri, K.A., Sin, J.I., Dang, K., Oh, J., Dentchev, T., Lee, D., Nottingham, L.K., Chalian, A.A., and Mccallus, D. (1999). Cytokine molecular adjuvants modulate immune responses induced by DNA vaccine constructs for HIV-1 and SIV*, Journal of interferon & cytokine research,* 19, pp. 77-84.

Kufer, T.A. and Sansonetti, P.J. (2007). Sensing of bacteria: NOD a lonely job*, Current Opinion in Microbiology,* 10, pp. 62-69.

Kutzler, M.A. and Weiner, D.B. (2008). DNA vaccines: ready for prime time?*, Nat Rev Genet,* 9, pp. 776-788.

Lemesre, J.-L., Holzmuller, P., Gonçalves, R.B., Bourdoiseau, G., Hugnet, C., Cavaleyra, M., and Papierok, G. (2007). Long-lasting protection against canine visceral leishmaniasis using the LiESAp-MDP vaccine in endemic areas of France: Double-blind randomised efficacy field trial*, Vaccine,* 25, pp. 4223-4234.

Limbach, L.K., Li, Y., Grass, R.N., Brunner, T.J., Hintermann, M.A., Muller, M., Gunther, D., and Stark, W.J. (2005). Oxide nanoparticle uptake in human lung fibroblasts: effects of particle size, agglomeration, and diffusion at low concentrations*, Environmental science & technology,* 39, pp. 9370-9376.

Lindblad, E.B., Elhay, M.J., Silva, R., Appelberg, R., and Andersen, P. (1997). Adjuvant modulation of immune responses to tuberculosis subunit vaccines*, Infection and Immunity,* 65, pp. 623-629.

Marichal, T., Ohata, K., Bedoret, D., Mesnil, C., Sabatel, C., Kobiyama, K., Lekeux, P., Coban, C., Akira, S., and Ishii, K.J. (2011). DNA released from dying host cells mediates aluminum adjuvant activity*, Nature Medicine,* 17, pp. 996-1002.

Moschos, S.A., Bramwell, V.W., Somavarapu, S., and Alpar, H.O. (2005). Comparative immunomodulatory properties of a chitosan-MDP adjuvant combination following intranasal or intramuscular immunisation*, Vaccine,* 23, pp. 1923-1930.

Patil, S., Sandberg, A., Heckert, E., Self, W., and Seal, S. (2007). Protein adsorption and cellular uptake of cerium oxide nanoparticles as a function of zeta potential*, Biomaterials,* 28, pp. 4600-4607.

Poecheim, J., Barnier Quer, C., Heuking, S., Brunner, L., Collin, N., and Borchard, G. (submitted). Nanocarriers for DNA vaccines: co-delivery of TLR-9 and NLR-2 leads to synergistic enhancement of proinflammatory cytokine release*, Manuscript submitted for publication.*

Poecheim, J. and Borchard, G. (2015) *Controlled Release Systems: Advances in Nanobottles and Active Nanoparticles* eds. J. Forcada, A. v. Herk, and Pastorin, G., 17 "Immunotherapie and Vaccines", (Pan Stanford Publishing, Singapore) pp. 523-551.

Pye, D., Vandenberg, K.L., Dyer, S.L., Irving, D.O., Goss, N.H., Woodrow, G.C., Saul, A., Alving, C.R., Richards, R.L., Ballou, W.R., Wu, M.-J., Skoff, K., and Anders, R.F. (1997). Selection of an adjuvant for vaccination with the malaria antigen, MSA-2*, Vaccine,* 15, pp. 1017-1023.

Russell, D.G. (2007). Who puts the tubercle in tuberculosis?*, Nature Reviews Microbiology,* 5, pp. 39-47.

Slütter, B., Plapied, L., Fievez, V., Alonso Sande, M., des Rieux, A., Schneider, Y.-J., Van Riet, E., Jiskoot, W., and Préat, V. (2009). Mechanistic study of the adjuvant effect of biodegradable nanoparticles in mucosal vaccination*, Journal of Controlled Release,* 138, pp. 113-121.

Tada, H., Aiba, S., Shibata, K.-I., Ohteki, T., and Takada, H. (2005). Synergistic Effect of Nod1 and Nod2 Agonists with Toll-Like Receptor Agonists on Human Dendritic Cells To Generate Interleukin-12 and T Helper Type 1 Cells*, Infect. Immun.,* 73, pp. 7967-7976.

Tameris, M., Geldenhuys, H., Luabeya, A.K., Smit, E., Hughes, J.E., Vermaak, S., Hanekom, W.A., Hatherill, M., Mahomed, H., and McShane, H. (2014). The candidate TB vaccine, MVA85A, induces highly durable Th1 responses*, PLoS ONE,* 9, pp. e87340. DOI: 0.1371/journal.pone.0087340

Thanou, M., Florea, B., Geldof, M., Junginger, H., and Borchard, G. (2002). Quaternized chitosan oligomers as novel gene delivery vectors in epithelial cell lines*, Biomaterials,* 23, pp. 153-159.

Thanou, M.M., Verhoef, J.C., Romeijn, S.G., Nagelkerke, J.F., Merkus, F.W.H.M., and Junginger, H.E. (1999). Effects of N-trimethyl chitosan chloride, a novel absorption enhancer, on Caco-2 intestinal epithelia and the ciliary beat frequency of chicken embryo trachea*, International Journal of Pharmaceutics,* 185, pp. 73-82.

Uehara, A., Sugawara, Y., Kurata, S., Fujimoto, Y., Fukase, K., Kusumoto, S., Satta, Y., Sasano, T., Sugawara, S., and Takada, H. (2005). Chemically synthesized pathogen-associated molecular patterns increase the expression of peptidoglycan recognition proteins via toll-like receptors, NOD1 and NOD2 in human oral epithelial cells*, Cellular Microbiology,* 7, pp. 675-686.

Van Heel, D.A., Ghosh, S., Butler, M., Hunt, K., Foxwell, B.M.J., Mengin-Lecreulx, D., and Playford, R.J. (2005). Synergistic enhancement of Toll-like receptor responses by NOD1 activation*, European Journal of Immunology,* 35, pp. 2471-2476.

Wang, C., Luo, X., Zhao, Y., Han, L., Zeng, X., Feng, M., Pan, S., Peng, H., and Wu, C. (2012). Influence of the polyanion on the physico-chemical properties and biological activities of polyanion/DNA/polycation ternary polyplexes*, Acta Biomaterialia,* 8, pp. 3014-3026.

WHO (2014). Global tuberculosis report 2014, *19th global report on tuberculosis* (Vol., 19).

Yuk, J.-M. and Jo, E.-K. (2014). Host immune responses to mycobacterial antigens and their implications for the development of a vaccine to control tuberculosis*, Clinical and Experimental Vaccine Research,* 3, pp. 155-167.

Summary and conclusion

The aim of this work was to formulate nanoparticles with DNA plasmid (pDNA), encoding the *Mycobacterium tuberculosis (Mtb)* antigen 85A. The design of cationic N-trimethylated chitosan (TMC) nanoparticles, adjuvanted with the pattern recognition ligands TLR-9 and NLR-2, is a novel approach for improving DNA vaccines. These adjuvanted pDNA-nanoparticle systems were investigated as a potential vaccine formulation to increase and polarize cell-mediated immune responses.

Nanoparticle application in vaccines to activate the immune systems is reviewed in Chapter 1. Key parameters of nanoparticles as immunostimulants, nanoparticles as delivery systems to enhance antigen processing, as well as current nanoparticle vaccines on the market and in clinical trials were discussed. Particle uptake and immunogenicity have been shown to be dependent on many factors, associated with size, surface charge, the bulk materials in nanoparticle composition, the antigen type transferred, the route of administration, as well as the vaccination regime. However, fundamental knowledge of nanoparticle mechanism of action in both immunostimulation and drug delivery are still urgently required for the rational design of nanoparticle-containing vaccines. To date, nanosized vaccines approved for human use are represented by virus-like nanoparticles, non-viral liposomal nanoparticles and oil-in-water nanoemulsions. The use of nanotechnology in vaccines has been increasing exponentially in the past decade and many more candidates are currently under investigation in clinical and pre-clinical trials.

Assessment of stability and integrity of the components implicated in TMC nanoparticle formulations with pDNA is described in Chapter 2. The introduction of permanent charges in chitosan by trimethylation of the primary amino groups enhanced cationic

properties and thus increased complexation of polyanions to form nanoparticles. TMC nanoparticles were investigated with regard to their stability in aqueous formulations and after lyophilization. pDNA was adsorbed to the TMC particles by electrostatic interactions between the cationic nanoparticle surface and the anionic charges of the pDNA phosphate backbone. The physicochemical characteristics of TMC nanoparticles were preserved during freeze-drying and storage, after reconstitution. Structural changes of pDNA were observed upon adsorption to the particles, however, the helical conformation was shown to be regained after release.

In Chapter 3, TMC nanoparticles were compared with a cationic squalene-in-water emulsion, and the cationic oil-in-water emulsion Cationorm® on their ability to enhance immunogenicity of pDNA in mice. It was demonstrated that TMC nanoparticles was the only carrier evaluated able to induce antigen-specific cell-mediated immune responses. Moreover, mechanistic *in vitro* studies revealed an immune response enhancing effect by simultaneous targeting of Toll-like receptor 9 *via* unmethylated CpG motifs present on pDNA and Nod-like receptor 2, targeted by co-administration of muramyl dipeptide (MDP). The delivery of pDNA with all three cationic nanocomplexes together with MDP was shown to significantly increase pro-inflammatory cytokine release in a synergistic manner.

In a last step the optimal dose of pDNA applied with TMC nanoparticles was evaluated *in vitro* and *in vivo*, as shown in Chapter 4. A systematic approach to formulation development was accomplished by detailed physicochemical and biophysical characterization of the pDNA/TMC nanoparticle formulations, to gain better understanding of their biological behavior. Variations in pDNA doses changed the outcome of immune responses and indicate that dose optimization is crucial for obtaining the desired outcome of cell-mediated immunity. Finally, having incorporated MDP in the formulation, an additional increase in Th1 dependent antigen-specific cell-mediated immune responses, induced by pDNA/TMC nanoparticles, was provoked.

To summarize, formulating pDNA with cationic polymeric TMC particles in the nano-range was shown to be a successful approach to increase potency of antigen expressing DNA vaccines. To provide a potential context for future design of DNA vaccines, important parameters of TMC nanoparticle formulations with pDNA were evaluated and characterized. Freeze-drying was demonstrated to be a reasonable approach for stabilization and storage of standardized batches of TMC nanoparticles. Successful binding of pDNA to the nanoparticles was confirmed as well as integrity of the secondary structure of pDNA after being released. It was shown that two pattern-recognition ligands co-delivered by nanoparticles synergistically activate innate immune responses *in vitro* and enhance cell-mediated immune responses *in vivo*. The combination of two pattern-recognition ligands co-delivered by nanoparticles was shown *in vitro* to synergistically activate innate immune responses and enhanced cell-mediated immune responses *in vivo*. Furthermore, *in vivo* studies revealed that investigations of the correct pDNA dose applied were crucial to obtain the desired outcome of immune responses.

TMC nanoparticles, formulated with *Mtb* antigen 85A expressing pDNA, successfully induced robust Th1 immune responses in mice and may render pDNA/TMC nanoparticles a potential vaccine candidate for further investigations of protective efficacy against *Mtb* infections in a challenge model. An adjuvant effect of MDP co-delivered with pDNA/TMC nanoparticles was proven however, further assays are needed to validate the appropriate dose combination of pDNA and MDP. CD4 T-cells of helper type 1 (Th 1) activated by cytokines including interferon-gamma (IFN-γ) and tumour necrosis factor-alpha (TNF-α) are considered central mediators of protection and are widely used as an indicator for vaccine efficacy. Nevertheless, observations of IFN-y secreting T-cells as a sole predictor of protection needs to be extended by investigations of the contributions of various types of T-cells, such as natural killer, gamma-delta, lipid-specific CD1-restriced, CD8 cytotoxic T-cells and T-cells of helper

type 17. Elucidating their relevance to protection may offer a valuable concept for continuing vaccine design.

Résumé et conclusion

L'objectif du travail présenté dans cette thèse était de formuler des nanoparticules chargées en plasmides (pADN) codant l'antigène 85 A de *Mycobacterium tuberculosis (Mtb)*. Le développement des nanoparticules de N-triméthyl chitosan (TMC), avec des ligands de TLR-9 et de NLR-2, est une nouvelle approche pour améliorer les vaccins ADN. Ces systèmes de nanoparticules-pADN ont éte étudiés et analysés comme une formulation potentielle de vaccin pour augmenter et polariser les réponses immunitaires à médiation cellulaire.

L'utilisation de nanoparticules comme vaccins pour activer le système immunitaire est abordée dans le Chapitre 1. Les caractéristiques clés des nanoparticules comme stimulants immunitaires, systèmes de livraison pour améliorer la production d'antigènes ainsi que les vaccins à nanoparticules actuellement sur le marché et en expérimentations cliniques y sont également traités. L'absorption cellulaire de particules et l'immunogénicité dépendant de beaucoup de facteurs, comme la taille, la charge de surface, la composition des nanoparticules, le type d'antigène vectorisé, la voie d'administration ainsi que les paramètres de vaccination. Cependant, la connaissance fondamentale du mécanisme d'action des nanoparticules à la fois dans l'immunostimulation et dans les systèmes de libération sont encore nécessaires pour la conception rationnelle de vaccins contenant des nanoparticules. A ce jour, les nanovaccins approuvés pour l'utilisation humaine comprennent des virosomes et des formes non virales comme des liposomes et des nanoémulsions huile dans eau. L'utilisation de nanotechnologies dans les vaccins a augmenté de façon exponentielle ces dix dernières années et de plus en plus de candidats sont actuellement en cours d'étude dans des tests cliniques et pré-cliniques.

L'évaluation de la stabilité et de l'intégrité des composants impliqués dans les formulations de nanoparticules TMC avec de l'ADN sont décrites dans le chapitre 2. L'introduction de charges permanentes sur le chitosan par triméthylation des groupes amines primaires a amélioré les propriétés cationique et la complexation des polyanions pour former des nanoparticules. La stabilité des nanoparticules TMC dans les formulations aqueuses et après lyophilisation ont été étudiées. Le pADN a été adsorbé sur les particules grâce aux interactions électrostatiques entre la surface des nanoparticules cationiques et les charges anioniques du pADN. Les caractéristiques physiochimiques des nanoparticules TMC ont été préservées lors des phases de congélation- séchage et stockage, après reconstitution. Des changements structurels de pADN ont été observés au moment de l'adsorption sur les particules, cependant la structure hélicoïdale s'est montrée stable après libération.

Dans le chapitre 3, les nanoparticules de TMC ont été comparées avec une émulsion de squalène cationique dans l'eau et l'émulsion huile dans eau Cationorm® pour leur capacité à améliorer l'immunogénicité du pADN chez les souris. Il a pu être démontré que les nanoparticules TMC étaient le seul candidat évalué capable de déclencher des réponses immunes à médiation cellulaire contre des antigènes spécifiques. De plus, des études d'*in vitro* ont révélé l'amélioration de la réponse immune en ciblant simultanément le récepteur Toll-like receptor 9 *via* les motifs CpG non-méthylés présents sur le pADN et le récepteur Nod-like receptor 2, ciblé par la co-administration du muramyl dipeptide (MDP). La libération du pADN avec les trois nanocomplexes cationiques associés au MDP a montré l'augmentation significativement de la libération de cytokine pro-inflammatoire en synergie.

Dans la dernière partie, la dose optimale de pADN appliquée avec les nanoparticules TMC a été évaluée *in vitro* et *in vivo*, comme décrit dans le Chapitre 4. Une approche méthodique du développement de la formulation a été accomplie par une description physiochimique et biophysique détaillée des formulations des nanoparticules pADN-TMC, pour avoir une meilleur compréhension de leur comportement biologique. Les

variations de doses de pADN ont influencé le résultat des réponses immunitaire et indiquent que l'étude de l'effet de la dose sur les réponses immunitaire est cruciale pour obtenir l'effet désiré d'immunité à médiation cellulaire. Finalement, après avoir incorporé le MDP dans la formulation, une augmentation supplémentaire des réponses immunitaires Th1 à médiation cellulaire antigène spécifique, induite par les nanoparticules pADN-TMC, a été obtenue.

En résumé, la formulation de pADN avec des nanoparticules TMC cationique s'est révélée être une approche réussie pour augmenter l'efficacité du vaccin avec antigène exprimé par le pADN. Pour fournir un contexte potentiel pour la conception future d'un vaccin ADN, des paramètres importants de la formulation de TMC nanoparticules avec pADN ont été évalués et caractérisés. La lyophilisation est une approche raisonnable pour stabiliser et stocker des lots standardisés de nanoparticules TMC. Le succès de la liaison entre pADN et les nanoparticules a été confirmé ainsi que l'intégrité de la structure secondaire du plasmide après libération. La combinaison de deux modèles de reconnaissance de ligands co-delivrés par des nanoparticules a montré activer en synergie *in vitro* des réponses immunes naturelles et améliorer *in vivo les réponses immunes*. De plus, les études *in vivo* ont révélé que les recherché sur la dose de pADN appliquée étaient cruciales pour obtenir le résultat des réponses immunes désirée.

Les nanoparticules TMC, formulées avec l'antigène *Mtb* 85A exprimant pADN, ont induit avec succès des réponses immunes Th1 robustes chez les souris et pourraient faire des particules pADN/TMC un potentiel candidat pour de plus amples recherches sur l'efficacité protective contre les infections *Mtb* dans un modèle de simulation. Un effet adjuvant de MDP co produit avec des nanoparticules pADN/TMC a été prouvé. Cependant, de plus amples analyses sont nécessaire pour valider la dose appropriée dans la combinaison de pADN et MDP.

Les lymphocytes CD4 de type helper 1 (Th1) activés par les cytokines y compris l'interferon gamma (IFN-γ) et le facteur de nécrose tumorale alpha (TNF- α) sont considérés comme des médiateurs centraux de la protection et sont largement utilisés

comme indicateurs de l'efficacité des vaccins. Cependant, les observations des cellules T secrétant l' IFN-γ comme le seul facteur prédictif de la protection doivent être élargies par des recherches sur les contributions de différents types de cellules T, telles que natural killer, gamma-delta, CD1, cytotoxique (CD8) et Th17. Expliciter leur pertinence dans l'effet protecteur pourrait offrir des concepts précieux pour poursuivre la conception de vaccins.

Abbreviations

Ag85A	Antigen 85A
AIDS	Acquired immunodeficiency syndrome
APC	Antigen presenting cell
ATCC	American Type Culture Collection
BCG	Bacillus Calmette–Guérin
BEI	Biodefense and Emerging Infections Research Resources
BGH	Bovine growth hormone
BSA	Bovine serum albumin
CD (cells/ receptor)	Cluster of differentiation protein
CD (method)	Circular dichroism
CMV	Cytomegalovirus
ConA	Concanavalin A
CpG	Cytosine-phosphate-guanine
CS	Chondroitin sulfate
CTL	Cytotoxic T lymphocytes
DAPI	4′,6-diamidino-2-phenylindole
DC	Dendritic cell
DLS	Dynamic light scattering
DMEM	Dulbecco's modified Eagle medium
DNA	Deoxyribonucleic acid
DOTAP	Phospholipid 1,2-dioleoyl-3-trimethylammonium-propane
dsDNA	Double stranded DNA
EDTA	Ethylenediaminetetraacetic acid
ELISA	Enzyme-linked immunosorbent assay
ELISPOT	Enzyme-Linked ImmunoSpot
FCS	Fetal calf serum

FDA	Food and Drug Administration
FTIR	Fourier transform infrared spectroscopy
HCV	Hepatitis C virus
HIV	Human immunodeficiency virus
HPV	Human papillomavirus
IFN-γ	Interferon gamma
Ig	Immunoglobulin
IL	Interleukin
ISCOM	Immune-stimulating complexes
LB	Luria Bertani medium
LE	Loading efficiency
LN	Lymph node
LPS	Lipopolysaccharide
MDP	Muramyl dipeptide
MHC	Major histocompatibility complex
Mtb	Mycobacterium tuberculosis
MyD88	Myeloid differentiation primary response 88
NF-κB	Nuclear factor kappa-light-chain-enhancer *of* activated B cells
NIAID	National Institute of Allergy and Infectious Diseases
NIH	National Institute of Health
NK	Natural killer cells
NLR	Nod-like receptor
NLRP	NOD-like receptor family pyrin domain containing protein
NMP	1-methyl-2-pyrrolidinone
NMR	Nuclear magnetic resonance
NOD	Nuclear binding domain
NP	Nanoparticle
OD	Optical density
OVA	Ovalbumin
PAMP	Pathogen-associated molecular pattern

PBS	Phosphate buffered saline
PDI	Polydispersity index
pDNA	Plasmid DNA
PEG	Polyethylene glycol
PES	Polyethersulfone
PLGA	Poly lactic-co-glycolic acid
PRR	Pattern recognition receptor
RIP	Receptor-interacting protein
ROS	Reactive oxygen species
RT	Room temperature
SDS	Sodium dodecyl sulfate
SEM	Scanning electron microscope
SFC	Spots forming cells
SLN	Solid lipid nanoparticles
SPION	Superparamagnetic iron oxide nanoparticles
SWE06	Squalene-in-water emulsion with DOTAP
TANK	TRAF family member-associated NF-κB activator
TCR	T-cell receptor
TEM	Transmission electron microscope
Th	T-helper cells
TLR	Toll-like receptor
TMB	3,3',5,5'-Tetramethylbenzidine
TMC	*N,N,N*-trimethylated chitosan
TNF-α	Tumor necrosis factor alpha
tPA	Tissue plasminogen activator
TRAF	TNF receptor associated factor
TSP	3-(trimethylsilyl) propionic-2,2,3,3-d_4 acid
VLP	Virus-like particles
XTT	Sodium 3′-[1-(phenylaminocarbonyl)-3,4-tetrazolium]-bis (4-methoxy-6-nitro) benzene sulfonic acid hydrate

Publications

1. K. Walker, M. Guo, Y. Guo, J. Poecheim, K. Velmurugan, L. Schrager. Novel approaches to preclinical research and TB vaccine development. *Submitted.*

2. J. Poecheim, C. Barnier Quer, N. Collin, G. Borchard. Ag85A DNA vaccine delivery by nanoparticles: Influence of the formulation characteristics on immune responses. *Submitted.*

3. J. Poecheim, S. Heuking, L. Brunner, C. Barnier Quer, N. Collin, G. Borchard. Nanocarriers for DNA vaccines: co-delivery of TLR-9 and NLR-2 ligands leads to synergistic enhancement of proinflammatory cytokine release. *Nanomaterials* 2015, *5*(4), 2317-2334.

4. J. Poecheim, G. Borchard. "Immunotherapy and Vaccines". Book chapter in: J. Forcada, A. van Herk, G. Pastorin (eds.), *Controlled Release Systems: Advances in Nanobottles and Active Nanoparticles* by Pan Stanford, 2015 425-446.

5. J. Poecheim, V. Patrulea, C. Reichert, G. Borchard. Characterization of pDNA/TMC nanoparticle interaction and stability. Curr Drug Delv. 2016, 13 (8), 1567-2018.

6. C. Primard, J. Poecheim, S. Heuking, E. Sublet, F. Esmaeili, G. Borchard. Multifunctional PLGA based nanoparticles encapsulating simultaneously hydrophilic antigen and hydrophobic immunomodulator for mucosal immunization. *Molecular Pharmaceutics* 2013, 10 (8), 2996–3004.

Oral presentations

1. "Dose effect of Ag85A-DNA and muramyl dipeptide on cellular immune responses in vivo*."* Annual Meeting of the European Federation for Pharmaceutical Sciences, Geneva, Switzerland, June 2015.

2. "Cationic nanoparticles for DNA delivery: Comparison of three nanovaccine formulations for their potential to enhance immune responses against *M. tuberculosis."* 9th *World Meeting* on Pharmaceutics, Biopharmaceutics and Pharmaceutical Technology, Lisbon, Portugal, April 2014.

3. "Nanocarriers as vaccine adjuvants: Strategies to enhance immunogenicity." PhD day, Brocher Foundation Hermance, Switzerland, May 2013.

4. **"**TLR and NLR agonist functionalized chitosan nanoparticles for mucosal immunization against tuberculosis." Swiss Galenic Meeting, ETH Zürich, Switzerland, January 2012.

5. **"**DNA vaccine to enhance cell-mediated immune responses against tuberculosis." 26ème Seminaire en sciences pharmaceutiques, Zermatt, Switzerland, September 2011.

Acknowledgements

First of all I would like to express my sincere gratitude to my advisor Prof. Gerrit Borchard for the continuos support of my PhD study, for his patience and motivation. Not only for your guicance I want to thank, but also for being a supervisor on the professional level as well as on the personal.

Thanks to the members of the jury Prof. Muriel Cuendet (University of Geneva), Prof. Eva Roblegg (University of Graz) and Prof. Bruno Gander (ETH Zurich) for taking the time to read and evaluate my thesis.

I want to thank the members of the Vaccine Formulation Laboratory in Lausanne : Dr. Nicolas Collin, Dr. Christophe Barnier-Quer, Dr. Livia Brunner, Maude Marti-Favre and Géraldine Frank, for their collaboration in my project, which incented me to widen my research from various perspectives. I very much enjoyed working in your lab and the insightful comments and encouragements I received from you were more than valuable. I especially want to thank Christophe for his mentorship, the great input he gave on this work as well as for his friendship.

I would also like to thank Dr. Simon Heuking for having introduced me to this very interesting project, for his precious advises and for having set up the collaboration with the VFL, where I was able to do a big part of my thesis project.

Thanks to all my colleagues from FABIO and FATEC for their stimulating discussions, and for the many hours we spent together in the office and in the lab. A special thanks goes to Christian for his friendship and support throughout the whole time of the thesis, and Viorica, Sakthi and Tayeb for the great lunch discussions and all the fun time we had together outside working hours. These moments really kept me going.

I also want to thank the Archamps crew Annasara, Charlotte, Ralitza, Gaelle, Emmanuelle and Valerie for sharing fun and memorable moments in our chateau.

I want to thank all my friends who have greatly inspired me throughout the last years, in seeing the world also though other eyes than with the science glasses on. Thanks for the great moments we shared, in Switzerland, in Austria, on the trips we did together as well as in the mountains.

Thank you Felix, for having entered my life and being a major part of it beyond my thesis defense, for having supported me in finalizing these very last steps and for sharing the joy of these smaller and larger achievements with me.

And finally, I would like to thank my family: my parents and my two brothers, for being there for me throughout my thesis time and my life in general. Without you I wouldn't be where I am today and a big part of this success I owe you. Your constant support in the background always gave me the stability I needed to take this project to its end.